Lateral Torsional Buckling of Built-Up Beams

by

Mohamed Mansor

Supervised by

Prof. Magdi Mohareb

Prof. Ghasan Doudak

Thesis submitted in partial fulfillment of
The requirements for the degree of
DOCTOR OF PHILOSOPHY
in Civil Engineering

Department of Civil Engineering
Faculty of Engineering
University of Ottawa

Abstract

Built-up timber beams are composed of multiple thin plies of equal depth, mechanically connected along their vertical interfaces using discrete fasteners to provide partial composite action. These beams are increasingly used in modern timber structures because thin plies are more economical and more readily available than wide solid sections. However, when such members are employed in long-span applications without adequate lateral bracing, their strength is often governed by lateral–torsional buckling (LTB). The LTB behaviour of these systems is further complicated by the presence of discrete mechanical fasteners, which provide only partial interaction between plies, rather than full composite action. Accurately quantifying this partial interaction and its influence on the critical moment remains a challenge in timber engineering and is not addressed in current American or European timber design standards. The former Canadian standard permitted the use of the LTB capacity of an equivalent monolithic section, provided that the plies were "securely connected." However, ambiguity surrounding what constitutes a secure connection prompted a shift to a more conservative approach in the most recent version of the standard, where the LTB capacity is taken as the sum of the individual capacities of the plies. Within this context, the present thesis investigates the elastic lateral–torsional buckling behaviour of built-up timber beams while accounting for partial interaction between plies. The first part of the study develops a three-dimensional finite element model to simulate the elastic LTB behaviour of two-ply built-up beams. The model captures relative slip between plies and idealizes fasteners as discrete springs at the ply interfaces by assigning shear stiffness in both longitudinal and transverse directions. This approach enables an investigation of the effect of fastener stiffness and spacing on the elastic LTB resistance and corresponding mode shapes of two-ply built-up beams.

Building on this, the second part of the study introduces a variational principle and a beam finite element formulation for the LTB analysis of two-ply built-up timber beams. The formulation accounts for relative transverse and longitudinal slip between plies and characterizes fastener shear stiffness at their interface as linearly elastic springs, leading to an eigenvalue-type solution. The proposed solution yields results that are comparable to 3D finite element models but requires only a one-dimensional discretization along the member span, significantly reducing modeling, computational, and post-processing efforts. This finite element is then used for a parametric investigation of the effects of fastener stiffness, beam geometry, moment gradient, and load height on the elastic LTB capacity of two-ply built-up beams. The study also explores the potential of non-uniform fastener spacing, as opposed to conventional uniform spacing, as a means of optimizing beam capacity.

The third part of the research extends the variational principle and finite element formulation to built-up timber beams composed of multiple plies. Predictions from the developed finite element model are verified against a 3D finite element model and full-scale experimental results reported by other researchers. The verified model is then used to conduct a comprehensive parametric study of 733 cases, investigating the effects of the number of plies, normalized fastener stiffness, longitudinal and transverse spacing, normalized span, ply aspect ratio, common load configurations, and load height on LTB resistance. The resulting database is used to develop dimensionless design equations through symbolic regression, characterizing elastic critical moments relative to the case of no interaction and deriving moment-gradient factors for common loading conditions and load-height coefficients. These proposed equations are integrated into a simplified design procedure, and their practical application is illustrated through design examples.

In summary, the present study advances the understanding of LTB behaviour in built-up timber beams and provides practical tools for characterizing their elastic LTB resistance. The proposed solutions enable engineers to achieve more accurate and economical designs and lay the groundwork for future revisions of timber design standards regarding the LTB of built-up beams

Acknowledgment

This thesis would not have been possible without the support of many people and institutions, and I am truly grateful for their help.

I would like to sincerely thank my supervisors, Professor Magdi Mohareb and Professor Ghasan Doudak, for their guidance and steady support throughout this research. Their expertise, thoughtful feedback, and rigorous academic standards greatly strengthened this work and contributed meaningfully to its development. I am especially grateful for the constructive discussions that refined the direction and depth of this study. Their mentorship and continued support have greatly contributed to my academic and professional growth.

I sincerely thank the members of my examining committee: Professor Alexander Salenikovich from Laval University, Professor Heng-Aik Khoo from Carleton University, and Professor Beatriz Martin-Perez and Professor Elena Dragomirescu from the University of Ottawa—for their time, careful review, and valuable feedback. Their thoughtful questions and constructive comments helped in refining and strengthening this thesis.

My deepest gratitude goes to my family. To my wife, Rawan, thank you for your patience, encouragement, and unwavering belief in me through the long days, late nights, and demanding stages of this journey. Your support carried me through the most challenging moments, and I owe more than words can express. To my parents, I am forever thankful. Your sacrifices, dedication, and constant encouragement laid the foundation for everything I have achieved. I also thank my brother for always being there, whether through advice, reassurance, or simply listening when things felt overwhelming.

I gratefully acknowledge the University of Ottawa for fostering an academic environment that supported my intellectual and professional development. I also sincerely thank the Natural Sciences and Engineering Research Council of Canada (NSERC) and the Canadian Wood Council for their financial support, which significantly contributed to the advancement of this work.

Finally, I am grateful to my colleagues and friends who shared this journey with me. The discussions, collaboration, and encouragement we exchanged over the years made this experience both meaningful and memorable.

Table of Contents

List of Figures

List of tables

Chapter 1: Introduction

1.1 General

Due to the high cost and limited availability of large wooden sections and engineered wood products, designers increasingly rely on built-up wooden beams, particularly in residential buildings and light wood-frame applications. These members are generally formed by assembling several plies of equal depth, which are connected using mechanical fasteners such as nails or screws (Figure 1.1). The degree of composite action developed within a built-up beam depends primarily on the shear stiffness of the fasteners, as well as their spacing and layout along the members. When fasteners exhibit low shear stiffness or are spaced far apart, the interaction between plies is weak, resulting in limited composite action. Under such conditions, each ply tends to act independently, and the critical moment of the built-up beam approaches the summation of the critical moments of the individual plies. In contrast, closely spaced fasteners with high shear stiffness promote stronger interaction between plies, leading to a higher level of composite behaviour.

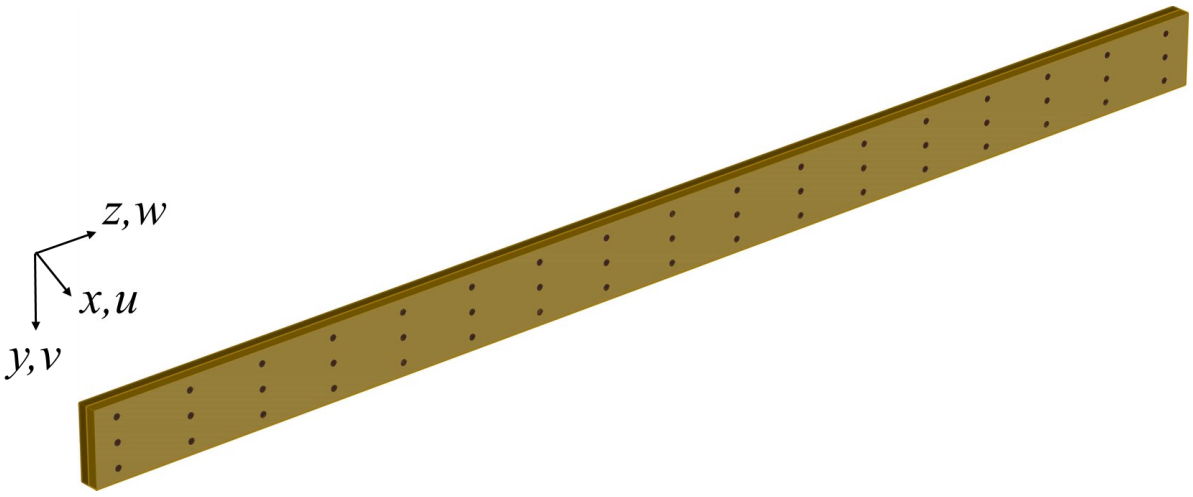

Figure 1.1 Built-up beam connected with fasteners

In this case, the critical moment may approach that of an equivalent monolithic beam whose width equals the total width of all plies. In practice, the behaviour of connections falls between these idealized extremes. Mechanical fasteners usually provide partial interaction, allowing relative slip between plies.

1.2 Lateral torsional buckling

The lateral torsional buckling (LTB) typically governs the resistance of long-span unbraced wooden monolithic beams subjected to major bending. Lateral torsional buckling is characterized by sudden lateral displacement combined with twisting. Similar to monolithic beams, long-span built-up beams may exhibit LTB. In this case, LTB is associated with more complex kinematics. Not only does the built-up beam exhibit weak-axis bending and torsion, but also it undergoes slippage in the transverse and longitudinal directions. As a result, its effective sectional properties, such as the moment of inertia and torsional constants, differ noticeably from those of an equivalent monolithic section [1.5].

Figure 1.2 illustrates a built-up beam as it progresses through the stages of lateral torsional buckling. In Stage 1, the member is shown in its undeformed state. Under the action of transverse loading, the beam undergoes transverse displacement, as depicted in Stage 2. Continued loading eventually brings the beam to the critical load level that triggers buckling (Stage 3). Once the onset buckling state is reached, the beam naturally tends toward the buckled configuration shown in Stage 4 without any additional increase in load. Throughout buckling, all plies undergo lateral displacement with a twist.

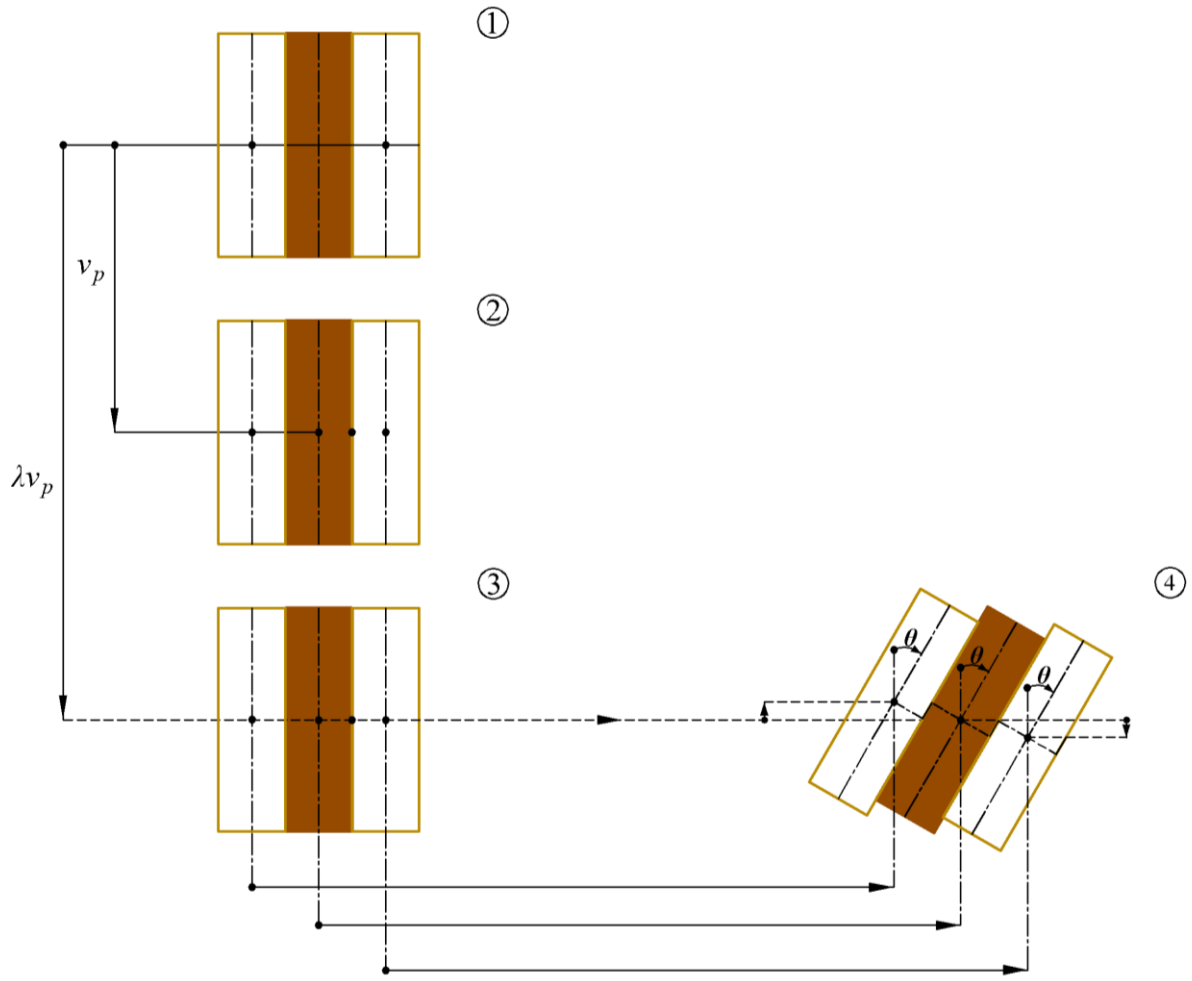

Figure 1.2 Buckling configuration of built-up beam consisting of three plies

1.3 Design Provisions

1.3.1 Canadian Standard

1.3.1.1 Treatment of monolithic sections

Under CAN/CSA-O86:19 [1.1], the LTB resistance of a laterally unbraced wooden beam subjected to bending about its major axis involves the following steps:

(1) Calculate the slenderness ratio C_B defined as

$$C_B = \sqrt{\frac{l_e d}{b^2}} \tag{1.1}$$

in which l_e is the effective length to be obtained from Table 7.4 in CAN/CSA-O86:19 [1.1], d is the section depth and b is its width.

(2) Ensure that the slenderness ratio C_B does not exceed 50.

(3) Compute the threshold slenderness $C_K = \sqrt{\left(0.97EK_{SE}K_T\right)/F_b}$ between elastic and inelastic LTB, where E is the modulus of elasticity (MPa) and the bending strength F_b is given by $F_b = f_b(K_D K_H K_{Sb} K_T)$ in which f_b is the specified bending strength, K_D is the load-duration factor, K_H is the system factor, K_{Sb} is the service-condition factor for bending, and K_T is the treatment factor.

(4) Depending on the slenderness ratio and the slenderness threshold, determine the lateral stability factor K_L from

$$K_L = \begin{cases} 1.0 & C_B \le 10 \text{ or } d/b \le 2.5 \\ 1 - \frac{1}{3}\left(\frac{C_B}{C_K}\right)^4 & 10 < C_B \le C_K \\ \frac{0.65EK_{SE}K_T}{C_B{}^2 F_b K_x} & C_K < C_B \le 50 \end{cases} \tag{1.2}$$

where K_x is the curvature factor, which is determined according to Clause 7.5.6.5.2.

(5) Determine the bending moment resistance M_r from

$$M_r = \phi F_b S K_{Zb} K_L \tag{1.3}$$

in which S is the section modulus and K_{Zb} is the size factor in bending.

Under the more recent CAN/CSA-O86:24 [1.2] the LTB resistance of laterally unsupported timber beams is determined by considering the individual unbraced segments along the member span. For a given segment, the elastic critical moment M_{cr} is given by

$$M_{cr} = \gamma C_r C_b C_l C_p \frac{\pi}{L_u} \sqrt{E_{05} I_y G_{05} J} K_{SE} K_T \tag{1.4}$$

where L_u is the unbraced segment length, E_{05} and G_{05} are the fifth-percentile modulus of elasticity and shear modulus, respectively, I_y is the moment of inertia about the weak axis, and J is the torsional constant of the cross-section. Coefficients K_{SE} and K_T are stiffness modifiers, while γ is a calibration factor that depends on the timber product type. Coefficient C_b accounts for the influence of the bending moment distribution within the unbraced segment. For general loading cases, it can be evaluated as

$$C_b = \frac{1.7 M_{\max}}{\sqrt{M_a^{\,2} + M_b^{\,2} + M_c^{\,2}}} \leq 2.5 \tag{1.5}$$

where $M_{\max}$ is the maximum absolute bending moment within the unbraced length, and M_a, M_b, and M_c are the bending moments at the quarter-point, mid-span, and three-quarter point of the unbraced segment, respectively. This factor accounts for the increase in the elastic buckling resistance when the moment diagram is non-uniform.

The load height factor C_l captures the detrimental position of gravity loads when they are applied above the shear centre of the cross-section. Loads applied above the shear center tend to destabilize

the member, while those applied below it have a stabilizing effect. The load height factor C_l can be obtained from Table 7.5 in CSA-O86:24 [1.2].

The partial torsional restraint coefficient C_r represents the degree of partial torsional restraint provided at the ends of the unbraced segment. Full restraint limits torsional rotation and increases buckling resistance, while unrestrained ends lead to reduced stability. The partial torsional restraint coefficient C_r is taken as 0.87 unless demonstrated otherwise. Coefficient C_p accounts for the pre-buckling deformation effect. For rectangular sections it takes the form

$$C_p = \frac{1}{\sqrt{1-(b/d)^2}} \tag{1.6}$$

where b and d are the width and depth of the member, respectively. This factor increases with the width to depth ratio. The pre-buckling factor C_p can conservatively be taken as 1.0. CSA-O86:24 [1.2] defines a slenderness parameter for each unbraced segment as

$$\lambda = \sqrt{\frac{L_u d}{C_l C_b C_r C_P b^2}} \tag{1.7}$$

which is then used to determine the lateral stability factor K_L from

$$k_L = \begin{Bmatrix} 1 & \text{for } \lambda \le 10 \\ 1-\frac{1}{3}\left(\frac{\lambda}{\lambda_e}\right)^4 & \text{for } 10 < \lambda_{rel,m} \le \lambda_e \\ \frac{M_{cr}}{F_b S K_x} & \text{for } \lambda_e < \lambda_{rel,m} \le 50 \end{Bmatrix} \tag{1.8}$$

where λ_e is the limiting slenderness separating inelastic and elastic buckling regions, S is the section modulus, and K_x is the curvature factor. The lateral stability factor k_L is then incorporated directly into the factored bending resistance. When lateral stability is ensured, the bending resistance is expressed as

$$M_{r1} = \varphi F_b S K_x K_{zbg} \tag{1.9}$$

whereas for laterally unsupported members, the governing resistance becomes

$$M_{r2} = \varphi F_b S K_x K_L \tag{1.10}$$

where φ is the resistance factor and K_{zbg} is the size factor for bending.

1.3.1.2 Considerations for Built-up Beams

Clause 7.5.6.3.3 in CAN/CSA-O86:19 [1.1] states "*For built-up beams consisting of two or more individual members of the same depth, the maximum (depth to width) ratio permitted in Clause 7.5.6.3.1 for laterally unsupported members may be based on the total width of the beam provided that the individual members are fastened together securely at intervals not exceeding four times the depth".* The clause suggests that, for a built-up beam, in order to determine the slenderness ratio as defined in Eq, (1.1), one would take the beam width b equal to the total width of all plies when all plies are fastened together "securely" at intervals not exceeding four times the depth. However, the standard does not provide a basis to determine whether the plies are securely attached together.

Clause 6.5.3.2.4 in the new standard CAN/CSA-O86:24 [1.2] states "*For built-up beams consisting of two or more individual members of the same depth, the lateral-stability factor, K_l, shall be determined in accordance with Clauses 6.5.3.2.1 and 6.5.3.2.2 based on individual ply width, unless demonstrated otherwise through analytical and engineering principles, documented test data, or both.".* The ambiguity of how to securely connect the plies prompted a shift in the current standard CSA O86:24 [1.2] to adopt a more conservative design provision, whereby the lateral-torsional buckling resistance of a built-up joist is evaluated as the sum of the capacities of the individual plies. This gap in the current state of knowledge flags the need for further investigation to quantify the LTB capacity while accounting for partial composite action which is one of the objectives of the present study.

1.3.2 US Standard

1.3.2.1 Treatment of monolithic sections

Obtaining the LTB capacity for a laterally unbraced wooden beam bent about its major axis, according to NDS 2024 [1.3] involves the following steps:

(1) Calculate the slenderness ratio R_B as follows:

$$R_B = \sqrt{\frac{l_e d}{b^2}} \tag{1.11}$$

where l_e is the effective length for bending members, which can be obtained from Table 3.3.3 in NDS (2024).

(2) Ensure that the slenderness ratio R_B does not exceed 50.

(3) Calculate the beam stability factor C_L from

$$C_L = \begin{cases} 1.0 & d/b \le 1 \\ \dfrac{1+\left(F_{be}/F_b^*\right)}{1.9} - \sqrt{\left[\dfrac{1+\left(F_{be}/F_b^*\right)}{1.9}\right]^2 - \dfrac{F_{be}/F_b^*}{0.95}} & d/b > 1 \,\&\, R_B \le 50 \end{cases} \tag{1.12}$$

in which F_b^* is the reference bending design stress value multiplied by all applicable adjustment factors and $F_{be} = 1.20E_{\min}'/R_b^2$ and $E_{\min}'$ is obtained from Appendix D in NDS (2024).

(4) Conduct the stress check

$$f_b \le C_L F_b^* \tag{1.13}$$

where f_b is the actual bending stress.

1.3.2.2 Limitations of US standards

The American standard NDS 2024 [1.3] does not provide guidance on obtaining the value of the beam width b in Eq. (1.11) to calculate the slenderness ratio R_B for built-up beams. The beam width b in Eq. (1.11) has two possible interpretations, either as (1) the width of a single ply and then capacity equals the number of plies times the capacity of a single ply, or (2) the total width of all plies. Therefore, the American standard [1.3] lacks clarification to obtain the LTB capacity of built-up beams.

1.3.3 European Standard

1.3.3.1 Treatment of monolithic beams

Eurocode 5 [1.4] addresses the lateral–torsional buckling resistance of timber beams through a reduction applied to the bending capacity when lateral restraints are insufficient to prevent LTB. To quantify the susceptibility of the beam to lateral–torsional instability, Eurocode introduces a

relative slenderness parameter $\lambda_{rel,m}$ that compares material strength to the elastic bending stress. This parameter is defined as

$$\lambda_{rel,m} = \sqrt{\frac{f_{m,k}}{\sigma_{crit}}} \tag{1.14}$$

where $\lambda_{rel,m}$ is the relative slenderness of the beam with respect to lateral–torsional buckling, $f_{m,k}$ is the characteristic bending strength of the timber material, and σ_{crit} is the elastic critical bending stress associated with lateral–torsional instability. The elastic critical bending stress σ_{crit} is obtained from the elastic critical moment $M_{y,crit}$ for LTB divided by the section modulus about the major axis W_y, i.e.,

$$\sigma_{crit} = \frac{M_{y,crit}}{W_y} = \frac{\pi}{W_y l_e}\sqrt{E_{0,05} I_z G_{0,05} J} \tag{1.15}$$

where l_e is the effective unbraced length of the beam that can be obtained from Table 6.1 in Eurocode 5 [1.4], I_z is the moment of inertia around the weak axis, $E_{0,05}$ and $G_{0,05}$ are the fifth percentile modulus of elasticity and shear modulus, respectively. The stability requirement for a laterally unrestrained beam is satisfied by limiting the design bending stress to a reduced design strength that accounts for lateral–torsional buckling effects. This condition is expressed as

$$\sigma_{m.d} \le k_{crit} f_{m,d} \tag{1.16}$$

where $\sigma_{m.d}$ is the design bending stress, $f_{m,d}$ is the design bending strength, and k_{crit} is the reduction factor accounting for lateral–torsional buckling. The reduction factor k_{crit} is defined in terms of the relative slenderness and reflects the transition from strength-controlled behaviour to

elastic buckling behaviour. Eurocode 5 defines this factor using the following piecewise relationship

$$k_{crit} = \begin{cases} 1 & \text{for } \lambda_{rel,m} \le 0.75 \\ 1.56 - 0.75\lambda_{rel,m} & \text{for } 0.75 < \lambda_{rel,m} \le 1.4 \\ \dfrac{1}{\lambda^2_{rel,m}} & \text{for } 1.4 < \lambda_{rel,m} \end{cases} \tag{1.17}$$

1.3.3.2 Limitations of the European standards

Eurocode 5 [1.4] does not provide guidance on incorporating the partial composite action in mechanically connected built-up beams when estimating the lateral–torsional buckling resistance. As a result, the designer must assume a specific level of composite action and then apply the standard beam-stability framework using the cross-sectional properties consistent with that assumption. In practical terms, this typically leads to bounding interpretations: either treating the member as monolithic or conservatively ignoring the interaction between plies.

1.4 Objectives

The overall objective of this thesis is to quantify the elastic lateral torsional buckling resistance of built-up wooden beams while accounting for partial composite action provided by discrete mechanical fasteners, and to translate these findings into tools suitable for design-oriented assessment. This overall objective is achieved through the following specific objectives:

1. Develop and verify a 3D finite element model for two-ply built-up wooden beams under elastic LTB which models the orthotropic behaviour of wood, discrete fasteners, and relative slip between plies.

2. Formulate a variational principle and beam finite element formulation for two-ply built-up beams. The formulation captures lateral displacement, twist, and interfacial slip mechanisms, and leads to an eigenvalue problem that efficiently predicts elastic critical moments for varying connector stiffness, spacing, moment gradient, and load height.
3. Extend the formulation to built-up beams with an arbitrary number of plies. A more general variational principle and FE formulation is to be developed. The generalized model characterizes multi-interface slip mechanisms. The resulting model provides a relatively simple means to quantify the elastic critical moment capacity of built-up beams.
4. Develop simplified, design-oriented predictive equations. Using the developed parametric database, develop dimensionless regression-based expressions that predict normalized elastic critical moments, moment-gradient factors, and load-height effects for built-up beams. The proposed equations provide a simple and universal design framework, implemented with the dimensionless parameters, that bridges the gap between advanced numerical simulations and practical design.

1.5 Thesis Outline

The thesis consists of five chapters[*] as follows:

- Chapter 1 presents the background, motivation, and objectives of the research. It discusses the limitations of current design approaches for built-up wooden beams and discusses the motivation for considering the partial interaction effect when evaluating elastic LTB resistance.

[*] Chapters 2, 3 and 4 are written in a paper format.

- Chapter 2 develops a three-dimensional finite element model for the elastic lateral torsional buckling in two-ply built-up wooden beams. The study examines the influence of fastener stiffness and spacing on buckling capacity and mode shapes.
- Chapter 3 investigates the elastic LTB behaviour of two-ply built-up wooden beams connected with discrete fasteners by developing a variational-based finite element model that captures transverse and longitudinal slip between plies as well as the shear stiffness of the fasteners. A parametric study is carried out to quantify the influence of fastener stiffness, spacing, and distribution (uniform and non-uniform), moment gradient, load height, and beam dimensions on the elastic critical moment and the level of composite action achieved in practice.
- Chapter 4 develops a general finite element formulation for predicting the elastic lateral-torsional buckling resistance of multi-ply built-up beams. The formulation captures the partial composite action between plies by considering the transverse slip, longitudinal slip, and the shear stiffness of the fasteners. It provides a unified framework applicable to any number of plies. The solution developed is validated against detailed 3D finite element models and full-scale experimental LTB tests. To characterize the behaviour of built-up systems across practical design ranges, the chapter presents a parametric study consisting of 733 runs examining the influence of key factors on the LTB resistance of built-up beams consisting of multiple plies. Using symbolic regression and the developed database, the chapter introduces practical design-oriented expressions for the normalized critical moment, the moment-gradient factors, and the load-height factor.

- Chapter 5 summarizes the main findings of the thesis, outlines the primary contributions to the understanding of elastic LTB of built-up wooden beams, and provides recommendations for future research and potential improvements to design standards.

1.6 References

[1.1] Canadian Standard Association (CSA), *CSA Standard O86-19 Engineering design in wood*. 2019.

[1.2] Canadian Standard Association (CSA), *CSA Standard O86-24 Engineering design in wood*, vol. 1, no. 1. 2024.

[1.3] American Wood Council, *National design specification for wood construction*. Leesburg, VA, USA, 2024.

[1.4] CEN, *Eurocode 5: Design of timber structures - Part 1-1: General - Common rules and rules for buildings Eurocode*, vol. 1. 2004.

[1.5] N. Challamel and U. A. Girhammar, "Lateral-torsional buckling of vertically layered composite beams with interlayer slip under uniform moment," *Eng. Struct.*, vol. 34, pp. 505–513, 2012, doi: 10.1016/j.engstruct.2011.10.004.

Chapter 2: Numerical Investigation of Elastic Lateral Torsional Buckling Behaviour of Two-Ply Built-up Wooden Beams[1]

Abstract

Current lateral torsional buckling design provisions in the Canadian wood design standard CSA O86:19 stipulate that the lateral buckling capacity of built-up beams consisting of multiple plies is equivalent to that of a solid beam with the full width of the built-up system, provided that individual plies are securely connected at intervals that do not exceed four times the depth. Within this context, the present study numerically examined the lateral torsional buckling behaviour of built-up wooden beams consisting of two lumber plies of identical depth connected together through mechanical fasteners such as nails. The analysis was conducted using 3D finite element simulation that enabled the relative slip between plies. The study investigated the effect of fastener stiffness and spacing on the elastic lateral torsional buckling resistance and corresponding mode shapes for the built-up system. Comparisons were made against the buckling resistance of a single ply and that of a solid beam with a width of both plies. The study shows that the critical moment of the built-up system is found to be significantly lower than that implied by present design provisions based on a solid beam with full width.

Keywords: Lateral torsional buckling, built-up beam, timber beam, fasteners, finite element.

[1] This chapter was published and presented in Canadian Society of Civil Engineering Annual Conference 2024 as: Mansor, M., Mohareb, M., Doudak, G. Numerical Investigation of Elastic Lateral Torsional Buckling Behaviour of Two-Ply Built-Up Wooden Beams. Proceedings of the Canadian Society for Civil Engineering Annual Conference 2024, Volume 10. Lecture Notes in Civil Engineering, vol 682. Springer, Cham, pp. 61–74. https://doi.org/10.1007/978-3-031-96767-2_6

2.1 Introduction and Scope

Built-up wooden beams consist of multiple plies of the same depth that are connected together [2.1]. Typically, these beams are made of sawn lumber or engineered wood products. The preference for using plies of a smaller dimension over the use of solid sawn beams with full width is primarily due to their availability and economic efficiency. In long and deep built-up beams without adequate lateral support, lateral-torsional buckling is a potential failure mode.

The buckling strength is greatly affected by the stiffness of the connection between plies. When using discrete fasteners that do not provide complete rigid connections, a slippage may occur between plies during buckling as shown in Figure 2.1. The transverse slippage of fasteners v_s is resisted by the transverse stiffness k_v of the fasteners and the longitudinal slippage w_s is resisted by their longitudinal stiffness k_w, while the separation between plies is resisted by the withdrawal stiffness k_u. The potential slippage between plies affects the effective sectional properties such as the torsional rigidity and the moment of inertia [2.2]. Past experimental and analytical studies on wood beams were limited to the lateral torsional buckling (LTB) of members with rectangular and I-shaped sections (e.g. [2.3], [2.4], [2.5]). Sahraei et al. [2.6] conducted analytical research on the LTB of solid rectangular sections that considers the effects of load height, pre-buckling deformation, moment gradient, and partial twist end restraints. The critical moment for built-up beams was reported to depend on the shear stiffness k_v, k_w of the fasteners but is insensitive to the withdrawal stiffness k_u if the minimum withdrawal stiffness is provided to ensure that the plies buckle in the same direction [2.7]. Yet, present design provisions for the lateral torsional buckling of built-up beams of the Canadian wood design standard CSA-O86:19 [2.1] do not reflect this dependence.

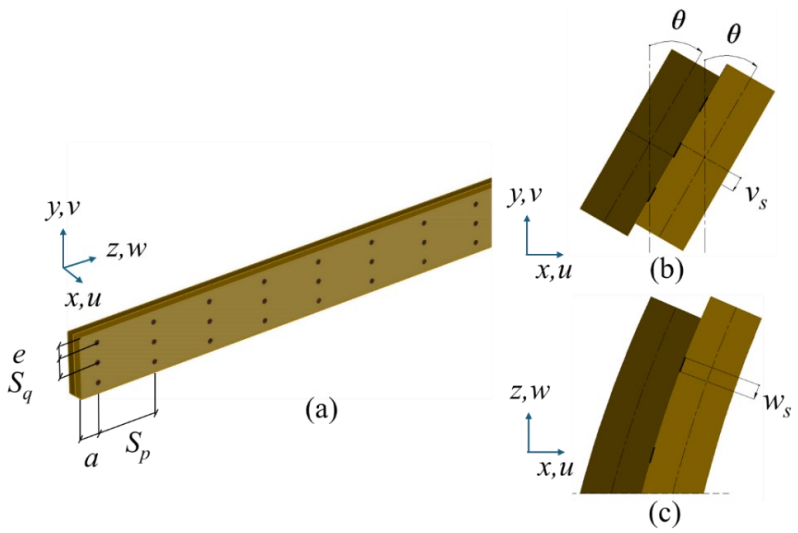

Figure 2.1 Two-ply beam (a) Undeformed 3D view (b) Deformed cross-sectional view and (c) Deformed plan view

Owing to the scarcity of relevant studies, the present study aims to evaluate the lateral torsional buckling of built-up timber beams connected together with nails through a series of 3D finite element analyses.

2.2 Reference Case

As a reference case, a built-up beam with two plies made of SPF No.1/No.2 grade sawn lumber was considered. This wood species is commonly used for built-up beams in Canada. The beam span was 5000 *mm* and each ply had dimensions of 38 *mm* × 286*mm*. The beam was simply supported relative to transverse and lateral displacements as well as twist, and the beam was subjected to a uniform moment. The plies were assumed to be fastened together using 3" common nails with 3.76 *mm* diameter. The nail length of 76 *mm* is twice the width of a single ply, and as such fully penetrates the second ply. The geometric parameters of the reference nailing pattern were spacing parallel to grain $S_p = 300mm$, end distance parallel to grain $a = 100mm$, spacing perpendicular to grain $S_q = 93mm$ and edge distance perpendicular to grain $e = 50mm$ (Figure 2.1).

These distances were chosen based on practical practices and they meet the minimum requirement of CSA-O86:19 [2.1]. The lateral and transverse stiffnesses k_v, k_w for the nail were estimated from the Eurocode 5 [2.8]* using the relationship

$$k_v = k_w = \rho_m^{1.5} d^{0.8} / 30 \tag{2.1}$$

in which k_v and k_w are in *N/mm*, ρ_m is the wood density in kg/m^3 and d the diameter in millimeters. The density of SPF-sawn lumber was taken as $\rho_m = 420\ Kg/m^3$ [2.1]. For a diameter $d = 3.76mm$, one obtains $k_v = k_w =$ 830 N/mm. The withdrawal stiffness was taken as k_u = 500 *N/mm* based on the experimental tests [2.9].

2.3 Finite Element Model Description

A 3D finite element model was developed to obtain the critical moments for two-ply built-up beam. The model was based on a linearly elastic orthotropic material characterization. The model was based on an eigenvalue analysis. As such, it omits initial out-of-straightness effects and inelastic deformations.

2.3.1 Eigenvalue Analysis

An eigenvalue buckling analysis was conducted to obtain the critical load level characterized by the critical load multiplier λ, i.e.,

$$\left([K_E] + \lambda_i [K_G]\right)\{v_i\} = 0 \tag{2.2}$$

where $[K_E]$ is the elastic stiffness matrix, $[K_G]$ is the geometric stiffness matrix induced by the loads, λ_i is the load multiplier that corresponds to the mode shape $\{v_i\}$. The critical moment $M_{cr} = \lambda_i M$, in which i corresponds to the lowest eigenvalue.

* Eurocode 5 provides Eq. (2.1) to characterize the shear stiffness for the connection between the fastener and the timber component in which it is embedded. This shear stiffness is termed as the fastener stiffness in the present study.

2.3.2 Elements and FEA Mesh

The finite element model was developed using commercial software Abaqus [2.10]. The eight-node-brick element C3D8 from the Abaqus library was chosen to model the plies of built-up beams. Element C3D8 has 8 nodes at the corners with three translational degrees of freedom per node. This element was successfully used by other studies [2.3], [2.4], [2.11] to investigate the lateral torsional buckling behaviour of wooden beams. To ensure the model accuracy, the width to depth-to-length aspect ratios of the element C3D8 have to be as close to unity as possible. A mesh study* indicated that convergence was reached when an element size of nearly 20 mm was used throughout the beam with four elements along the width of the beam, 15 elements along the depth of the beam and 250 elements along the span. In order to simulate the fasteners connecting the two plies, the two-node SPRING2 element was selected from the Abaqus library. This element connects two nodes within the model through three relative elastic springs defined along the global directions of the model. Three SPRING2 elements were used at each fastener location to represent the withdrawal stiffness k_u of the nail along the x-direction, the transverse stiffness k_v along the y-direction, and the longitudinal stiffness k_w along the z-direction.

2.3.3 Constitutive model and mechanical material properties

Wood can be considered a cylindrically orthotropic material and is characterized by twelve constitutive constants: three moduli of elasticity E_L, E_T and E_R along the longitudinal L, the tangential T, and the radial R directions and three shear moduli G_{LT}, G_{LR} G_{RT}. The model has six Poisson's ratios $\mu_{LR}, \mu_{RL}, \mu_{RT}, \mu_{TR}, \mu_{LT}$, and μ_{TL} [2.12]. However, the symmetry of the constitutive tensor requires satisfying the three constraints [2.12]:

* The details of the mesh sensitivity analysis are provided in Appendix A.

$$\mu_{ij}/E_i = \mu_{ij}/E_j,\ i \neq j, \quad i,j = L,R,T \tag{2.3}$$

therefore, the model is characterized by nine independent constants. The longitudinal modulus of elasticity E_L = 9500 *MPa* and the two shear moduli $G_{LT} = G_{LR} = E_L/16$ were taken from CSA-O86:19 [2.1]. Other properties were taken from the wood handbook [2.12] for Lodgepole Pine, a constituent species under the SPF species combinations (Column 2 of Table 2.1). Such a cylindrically orthotropic constitutive model is not supported in Abaqus. Instead, the software is equipped with a Cartesian orthotropic model, with three moduli of elasticity E_X, E_Y and E_Z along the global coordinates, three shear moduli G_{XY}, G_{XZ} and G_{XZ} and three Poisson's ratios $\mu_{XY}, \mu_{XZ}, \mu_{YZ}$. The stress-strain relationship takes the form [2.10]:

$$\begin{Bmatrix} \varepsilon_{XX} \\ \varepsilon_{YY} \\ \varepsilon_{ZZ} \\ \gamma_{XY} \\ \gamma_{XZ} \\ \gamma_{YZ} \end{Bmatrix} = \begin{bmatrix} 1/E_X & -\mu_{XY}/E_Y & -\mu_{ZX}/E_Z & 0 & 0 & 0 \\ -\mu_{XY}/E_Y & 1/E_Y & -\mu_{ZY}/E_Z & 0 & 0 & 0 \\ -\mu_{ZX}/E_Z & -\mu_{ZY}/E_Z & 1/E_Z & 0 & 0 & 0 \\ 0 & 0 & 0 & 1/G_{XY} & 0 & 0 \\ 0 & 0 & 0 & 0 & 1/G_{XZ} & 0 \\ 0 & 0 & 0 & 0 & 0 & 1/G_{YZ} \end{bmatrix} \begin{Bmatrix} \sigma_{XX} \\ \sigma_{YY} \\ \sigma_{ZZ} \\ \tau_{XY} \\ \tau_{XZ} \\ \tau_{YZ} \end{Bmatrix} \tag{2.4}$$

both constitutive orthotropic models would match when the properties along two directions (i.e., R,T or X,Y) coincide. Since the tangential and radial properties of wood are close [2.13], one can assume that $E_T \approx E_R$, $G_{LT} \approx G_{LR}$, $\mu_{LT} \approx \mu_{LR}$; thus, reducing the number of constants from nine to six. As an idealization, the Cartesian orthotropic model in Abaqus was adopted using the following simplifications $E_Z = E_L$, $E_x = E_Y = (E_R + E_T)/2$, $G_{ZX} = G_{ZY} = (G_{LT} + G_{LR})/2$, $G_{XY} = G_{RT}$, $\mu_{ZX} = \mu_{ZY} = (\mu_{LR} + \mu_{LT})/2$, and $\mu_{RT} = \mu_{XY}$ (Column 4 of Table 2.1). The transverse and longitudinal stiffnesses k_v, k_w for the nails were set to 830 *N/mm* and k_u was taken as 500 *N/mm* as mentioned in section 2.2.

2.3.4 Boundary Conditions

The beam was assumed to be simply supported at both ends relative to strong-axis bending, weak-axis bending, and twist, while being allowed to warp freely. To simulate these boundary conditions, each ply was laterally restrained at both ends, i.e., the nodes along vertical lines EF, GJ, E'F', and G'J' were restrained from lateral movement (Figure 2.2). In addition, the nodes along the horizontal lines AD and A'D' were restrained from transverse movement. Besides, both plies were restrained from longitudinal movement at one end ($z = 0$) at the centroids B' and C' but free to move longitudinally at the other end.

2.3.5 Details of Load Application

In order to apply uniform moment about the major axis, two equal compressive forces were applied at the top corner points of each ply and two equal tensile forces were applied at the bottom corner points. Additionally, longitudinal displacement equation constraints were applied between the four corner points of each ply (as master nodes) and the other nodes at the ends of each ply (as slave nodes), except the center of the ply.

Table 2.1 Constitutive parameters

Reported values[1,2]		Abaqus Input[2]	
Parameter	Tabulated values (*MPa*)	Parameter	Idealized values (*MPa*)
E_L	9500	E_Z	9500
E_T	646	E_Y	808
E_R	969	E_X	808
G_{LR}	594	G_{ZX}	594
G_{LT}	594	G_{ZY}	594
G_{RT}	64.57	G_{XY}	64.6
μ_{LR}	0.316	μ_{ZX}	0.332
μ_{LT}	0.347	μ_{ZY}	0.332
μ_{RT}	0.469	μ_{XY}	0.469

[1] SPF No.1/No.2 grade ([2.1], [2.12])

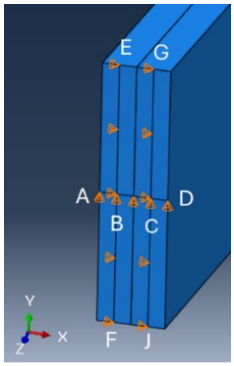

(a)

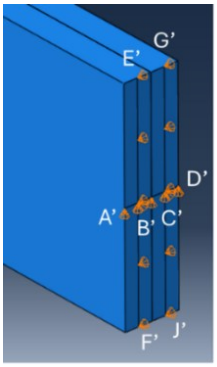

(b)

Figure 2.2 Boundary conditions (a) left end, and (b) right end

Therefore, localized deformations at both ends were successfully suppressed while maintaining consistency with the kinematics of the Vlasov beam [2.14] forming the basis of the classical lateral torsional buckling solution [2.15]. Under the Vlasov's theory [2.14], the longitudinal displacement w of a point (x, y) in a rectangular section z is

$$w(x,y,z) = \zeta(z) - \xi'(z)x - \eta'(z)y - \beta'(z)xy \tag{2.5}$$

where ζ, ξ and η are the longitudinal, lateral and transverse displacements of the center of the section respectively, β is the angle of twist, and all primes represent the derivative with respect to the longitudinal coordinate. By applying Equation (2.5) at the four corners points ($i = 1$ through 4) of each ply with coordinates (x_i, y_i), the longitudinal displacements of the corner points are:

$$\begin{Bmatrix} w_1(l_e) \\ w_2(l_e) \\ w_3(l_e) \\ w_4(l_e) \end{Bmatrix} = \begin{bmatrix} 1 & x_1 & y_1 & x_1y_1 \\ 1 & x_2 & y_2 & x_2y_2 \\ 1 & x_3 & y_3 & x_3y_3 \\ 1 & x_4 & y_4 & x_4y_4 \end{bmatrix} \begin{Bmatrix} \zeta(l_e) \\ \xi'(l_e) \\ \eta'(l_e) \\ \beta'(l_e) \end{Bmatrix} \tag{2.6}$$

by solving Equation (2.6) for the displacements $\langle \zeta(l_e) \quad \xi'(l_e) \quad \eta'(l_e) \quad \beta'(l_e) \rangle$ and substituting in Equation (2.5), one obtains

$$w(l_e,x,y)-\langle 1 \quad x \quad y \quad xy\rangle \begin{bmatrix} 1 & x_1 & y_1 & x_1y_1 \\ 1 & x_2 & y_2 & x_2y_2 \\ 1 & x_3 & y_3 & x_3y_3 \\ 1 & x_4 & y_4 & x_4y_4 \end{bmatrix}^{-1} \begin{Bmatrix} w_1(l_e) \\ w_2(l_e) \\ w_3(l_e) \\ w_4(l_e) \end{Bmatrix} = 0 \qquad (2.7)$$

Equation (2.7) provides the relationship between the longitudinal displacement of the corner points and the longitudinal displacement of any other point at the end of the ply, except the center of the ply. This condition was applied using the Equation constraint feature of Abaqus.

2.3.6 Modelling Interface between Plies

Two methods were used to model the interaction at the interface of the two plies, i.e., the finite slide approach and the lateral displacement constraint approach.

2.3.6.1 Finite Sliding Model

Under this method, the interaction between the interface was modelled using the finite sliding, surface to surface contact feature in Abaqus [2.10]. This feature enables sliding between two surfaces in contact. The hard contact pressure over-closure sub-feature was adopted to prevent penetration between surfaces (Figure 2.3).

2.3.6.2 Lateral Displacement Constraint Model

In this method, the two plies were modelled separately while introducing a small gap between them. To ensure compatibility, the lateral displacements of adjacent nodes of both plies at the interface were coupled using a built-in coupling kinematic constraint feature in Abaqus Figure 2.4. Transversely and longitudinally, the two nodes were connected through relative springs.

2.4 Verification

The critical moment M_u [2.15] of a simply supported beam under a uniform moment is

$$M_u = (\pi/L_u)\sqrt{EI_yGJ + (\pi E/L_u)^2 I_y C_w} \quad (2.8)$$

where I_y is the moment of inertia about the weak axis, L_u is the unbraced length between lateral and torsional supports, G is the shear modulus, the Saint-Venant torsional constant J is given by $J = kdb^3$ where k is a constant that depends on the cross section aspect ratio [2.16], and the warping

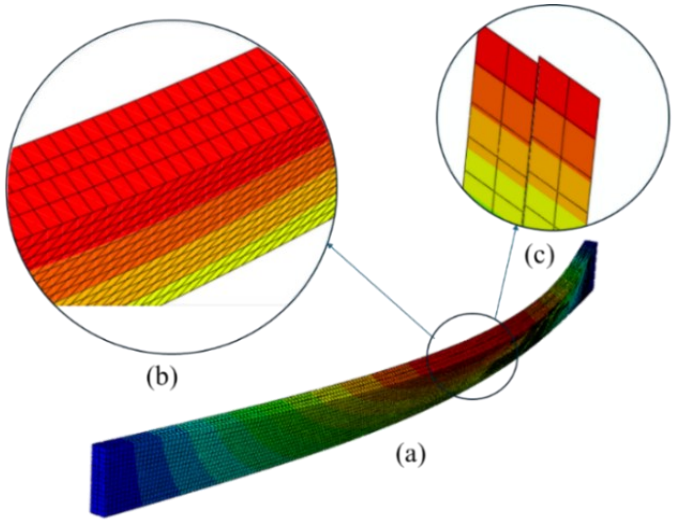

Figure 2.3 (a) Buckling mode of a built-up beam modeled with a finite sliding contact surface, (b) relative longitudinal slip between both plies looking from top b, and (c) cross-sectional view showing relative vertical slip between both plies

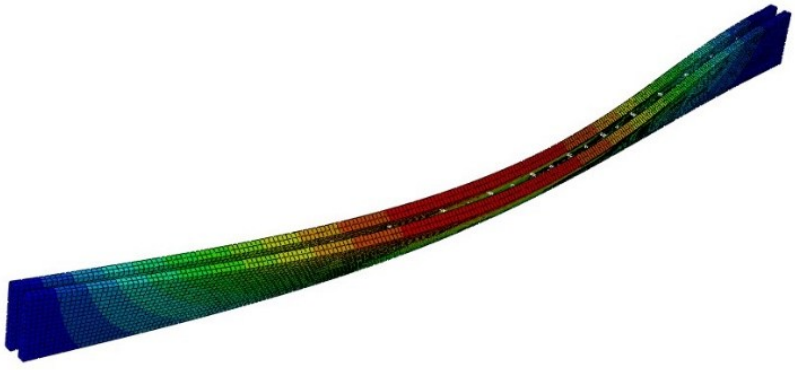

Figure 2.4 Buckling mode of a built-up beam modelled with lateral displacement constraint Model

constant C_w for a rectangular section is given by $C_w = \int_A (xy)^2 \, dA = b^3 d^3 / 144$. The elastic critical moment of the reference beam was predicted by the finite element model. Two cases were considered for verification against the theoretical solutions: 1) a non-composite beam with no springs between both plies which was compared to twice the theoretical solution of a single ply of the reference beam that has $I_y = 1.3 \times 10^6 \, mm^4$, $J = 4.8 \times 10^6 \, mm^4$ and $C_w = 8.91 \times 10^9 \, mm^6$ (Table 2.2). 2) a monolithic beam in which the connection at the interface between both plies was assumed to be rigid. Thus, SPRING2 relative spring elements were placed between each pair of nodes on the interface with the reference stiffnesses value $k_w = k_v = 830 \; N/mm$. For the finite sliding model, the withdrawal stiffness was taken as $k_u = 500 \; N/mm$. The results were compared to the theoretical solution of a solid beam with the full width with sectional properties $I_y = 10.5 \times 10^6 \, mm^4$, $J = 34.5 \times 10^6 \, mm^4$ and $C_w = 71.3 \times 10^9 \, mm^6$. Close agreement was observed between FE and the theoretical solutions (Table 2.2).

Table 2.2 Comparison between FE and classical solutions

Case	Connection between plies	Critical Moment (*kNm*)			Ratio	
		FE lateral constraint [1]	FE finite sliding [2]	Classical Solution [3]	$\frac{[1]}{[3]}$	$\frac{[2]}{[3]}$
Non-composite	No springs	7.05	7.05	7.51	0.939	0.939
Monolithic	Continuum connection	28.2	28.3	28.6	0.986	0.989

2.5 Parametric Study

2.5.1 Effect of fastener stiffness k_w and k_v

The effect of the fastener stiffness was investigated by varying stiffness $k_v = k_w$ to take the values from 10 to 10^8 for three nailing patterns corresponding to the reference spacing, the minimum

spacing for connections as specified in CSA-O86:19 [2.1], and a continuum connection in which all nodes on the interface were connected (Table 2.3). In this case, for a given $k_v = k_w$, the total stiffness $nk_v = nk_w$ differs for the three spacings considered because the total number of fasteners n varies for each spacing. The critical moment and mode shape predictions of finite sliding and lateral displacement constraint techniques are observed to be in close agreement (Figure 2.5, Figure 2.6).

Table 2.3 Nailing patterns (*mm*)

Cases	Spacing parallel to grain *Sp*	End dist. parallel to grain *a*	Spacing normal to grain *Sq*	Edge distance normal to grain *e*
Reference Spacing	300	100	93	50
Minimum Spacing	80	60	45	30
Continuum conn.[1]	20	20	20	20

[1]based on element size

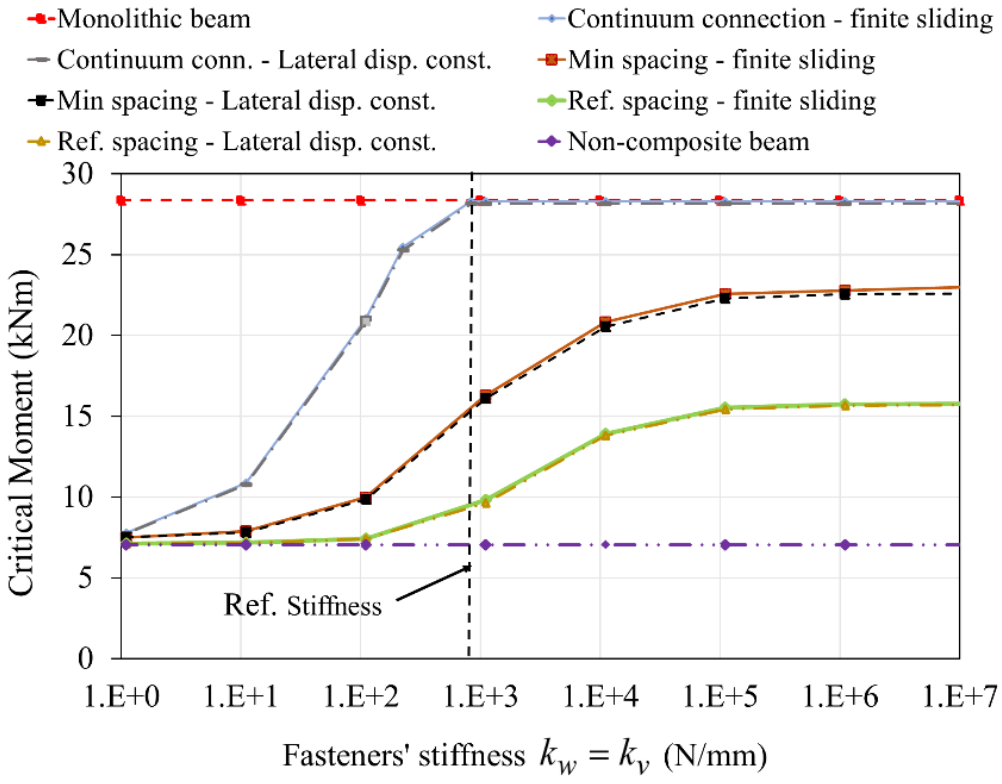

Figure 2.5 Critical moment vs fasteners' stiffness

The Canadian wood design standard CSA-O86:19 [2.1] requires the longitudinal spacing between fasteners not to exceed four times the ply depth for a beam to be considered as monolithic when determining its lateral torsional buckling resistance. Although the chosen reference nailing pattern has a longitudinal spacing of 300 *mm*, which represents quarter the standard requirement ($4d$ = 1144 *mm*), and for the reference nail stiffness $k_v = k_w = 830 N/mm$, the critical moment of the reference beam was found to be only 33% of that of the monolithic beam with the same cross-sectional geometry. Also, for the minimum spacing scenario, the critical moment increases only to 55% of that of a monolithic beam, signaling the unconservative nature of the standard in this case. Under both nailing patterns, the monolithic critical moment resistance is found unattainable. This stems from the fact that using flexible fasteners to connect both plies with the allowed spacings in the design provisions does not fully prevent the slip at the interface between the plies.Among the three considered cases, only the continuum connection enables the system to reach the critical moment of the monolithic beam (Figure 2.5) corresponding to a nail spacing much less than the minimum specified value in CSA-O86:19 [2.1].

2.5.2 Effect of the total fastener stiffness nk_w and nk_v

Three nail spacings were considered, two of them were the reference and the minimum spacings which were considered in section 2.5.1. The third one was based on the maximum spacing as per CSA-O86:19 [2.1] in which the spacing parallel to grain S_p was increased to four times the depth $4d$ while the perpendicular to grain spacing S_q remained the same as the reference spacing. Unlike Section 2.5.1 in which $k_w = k_v$ was kept constant for a specified stiffness value, the present section adjusted the individual fastener stiffness so as to keep constant the target total stiffness $nk_w = nk_v$ for the three considered nail spacings (Table 2.4, Figure 2.7). For a target total stiffness

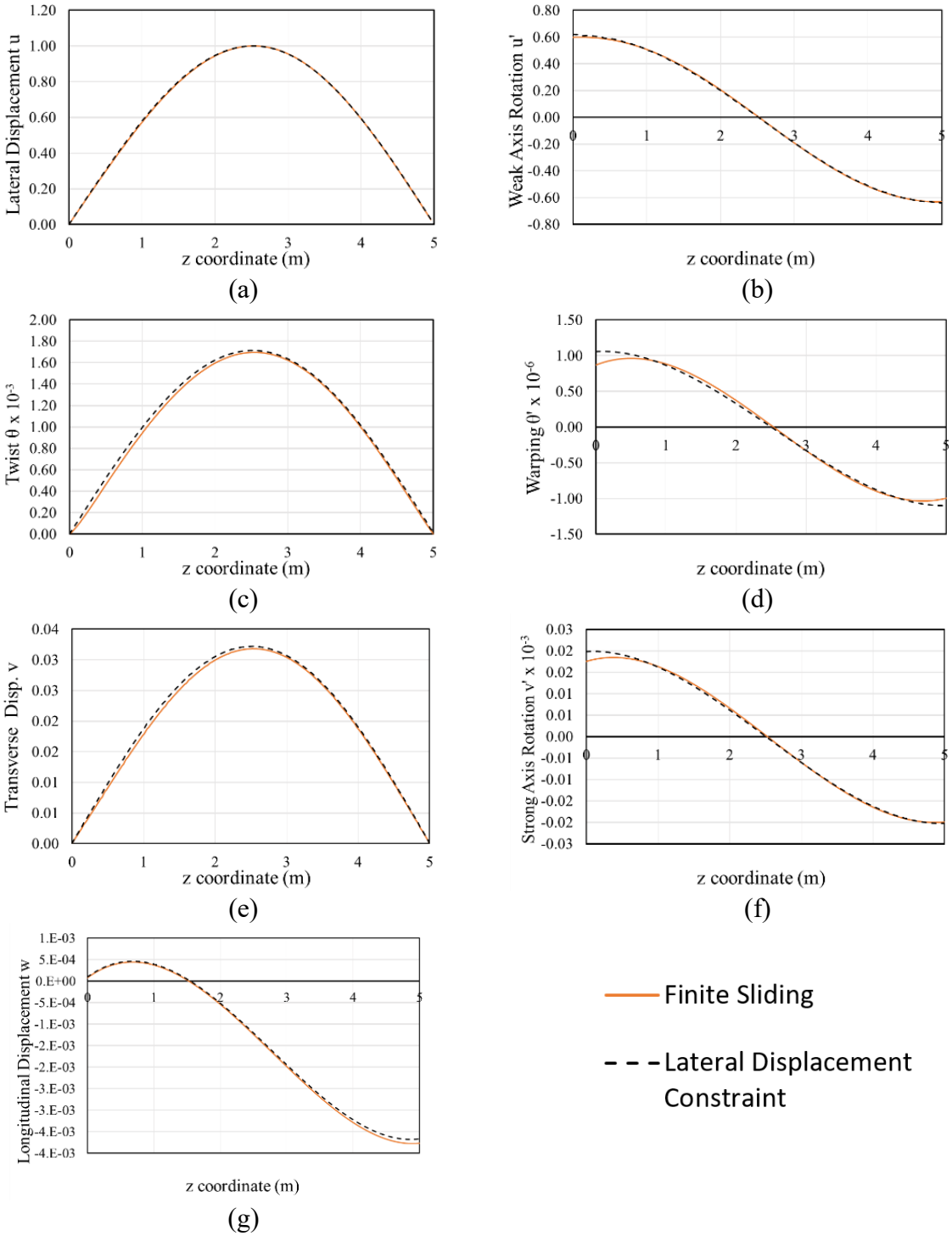

Figure 2.6 Normalized Mode Shapes for the reference beam (a) lateral displacement; (b) weak-axis rotation; (c) twist; (d) warping; (e) transverse displacement; (f) strong axis rotation; and (g) longitudinal displacement. All mode shapes have been normalized relative to the peak lateral displacement.

of $nk_w = nk_v = 10^2$, as an example, one had 455 fasteners for the case of minimum spacing with a stiffness of 0.22 *N/mm* per fastener. For the same target total stiffness, the reference spacing had a total of 51 nails with a higher stiffness of $k_v = k_w = 1.96$ *N/mm* such that both cases maintained the same total stiffness $nk_w = nk_v = 10^2$. As the difference between the finite sliding and lateral displacement approaches was shown to be negligible in Section 2.5.1, only the finite sliding approach was used in this section. Figure 2.7 shows that the critical moment corresponding to the minimum spacing is higher than the other two cases, i.e., signaling that, for a target total stiffness $nk_w = nk_v$, the increase in the number of fasteners is more favourable, in increasing the lateral torsional buckling capacity, than increasing the stiffness of the fastener.

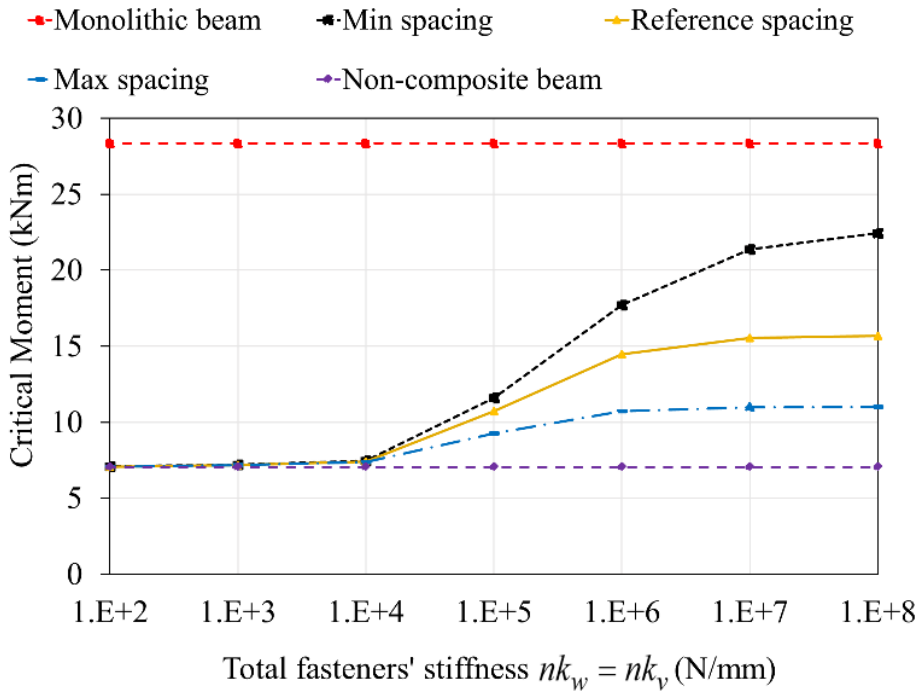

Figure 2.7 Critical moment vs total fasteners' stiffness

Table 2.4 Nailing Details

nk_w & nk_v N/mm	Min Spacing		Ref. Spacing		Max Spacing	
	n	k_v & k_w N/mm	n	k_v & k_w N/mm	n	k_v & k_w N/mm
10^2	455	2.2E-1	51	1.96E+0	15	6.67E+0
10^3	455	2.2E+0	51	1.96E+1	15	6.67E+1
10^4	455	2.2E+1	51	1.96E+2	15	6.67E+2
10^5	455	2.2E+2	51	1.96E+3	15	6.67E+3
10^6	455	2.2E+3	51	1.96E+4	15	6.67E+4
10^7	455	2.2E+4	51	1.96E+5	15	6.67E+5
10^8	455	2.2E+5	51	1.96E+6	15	6.67E+6
10^9	455	2.2E+6	51	1.96E+7	15	6.67E+7

2.6 Summary and Conclusions

A 3D finite element model was developed for built-up wooden beams consisting of two lumber plies connected using mechanical fasteners to predict their elastic lateral torsional buckling analysis. A parametric study was conducted to examine the effect of fastener stiffness and spacing on the critical moment. The main conclusions drawn from the study are:

1- For the reference beam considered, the critical moment of built-up beams with common spacings and fastener stiffnesses is significantly lower than that of the monolithic beam. The critical moment of a beam with a fastener spacing equal to a quarter of the maximum spacing allowed by CSA O86:19 [2] is around 33% of that of a monolithic beam with full width. Using the minimum nail spacing, the critical moment leads to a capacity of 55% of the monolithic capacity.

2- For a target total fastener stiffness, reducing the spacing between fasteners (i.e., increasing the number of fasteners) is a more effective measure to increase the lateral torsional buckling capacity than increasing the stiffness of the individual fasteners.

3- The present pilot study suggests that present design rules in design standards may need to be revised to account for the effect of fastener spacing and stiffness on the predicted critical

moments. Further analytical and experimental studies are needed prior to developing such criteria.

2.7 References

[2.1] Canadian Standard Association (CSA), *CSA Standard O86-19 Engineering design in wood*. 2019.

[2.2] N. Challamel and U. A. Girhammar, "Lateral-torsional buckling of vertically layered composite beams with interlayer slip under uniform moment," *Eng. Struct.*, vol. 34, pp. 505–513, 2012, doi: 10.1016/j.engstruct.2011.10.004.

[2.3] Q. Xiao, G. Doudak, and M. Mohareb, "Numerical and experimental investigation of lateral torsional buckling of wood beams," *Eng. Struct.*, vol. 151, pp. 85–92, 2017, doi: 10.1016/j.engstruct.2017.08.020.

[2.4] Y. Hu, M. Mohareb, and G. Doudak, "Lateral Torsional Buckling of Wooden Beams with Midspan Lateral Bracing Offset from Section Midheight," *J. Eng. Mech.*, vol. 143, no. 11, pp. 1–13, 2017, doi: 10.1061/(asce)em.1943-7889.0001359.

[2.5] Y. Du, M. Mohareb, and G. Doudak, "Nonsway Model for Lateral Torsional Buckling of Wooden Beams under Wind Uplift," *J. Eng. Mech.*, vol. 142, no. 12, 2016.

[2.6] A. Sahraei, P. Pezeshky, M. Mohareb, and G. Doudak, "Simplified expressions for elastic lateral torsional buckling of wooden beams," *Eng. Struct.*, vol. 174, no. February, pp. 229–241, 2018, doi: 10.1016/j.engstruct.2018.07.042.

[2.7] G. Robatmili, Robabeh, Du, Yang and Doudak, "Effect of fastener stiffness on buckling behaviour of wooden built-up beams," *CSCE 2022 Annu. Conf. Whistler, Br. Columbia*, 2022.

[2.8] CEN, *Eurocode 5: Design of timber structures - Part 1-1: General - Common rules and*

rules for buildings Eurocode, vol. 1. 2004.

[2.9] L. A. Winistorfer, S.G. and Soltis, "Lateral and Withdrawal Strength of Nail Connections for Manufactured Housing," *J. Struct. Eng.*, vol. 120, no. 12, pp. 3577–3594, 1994.

[2.10] Simulia, "Abaqus/CAE," 2016, *ABAQUS analysis user's manual*.

[2.11] Y. Hu, M. Mohareb, and G. Doudak, "Effect of Eccentric Lateral Bracing Stiffness on Lateral Torsional Buckling Resistance of Wooden Beams," vol. 18, no. 02, pp. 1–34, 2018.

[2.12] FPL, *Wood Handbook*, 2010th ed. Madison, USA, 2010.

[2.13] B. J. F. Davalos, A. Member, J. R. Loferski, and V. Yadama, "Transverse Isotropy Modelling of 3-D glulam timber beams," *ASCE*, vol. 3, no. 2, pp. 125–139, 1991.

[2.14] Vlasov, *Thin walled elastic beams*, Second edn. Israel Program for Scientific Translations, 1961.

[2.15] S. P. and G. Timoshenko, *Theory of Elastic Stability*, 2nd ed. New York: New York, Mcgraw-Hill, 1961.

[2.16] A. P. BORESI and R. J. SCHMIDT, *Advanced Mechanics of Materials*, 6th Ed. New York: Wiley, 2003.

2.8 Notation

The following symbols are used in the paper:

A: Cross sectional Area

a: End distance of fasteners.

b: Ply width.

d: Ply depth.

E: Young's modulus of timber.

E_X, E_Y and E_Z: Three moduli of elasticity along the global coordinates X, Y, Z.

E_L, E_T and E_R: Three moduli of elasticity along the longitudinal L, the tangential T, and the radial R directions in Abaqus.

e: Edge distance

G: Shear modulus of timber.

G_{XY}, G_{XZ} and G_{YZ}: Three shear moduli on the three global faces of the beam XY, XZ, YZ.

G_{LT}, G_{LR} G_{RT}: Three shear moduli on the three main faces LT, LR, RT in Abaqus.

I_x: Major-axis moment of inertia.

I_y: Minor-axis moment of inertia.

J: Saint-Venant torsional constant of a single ply.

j: Fastener index within a fastener group.

k : Constant depending on the cross-sectional aspect ratio used in torsional constant expressions.

k_u : Fastener withdrawal stiffness

k_v : Fastener transverse stiffness

k_w : Fastener longitudinal stiffness

K_E : Elastic stiffness matrix

K_G : Geometric stiffness matrix

L : Span of the built-up beam.

M : Bending moment of the beam.

M_{cr} : Elastic lateral–torsional buckling critical moment.

M_{cru} : Uniform critical moment of the built-up beam

S_P : Longitudinal fastener spacing (parallel to the grain).

S_q : Transverse fastener spacing (perpendicular to the grain).

u : Lateral displacement of the plies during buckling.

v :Transverse displacement of ply during buckling.

w : Longitudinal displacement of ply during buckling.

y : Transverse coordinate across the beam.

z : Longitudinal coordinate along the beam axis.

λ : Load multiplier to be determined from the buckling analysis.

ρ_m : Mean wood density.

θ : Angle of twist of the built-up beam.

ζ , ξ , η and β : The Vlasov theory displacements in the longitudinal, lateral and transverse directions and Vlasov angle of twist respectively.

$\mu_{XY}, \mu_{XZ}, \mu_{YZ}$: Three major Poisson's ratios on the three global faces of the beam XY, XZ, YZ.

$\mu_{LR}, \mu_{RL}, \mu_{RT}, \mu_{TR}, \mu_{LT}$, and μ_{TL} : Six Poisson's ratios in Abaqus.

Chapter 3: Elastic lateral torsional buckling of two-ply built-up wooden beams connected with discrete fasteners[1]

Abstract

The present study investigates the elastic lateral torsional buckling of built-up wooden beams formed by two plies of equal depth connected through fasteners at their vertical interface. Towards this goal, the study develops a variational principle for the problem and then develops a finite element formulation, leading to an eigenvalue problem. The formulation captures the transverse, longitudinal slippage between both plies and the shear stiffness provided by the fasteners at the interface. A systematic parametric study is then conducted to investigate the effect of the fasteners' stiffness, their distribution, moment gradient, load height, and beam dimensions on the resulting elastic critical moment. The model provides a basis to quantify the level of the composite action achieved by various nailing patterns and stiffnesses and their effect on the lateral torsional buckling capacity of two-ply built-up beams. The study then explores the effect of uniform and non-uniform nail patterns in a bid to optimize the design of built-up beams. The study shows that the critical moment of built-up beams with fastener spacings conforming with the Canadian Standards requirements is considerably lower than that of a monolithic beam with identical total width.

Keywords: Lateral torsional buckling, built-up wooden beam, fasteners, nails, slip, connection stiffness, finite element.

[1] This chapter was published as: Mansor, M., M. Mohareb and G. Doudak (2025). "Elastic lateral torsional buckling of two-ply built-up wooden beams connected with discrete fasteners." Engineering Structures, 331: 119944.

3.1 Introduction

Built-up wooden beams consist of multiple plies with the same depth that are connected using mechanical fasteners such as nails or screws (Figure 3.1). Such plies are commonly made from sawn lumber or engineered wood products. Built-up beams are considered an economic alternative to solid beams since small wood plies are more available and economical than larger timber sections. As is the case for monolithic beams, the lateral torsional buckling (LTB) typically governs the resistance of long-span unbraced built-up beams. The level of the composite action achieved by the built-up beams is expected to depend on the shear stiffness, spacing, and arrangement of the fasteners connecting the plies. A lower fastener shear stiffness and large spacing between fasteners offer limited interaction between plies resulting in a weak composite action. In this case, the critical moment of the assembly is expected to approach that of the sum of the critical moment capacities of each ply. Conversely, a higher connection stiffness and narrow spacing between fasteners offer significant interaction between plies resulting in a strong composite action. In such a case, the critical moment of the assembly may approach that of a monolithic beam with a total width equal to the sum of the widths of the plies. The Canadian wood design standard CSA O86:19 [3.1] enables designers to adopt the monolithic capacity, provided that the plies are securely fastened together at an interval of four times the ply depth but does not provide guidance on the required shear stiffness for the fasteners to attain the securely fastened condition. Guidance is also missing on this topic in the American and European wood design standards [3.2], [3.3]. Within this context, the present study developed a variational principle and finite-element formulation that quantifies the elastic lateral torsional buckling capacity of built-up beams consisting of two plies connected with discrete fasteners. The present study investigated the effect of the fasteners' stiffness, their distribution, and beam dimensions on the elastic LTB

resistance of built-up beams under different load patterns, and load heights. The study also investigated the effect of uniform and non-uniform nail patterns on the critical moment.

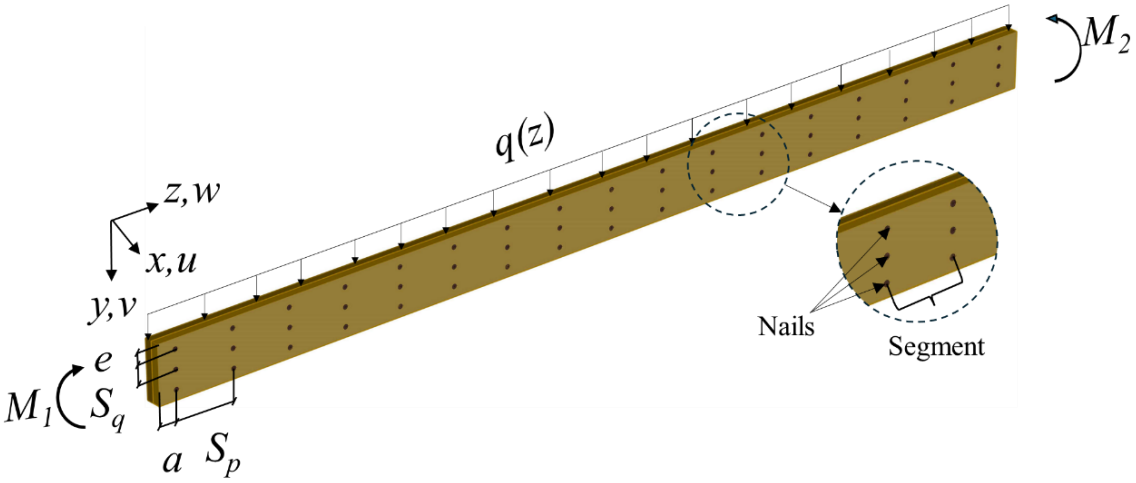

Figure 3.1 Two-ply beam loading and geometry[*]

3.2 Literature Review

The lateral torsional buckling for wood beams has been investigated in several studies including the experimental work of Hooley and Madsen [3.4] on the LTB behavior of wooden beams with rectangular monolithic cross-sections. The study then used the results to develop design formulas for the elastic and inelastic LTB capacity. Hindman et al. [3.5] performed an experimental study to investigate the LTB behaviour of unbraced cantilevers; in addition, Hindman et al. [3.6] studied the lateral-torsional buckling of I-joists. Xiao et al. [3.7] carried out a full-scale experimental study on the elastic LTB of simply supported beams with rectangular cross-sections. A 3D model was developed and verified with the results of the experimental study and then used to assess the European provisions [3.3] for the LTB of wooden beams.

[*] The origin of the local coordinate system for each ply is located at the ply centroid.

St-Amour and Doudak [3.8] conducted experimental tests on I-joist and developed a 3D FE model using material properties and initial imperfections obtained from the experimental tests. Pelletier and Doudak [3.9] experimentally investigated the LTB of wooden I-joists with realistic boundary conditions such as commercial joist hangers. A reduction factor to the critical moment was proposed when using joist hangers. Also, a 3D model was conducted to investigate the effect of the initial imperfections on the non-linear behavior of the I-joists. Töpler and Kuhlmann [3.10] investigated experimentally and numerically the effect of geometric imperfections and shear stresses from torsion on the LTB behavior of glulam beams. In addition, several analytical studies investigated the LTB of wooden beams such as Du et al. [3.11] who developed analytical and numerical non-sway models for the LTB of wooden beams under wind uplift. The study assessed the effect of the restraints provided by the deck boards on the LTB capacity of a twin beam without a sway. Du et al. [3.12] then provided a formulation for the problem that captures the sway effects by modelling the deck boards as continuous partial lateral and torsional restraints. Du et al. [3.13] complemented the previous studies by providing a finite element formulation that captures the rotational flexibility that is provided by the connections between the deck and the beams and then quantifies the buckling capacity for the beam-deck systems. Sahraei et al. [3.14] analytically investigated the LTB of wooden beams with rectangular sections and developed a formulation that considers the effects of moment gradient, load height, pre-buckling deformation and partial twist end restraints. Based on the study of Sahraei et al. [3.14], Doudak et al. [3.15] proposed a design procedure to determine the elastic LTB capacity for beams with single and multi-segments.

The lateral-torsional buckling behaviour of built-up beams is closely related to the load-slip behaviour of fasteners connecting wood plies. The load-slip relationship was investigated for single and group of fasteners by several studies. Ribeiro and Pellicane [3.16] experimentally

investigated the load-slip behavior of nailed joints. Girhammar and Gopu [3.17] conducted first and second-order analyses for composite timber beam-columns. Mascia et al. [3.18], [3.19] analytically and experimentally investigated the slip modulus for plywood timber beams. The fastener response was idealized based on beam on elastic foundation approach.

While the above studies were limited to the LTB of monolithic beams and slip modulus of fasteners, only a few studies focused on the LTB of built-up beams consisting of multiple plies. Miller and Bulleit [3.20] experimentally and analytically investigated the LTB of built-up beams with horizontal laminations that are connected with inclined and square shear keys. The study indicated that the stiffness of the shear keys has a significant effect on the capacity of the built-up beam. Challamel and Girhammar [3.21] developed an analytical solution for the LTB of built-up beams with two vertical plies. The study considered a pinned-pinned beam under a uniform moment. The study assumed sinusoidal displacement functions along the beam for all displacements (transverse, rotational, longitudinal displacements). In addition, the study assumed that both plies were connected with a continuous shear layer as glue with uniformly distributed stiffness per unit area [N/mm^2] which is different from the case of the present study where the plies are assumed to be connected through discrete fasteners with stiffness per unit length k [N/mm] and subjected to different load patterns and load heights. Robatmili et al. [3.22] and Robatmili [3.23] investigated the LTB of built-up beams consisting of multiple vertical plies connected together by nails and screws. The studies included an experimental test to determine the shear stiffness of the nails and screws, followed by a 3D finite element (FE) buckling analysis to characterize the elastic LTB resistance of the beam. The studies showed that the LTB capacity of built-up beams is influenced by the transverse and longitudinal stiffness of the mechanical fasteners, but not by their withdrawal stiffness, given that the withdrawal stiffness is sufficient to keep both plies in contact.

None of the previous studies provided a beam formulation to quantify the elastic lateral torsional buckling capacity of built-up wooden beams consisting of vertical plies connected together using fasteners.

3.3 Statement of the Problem

A built-up wooden beam consists of two plies that are subdivided into n_e segments. Both plies are connected at the interfaces of the segments by $i = 1,2...n = n_e - 1$ groups of fasteners, each group being located at the longitudinal coordinate z_i. Fastener group i consists of $j = 1,2....n_i$ fasteners located at a height $y_{i,j}$ below the shear center of the beam (Figure 3.1). Each ply is subjected to a transverse loading $q(z)$ at a height $y_q(z)$ measured from the shear center, and/or end moments M_1 at $z = 0$ and M_2 at $z = L$. The present study aims to develop a variational principle that governs the elastic lateral torsional buckling behaviour of built-up beams consisting of two plies connected by fasteners and then develop a finite element formulation for the problem. The solution is primarily intended to characterize the LTB capacity of slender built-up beams whose strength is governed by the elastic critical moment.

3.4 Assumptions

The assumptions of the present study are:

1. Warping effects within both plies are omitted as past studies (e.g., [3.7], [3.24], [3.25], [3.26]) have shown that omitting the warping stiffness slightly underestimates the lateral torsional buckling capacity of rectangular sections.
2. The wood constitutive model is fully characterized by Young's modulus in the longitudinal direction and the shear modulus on the transverse plane. Other constants of orthotropic

constitutive models were shown to have a negligible effect on the lateral torsional buckling resistance [3.27].

3. The present study assumes that the beam cross-section displaces and twists but does not deform in its own plane, i.e., it omits cross-sectional distortion (e.g., [3.13], [3.24])
4. Pre-buckling deformation effects are omitted. For rectangular cross-sections with a minor to a major moment of inertia ratio I_y/I_x less than 1/13, it was shown in [3.14] that the omission of pre-buckling effects would underpredict the critical moment by less than 4%.
5. As transverse loads in timber beams are frequently offset from the beam shear center, the formulation accounts for the load height effect.
6. As a simplification, the stiffness of the fasteners k is assumed to be identical in the transverse direction (along y axis) and the longitudinal direction (along z axis) as stated in Eurocode 5 [3.3]. This condition is approached in situations where the connectors are relatively small in diameter and applied without pre-drilling, the effect of grain direction becomes less pronounced as reported in the experimental work of Soltis et al. [3.28]. This is in part because the mechanism of failure is dominated in this case by fastener yielding rather than wood crushing.
7. The friction between both plies is neglected. The contribution of friction is assumed negligible due to wood shrinkage and the inability of typical fasteners (e.g., nails, fully threaded screws) to exert significant normal pressure between plies. Previous analytical solutions (e.g.[3.20]) that omitted the friction contribution attained close agreement with the experimental results.

8. The present formulation is based on moderate displacements and rotations, e.g., for the angle of twist θ by adopting the approximations $\sin\theta \approx \tan\theta \approx \theta$ and $\cos\theta \approx 1-\theta^2/2$ and omitting second-order terms related to the kinematics of the fasteners.
9. The mean values of the density, modulus of elasticity, and shear modulus were adopted in the analysis.

3.5 Kinematics

3.5.1 Beam Kinematics

Figure 3.2 depicts the system in the undeformed state prior to loading (Stage 1). Under reference loads $q(z)$ M_1 M_2, the system is assumed to undergo a transverse displacement $v_p(z)$ (Stage 2), the loads are then assumed to increase by a factor λ to attain the state of onset of bucking (Stage 3). At this state, the system has a tendency to undergo lateral torsional buckling to reach the buckled state (Stage 4) characterized by a common angle of twist $\theta(z)$, lateral displacements $u_1(z)$ for ply 1, and $u_2(z)$ for ply 2, both defined as positive along the positive x direction. Unlike the classical solution for a monolithic beam in which the beam displaces only laterally, the present two-ply system will undergo additional transverse and longitudinal displacements, i.e., ply 1 undergoes a transverse displacement $v_1(z)$ and longitudinal displacement $w_1(z)$ while ply 2 undergoes a transverse displacement $v_2(z)$ and longitudinal displacement $w_2(z)$. Both $v_1(z)$, $v_2(z)$ are defined as positive along the positive y direction and $w_1(z)$, $w_2(z)$ are taken as positive along the positive z direction.

Figure 3.2 depicts the buckling deformation of the system. The lateral displacement u_2 for ply 2 can be expressed in terms of the lateral displacement u_1 for ply 1 from the relation $u_2 - u_1 = \overline{A''G''} - 2c$ in

which $\overline{A''G''}$ is the length of the line segment between A'' and G'' as depicted in Figure 3.2 and c is the half ply-width (as defined in view 1 of Figure 3.2). Therefore, the difference between the lateral displacements of both plies $u_2 - u_1$ can be expressed as $u_2 - u_1 = \overline{A''F''} - \overline{G''F''} - 2c$. From the triangle $A''E''F''$, one has $\overline{A''F''} = 2c/\cos\theta$ and from the triangle $C''G''F''$, one has $\overline{G''F''} = (v_2 - v_1)\tan\theta$, yielding the relation $u_2 - u_1 = 2c/\cos\theta - (v_2 - v_1)\tan\theta - 2c$. By adopting the small rotation assumption where $\tan\theta \approx \theta$ and $1/\cos\theta \approx 1 + (\theta^2/2)$, the relation can be simplified to

$$u_2 \approx u_1 + c\theta^2 - (v_2 - v_1)\theta \tag{3.1}$$

i.e., displacements u_1 and u_2 differ by the second order term $c\theta^2 - (v_2 - v_1)\theta$ which is negligible compared to u_1; thus, the approximation $u \approx u_2 \approx u_1$ will be adopted in this paper. In addition, the longitudinal and the transverse displacements of the two plies are equal and opposite (Appendix A), i.e.,

$$v_1(z) = -v_2(z) = v(z) \qquad w_1(z) = -w_2(z) = w(z) \tag{3.2a-b}$$

3.5.2 Fastener Kinematics

At stage 4, the relative tangential displacement $v_{s,i}$ (Figure 3.2.a) of a shear connector located at the longitudinal coordinate z_i and height $y_{i,j}$ at the vertical interface between both plies is obtained by tracking the displacement of point D relative to B. The horizontal component of the relative displacement between the shear centers of both plies (Point C relative to A) is $2c/\cos\theta_i + (v_{2,i} - v_{1,i})\tan\theta_i$, while the vertical component is $v_{2,i} - v_{1,i}$. As a result, the relative displacement between Points D and B at the vertical interface of both plies has a horizontal component $2c/\cos\theta_i + (v_{2,i} - v_{1,i})\tan\theta_i - 2c\cos\theta_i$, a vertical component $v_{2,i} - v_{1,i} - 2c\sin\theta_i$ and an inclined

resultant $v_{s,i}=\sqrt{\left(2c/\cos\theta_i+\left(v_{2,i}-v_{1,i}\right)\tan\theta_i-2c\cos\theta_i\right)^2+\left(v_{2,i}-v_{1,i}-2c\sin\theta_i\right)^2}$. For small rotations, one has $\sin\theta_i\approx\tan\theta_i\approx\theta_i$, $\cos\theta_i=1-\theta_i^2/2$, $1/\cos\theta_i\approx1+\theta_i^2/2$, which simplifies the relation to $v_{s,i}{}^2=\left[2c\left(1+\theta_i^2/2\right)+\left(v_{2,i}-v_{1,i}\right)\theta_i-2c\left(1-\theta_i^2/2\right)\right]^2+\left(v_{2,i}-v_{1,i}-2c\theta_i\right)^2$. By omitting second-order terms, the following relation is obtained

$$v_{s,i}=v_{2,i}-v_{1,i}-2c\theta_i \tag{3.3}$$

Similarly, the longitudinal displacement of the shear center of the right ply C relative to that of the left ply A is $w_{s,i,j}=w_{2,i}-w_{1,i}+2cu_i'$. Therefore, the longitudinal fastener slip $w_{s,i,j}$ can be expressed as

$$w_{s,i,j}=w_{2,i}-w_{1,i}+2cu_i'-y_{i,j}v_{1,i}'+y_{i,j}v_{2,i}' \tag{3.4}$$

3.6 Formulation

3.6.1 Variational Principle

The total potential energy of the system π from stage 3 to stage 4 can be expressed as follows:

$$\pi=\sum_{e=1}^{e=n_e}\pi_{b,e}+\sum_{i=1}^{n=n_{e-1}}\pi_{s,i} \tag{3.5}$$

Where $\pi_{b,e}$ is the total potential energy stored in both plies for the beam element e and the total internal strain energy $\pi_{s,i}$ for a column of n_i fasteners located at a coordinate z_i along the span of the beam. The total potential energy $\pi_{b,e}$ stored in both plies is

$$\pi_{b,e}=U_{b,e,1}+U_{b,e,2}+U_{b,e,3}+U_{b,e,4}+V_{b,e,1}+V_{b,e,2} \tag{3.6}$$

where

$$U_{b,e,1}=\int_0^{l_e} EI_y\left(u''\right)^2 dz \qquad U_{b,e,2}=\int_0^{l_e} EI_x\left(v''\right)^2 dz$$
$$U_{b,e,3}=\int_0^{l_e} GJ\left(\theta'\right)^2 dz \qquad U_{b,e,4}=\int_0^{l_e} EA\left(w'\right)^2 dz \qquad (3.7a\text{-}e)$$
$$V_{b,e,1}=2\lambda\int_0^{l_e} M\theta u'' dz \qquad V_{b,e,2}=\lambda\int_0^{l_e} qy_q\theta^2 dz$$

where E is Young's modulus of elasticity, I_y is the moment of inertia about the weak axis, I_x is the moment of inertia about the major axis, G is the shear modulus, and J is the Saint-Venant torsional constant. In Eq. (3.5), the total internal strain energy $\pi_{s,i}$ for a column of n_i fasteners is given by

$$\pi_{s,i}=U_{sv,i}+U_{sw,i} \qquad (3.8)$$

in which $U_{sv,i}$ is the internal strain energy contribution due to the relative transverse displacement $v_s\left(z_i\right)$ at the ply interface, $U_{sw,i}$ is that due to the relative longitudinal displacement $w_s\left(y_j,z_i\right)$, $\left(y_i,z_i\right)$are the coordinates of the fastener. The fasteners' transverse internal strain energy contribution $U_{sv,i}$ is given by $U_{sv,i}=\frac{1}{2}\sum_{j=1}^{j=n_i} kv_s\left(z_i\right)^2$ or $U_{sv,i}==\frac{1}{2}\sum_{j=1}^{j=n_i} k\left(2v_{1,i}+2c\theta_{,i}\right)^2$ which can be presented in the matrix form as

$$U_{sv,i}=2\sum_{j=1}^{j=n_i} k\left\langle v_1 \quad \theta\right\rangle_i\begin{bmatrix}1 & c\\ c & c^2\end{bmatrix}\begin{Bmatrix}v_1\\ \theta\end{Bmatrix}_i \qquad (3.9)$$

The fasteners' longitudinal internal strain energy contribution $U_{sw,i}$ can be expressed as

$$U_{sw,i}=\frac{1}{2}\sum_{j=1}^{j=n_i} kw_s\left(y_j,z_i\right)^2=\sum_{j=1}^{j=n_i} 2k\left\langle w_1 \quad u' \quad v'\right\rangle\begin{bmatrix}1 & -c & y_{i,j}\\ -c & c^2 & -cy_{i,j}\\ y_{i,j} & -cy_{i,j} & y^2\end{bmatrix}\begin{Bmatrix}w_1\\ u'\\ v'\end{Bmatrix} \qquad (3.10)$$

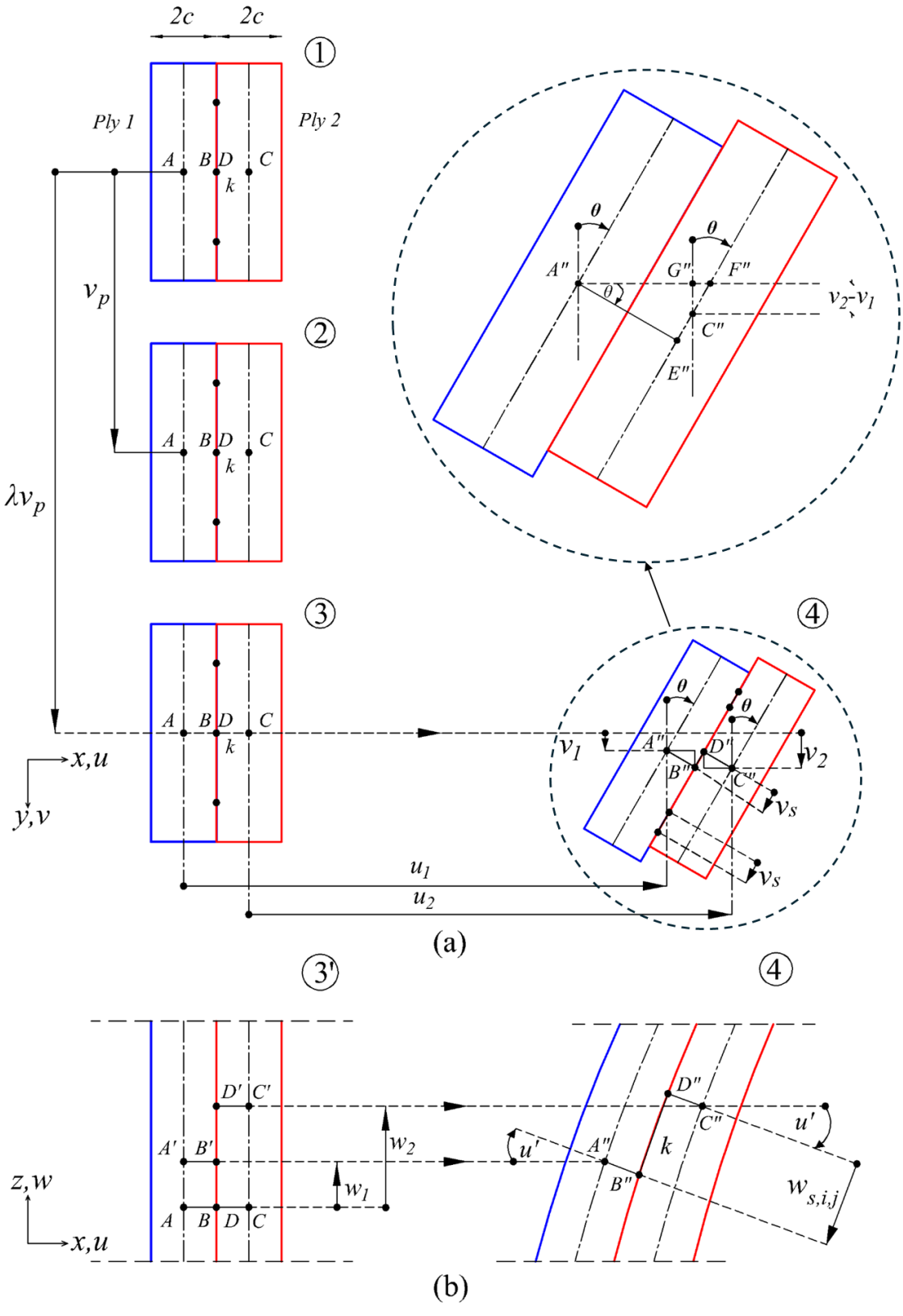

Figure 3.2 Kinematics (a) Elevation view and (b) Plan view

3.6.2 Finite Element Formulation

Displacements $(u,\theta,v)_e$ are related to the nodal displacement vector $\mathbf{u}_e^{\mathbf{T}} = \langle u_{N1} \quad u'_{N1} \quad u_{N2} \quad u'_{N2} \rangle_e, \boldsymbol{\theta}_e^{\mathbf{T}} = \langle \theta_{N1} \quad \theta'_{N1} \quad \theta_{N2} \quad \theta'_{N2} \rangle_e, \mathbf{v}_e^{\mathbf{T}} = \langle v_{N1} \quad v'_{N1} \quad v_{N2} \quad v'_{N2} \rangle_e$ through Hermitian polynomials, i.e.,

$$u_e = \mathbf{H}_{\mathbf{1},e}{}^{\mathbf{T}}\mathbf{u}_e \qquad \theta_e = \mathbf{H}_{\mathbf{1},e}{}^{\mathbf{T}}\boldsymbol{\theta}_e \qquad v_e = \mathbf{H}_{\mathbf{2},e}{}^{\mathbf{T}}\mathbf{v}_e \tag{3.11 a-c}$$

in which $\mathbf{H}_{\mathbf{1},e}{}^{\mathbf{T}}, \mathbf{H}_{\mathbf{2},e}{}^{\mathbf{T}}$ are vectors of Hermitian polynomials defined as

$$\begin{aligned} \mathbf{H}_{\mathbf{1},e}{}^{\mathbf{T}} &= \left\langle \; 1-3\xi_e{}^2+2\xi_e{}^3 \;\vdots\; \xi l\left(1-\xi_e\right)^2 \;\vdots\; 3\xi_e{}^2-2\xi_e{}^3 \;\vdots\; l\xi_e{}^2\left(\xi_e-1\right) \right\rangle \\ \mathbf{H}_{\mathbf{2},e}{}^{\mathbf{T}} &= \left\langle \; 1-3\xi_e{}^2+2\xi_e{}^3 \;\vdots\; -\xi_e l\left(1-\xi_e\right)^2 \;\vdots\; 3\xi_e{}^2-2\xi_e{}^3 \;\vdots\; -l\xi_e{}^2\left(\xi_e-1\right) \right\rangle \end{aligned} \tag{3.12a-b}$$

where $\xi_e = z/l_e$. Also, displacement $w_{i,j}$ is linearly interpolated to the nodal displacements $\mathbf{w}^{\mathbf{T}} = \langle w_{1N} \quad w_{2N} \rangle$ through

$$w_e(z) = \mathbf{L}_e{}^{\mathbf{T}}\mathbf{w}_e \tag{3.13}$$

in which

$$\mathbf{L}_e{}^{\mathbf{T}} = \langle 1-\xi_e \;\vdots\; \xi_e \rangle \tag{3.14}$$

Also, the bending moment is linearly interpolated between end moments M_{e0}, M_{e1}, i.e.,

$$M_e(z) = -M_{e0}\left(1-\xi_e\right) + M_{e1}\xi_e \tag{3.15}$$

And the distributed load $q(z)$ is linearly interpolated between q_{e0}, q_{e1}, i.e.,

$$q_e(z) = q_{e0}\left(1-\xi_e\right) + q_{e1}\xi_e \tag{3.16}$$

By substituting Eqs. (3.11 a-c), (3.13), (3.15) and (3.16) into Eqs. (3.6) and (3.7a-e)a-e), one obtains

$$\pi_{b,e} = \mathbf{u}_e{}^{\mathrm{T}}\mathbf{K}_{\mathbf{uu},e}\mathbf{u}_e + \mathbf{v}_e{}^{\mathrm{T}}\mathbf{K}_{\mathbf{vv},e}\mathbf{v}_e + \boldsymbol{\theta}_e{}^{\mathrm{T}}\mathbf{K}_{\boldsymbol{\theta\theta},e}\boldsymbol{\theta}_e + \mathbf{w}_e{}^{\mathrm{T}}\mathbf{K}_{\mathbf{ww},e}\mathbf{w}_{ee} + 2\lambda\mathbf{u}_e{}^{\mathrm{T}}\mathbf{K}_{\mathbf{g1},e}\boldsymbol{\theta}_e + \lambda\boldsymbol{\theta}_e{}^{\mathrm{T}}\mathbf{K}_{\mathbf{g}2,e}\boldsymbol{\theta}_e \tag{3.17}$$

in which stiffness matrices $\mathbf{K}_{\mathbf{uu,i}}, \mathbf{K}_{\mathbf{vv,i}}, \mathbf{K}_{\boldsymbol{\theta\theta},\mathbf{i}}, \mathbf{K}_{\mathbf{ww,i}}, \mathbf{K}_{\boldsymbol{\theta u},\mathbf{i}}$ are defined as

$$\begin{aligned}
\mathbf{K}_{\mathbf{uu},e} &= EI_y\int_0^{l_e}\mathbf{H}''_{1,e}\mathbf{H}''_{1,e}{}^{\mathrm{T}}dz & \mathbf{K}_{\mathbf{vv,i}} &= EI_x\int_0^{l_e}\mathbf{H}''_{2,e}\mathbf{H}''_{2,e}{}^{\mathrm{T}}dz \\
\mathbf{K}_{\boldsymbol{\theta\theta},e} &= GJ\int_0^{l_e}\mathbf{H}'_{1,e}\mathbf{H}'_{1,e}{}^{\mathrm{T}}dz & \mathbf{K}_{\mathbf{ww,i}} &= EA\int_0^{l_e}\mathbf{L}'_e\mathbf{L}'^{\mathrm{T}}_e dz \\
\mathbf{K}_{\mathbf{g1},e} &= \int_0^{l_e}M(z)\mathbf{H}''_{1,e}\mathbf{H}_{1,e}{}^{\mathrm{T}}dz & \mathbf{K}_{\mathbf{g}2,e} &= \int_0^{l_e}q(z)y_q\mathbf{H}_{1,e}\mathbf{H}_{1,e}{}^{\mathrm{T}}dz
\end{aligned} \tag{3.18a-e}$$

in which

$$\mathbf{K}_{\mathbf{uu},e} = \frac{EI_y}{l_e^3}\begin{bmatrix} 12 & 6l_e & -12 & 6l_e \\ 6l_e & 4l_e^2 & -6l_e & 2l_e^2 \\ -12 & -6l_e & 12 & -6l_e \\ 6l_e & 2l_e^2 & -6l_e & 4l_e^2 \end{bmatrix} \qquad \mathbf{K}_{\mathbf{vv},e} = \frac{EI_x}{l_e^3}\begin{bmatrix} 12 & -6l_e & -12 & -6l_e \\ -6l_e & 4l_e^2 & 6l_e & 2l_e^2 \\ -12 & 6l_e & 12 & 6l_e \\ -6l_e & 2l_e^2 & 6l_e & 4l_e^2 \end{bmatrix}$$

$$\mathbf{K}_{\boldsymbol{\theta\theta},e} = \frac{GJ}{30l_e}\begin{bmatrix} 36 & 3l_e & -36 & 3l_e \\ 3l_e & 4l_e^2 & -3l_e & -l_e^2 \\ -36 & -3l_e & 36 & -3l_e \\ 3l_e & -l_e^2 & -3l_e & 4l_e^2 \end{bmatrix} \qquad \mathbf{K}_{\mathbf{ww},e} = \frac{EA}{l_e}\begin{bmatrix} 1 & -1 \\ -1 & 1 \end{bmatrix}$$

$$\mathbf{K}_{\mathbf{g1},e} = \frac{1}{30l_e}\left[\begin{array}{c|c|c|c} 33M_{e0}-3M_{e1} & 3M_{e0}l_e & -3M_{e0}+33M_{e1} & -3M_{e1}l_e \\ \hline 27M_{e0}l_e-6M_{e1}l_e & (3M_{e0}-M_{e1})l_e^2 & 3M_{e0}l_e+6M_{e1}l_e & -l_e^2M_{e0} \\ \hline -33M_{e0}+3M_{e1} & -3M_{e0}l_e & 3M_{e0}-33M_{e1} & 3M_{e1}l_e \\ \hline 6M_{e0}l_e+3M_{e1}l_e & M_{e1}l_e^2 & -6M_{e0}l_e+27M_{e1}l_e & l_e^2(M_{e0}-3M_{e1}) \end{array}\right]$$

For a uniformly distributed load $q(z)=q$ acting at a height y_q, $\mathbf{K}_{\mathbf{g}2,e}$ takes the form

$$\mathbf{K}_{\mathbf{g}2,e} = \frac{qy_ql_e}{420}\left[\begin{array}{c|c|c|c} 156 & 22l_e & 54 & -13l_e \\ \hline 22l_e & 4l_e^2 & 13l_e & -3l_e^2 \\ \hline 54 & 13l_e & 156 & -22l_e \\ \hline -13l_e & -3l_e^2 & -22l_e & 4l_e^2 \end{array}\right]$$

In Eq.(3.8), the internal strain energy $\pi_{s,i}$ stored in the group of fasteners n_i located at coordinate z_i is determined from Eqs. (3.3) and (3.4) by substituting into Eqs. (3.9) and (3.10) then using the relations (3.2a-b) yielding

$$U_{sv,i} = \mathbf{v}_{\mathbf{s},i}^{\mathrm{T}} \mathbf{K}_{\mathbf{sv},i} \mathbf{v}_{\mathbf{s},i} \qquad U_{sw,i} = \mathbf{w}_{\mathbf{s},i}^{\mathrm{T}} \mathbf{K}_{\mathbf{sw},i} \mathbf{w}_{\mathbf{s},i} \tag{3.19a-b}$$

in which

$$\mathbf{v}_{\mathbf{s},i}^{\mathrm{T}} = \langle v \quad \theta \rangle_i, \qquad \mathbf{K}_{\mathbf{sv},i} = \sum_{j=1}^{j=n_i} \overline{\mathbf{K}}_{\mathbf{sv},i,j} = n_i (2k) \begin{bmatrix} 1 & c \\ c & c^2 \end{bmatrix}$$

$$\mathbf{w}_{\mathbf{s},i}^{\mathrm{T}} = \langle w \quad u' \quad v' \rangle_i, \qquad \mathbf{K}_{\mathbf{sw},i} = \sum_{j=1}^{j=n_i} \overline{\mathbf{K}}_{\mathbf{sw},i,j}, \qquad \overline{\mathbf{K}}_{\mathbf{sw},i,j} = (2k) \begin{bmatrix} 1 & -c & y_{i,j} \\ -c & c^2 & -cy_{i,j} \\ y_{i,j} & -cy_{i,j} & y_{i,j}^{\ 2} \end{bmatrix}$$

3.7 Verification

The formulation presented in this study was verified by comparing the critical moments and mode shapes predicted by the current formulation and the 3D finite element model using Abaqus [3.29]. Results based on the formulation developed under the previous section will be referred to as the "Present Model".

3.7.1 Reference Case

As a reference case, a 5m span built-up beam composed of two plies of SPF No. 1/No. 2 grade sawn lumber is considered. Each ply has a 38 mm × 286 mm cross-section. The beam is simply supported with respect to transverse, lateral displacements, and twists and is subjected to uniform moment. The plies are fastened together using 3" common nails with 3.76 mm diameter. The nail length is 76 mm (i.e., equal to twice the width of a single ply); and thus, fully penetrates both plies. The geometric parameters of the nailing pattern are selected based on practical considerations while meeting the requirements of CSA-O86:19 [3.1]. Longitudinal spacing parallel to the grain

is $S_p = 300mm,$ with end distance $a = 100mm,$. Transverse spacing perpendicular to grain is $S_q = 93mm$ with edge distances $e = 50mm$ (Figure 3.1). The lateral and transverse stiffnesses k for the fasteners are estimated from Eurocode 5 [3.3]* using the relationship

$$k = \rho_m^{1.5} d^{0.8} / 30 \tag{3.20}$$

in which k is in N/mm, ρ_m is the mean wood density in kg/m^3 and d is the diameter in millimeters. The density of SPF-sawn lumber is taken as $\rho_m = 420\ kg/m^3$ [3.1]. For a diameter $d = 3.76mm$, one obtains $k = 830\ N/mm$. The withdrawal stiffness is taken as $k_u = 500 N/mm$ based on the experimental tests in [3.30].

3.7.2 Description of the Present Model

A mesh** sensitivity analysis was conducted on the present model that is based on the developed formulation. The study showed that convergence was achieved when 18 elements were taken along the beam span.

3.7.3 Description of Abaqus Model

A 3D finite element model was developed using the C3D8 brick element in Abaqus [3.29]. The C3D8 element has eight corner nodes with three translational degrees of freedom per node and is based on full integration. This element was successfully used in past studies (e.g.,[3.7], [3.24], [3.25]) to predict the lateral torsional buckling resistance of wooden beams. To ensure the model accuracy, the ratios of the width to depth to length of the C3D8 elements were chosen to be close to the unity. A mesh study**indicated that convergence was reached when the element size is nearly 20 mm. To model the nails connecting the two plies, the two-node SPRING2 element was selected

* Eurocode 5 provides Eq. (3.20) to characterize the shear stiffness for the connection between the fastener and the timber component in which it is embedded. This shear stiffness is termed as the fastener stiffness in the present study.

** The details of the mesh sensitivity analysis are provided in Appendix A.

from the Abaqus library. Three elastic relative springs were used at each nail location to represent the withdrawal stiffness of the nail along the x-direction, the transverse stiffness along the y-direction, and the longitudinal stiffness along the z-direction. Wood was modelled as an orthotropic material with 12 constitutive constants: three elastic moduli E_L, E_R, E_T in which L, R, T denote the longitudinal, radial and tangential directions, three shear moduli G_{LR}, G_{RT}, G_{TL}, and six Poisson ratios μ_{ij}, where $i, j = L, R, T$. However, the symmetry of the constitutive tensor requires satisfying three constraints (e.g., [3.31]) i.e.,

$$\mu_{ij}/E_i = \mu_{ij}/E_j, \quad i \neq j, \quad i, j = L, R, T \tag{3.21}$$

which reduces the number of constitutive constants to nine independent parameters. The longitudinal modulus of elasticity E and the shear moduli G_{LT}, G_{LR} were taken from CSA-O86:19 [3.1] as $E_z = E_L = 9500Mpa$ and $G_{LT} = G_{LR} = E_L/16$. Other properties were taken from the wood handbook [3.31] for Lodgepole Pine, a constituent species under the SPF species combinations. Given that a cylindrically orthotropic constitutive model of wood (defined along L, R, T) is not supported in Abaqus, a Cartesian orthotropic model (defined along the Cartesian coordinate X, Y, Z) f was used to model the problem. Both constitutive models would match when the properties along two directions (i.e., R, T or X, Y) are equal. Since the tangential and radial properties of wood are close (e.g., [3.32]), i.e., $E_T \approx E_R$, $G_{LT} \approx G_{LR}$, $\mu_{LT} \approx \mu_{LR}$, the number of independent parameters can be reduced from nine to six. The Cartesian orthotropic model in Abaqus was adopted using the approximation $E_X = E_Y = (E_R + E_T)/2 = 808MPa$, and $\mu_{ZX} = \mu_{ZY} = (\mu_{LR} + \mu_{LT})/2 = 0.332$. The remaining constants were taken as $G_{XY} = G_{RT} = 64.57MPa$, $\mu_{RT} = \mu_{XY} = 0.469$. Boundary conditions and load application details are shown in Figure 3.3. To

model the simply supported end conditions, transverse restraints were provided at both ends along lines

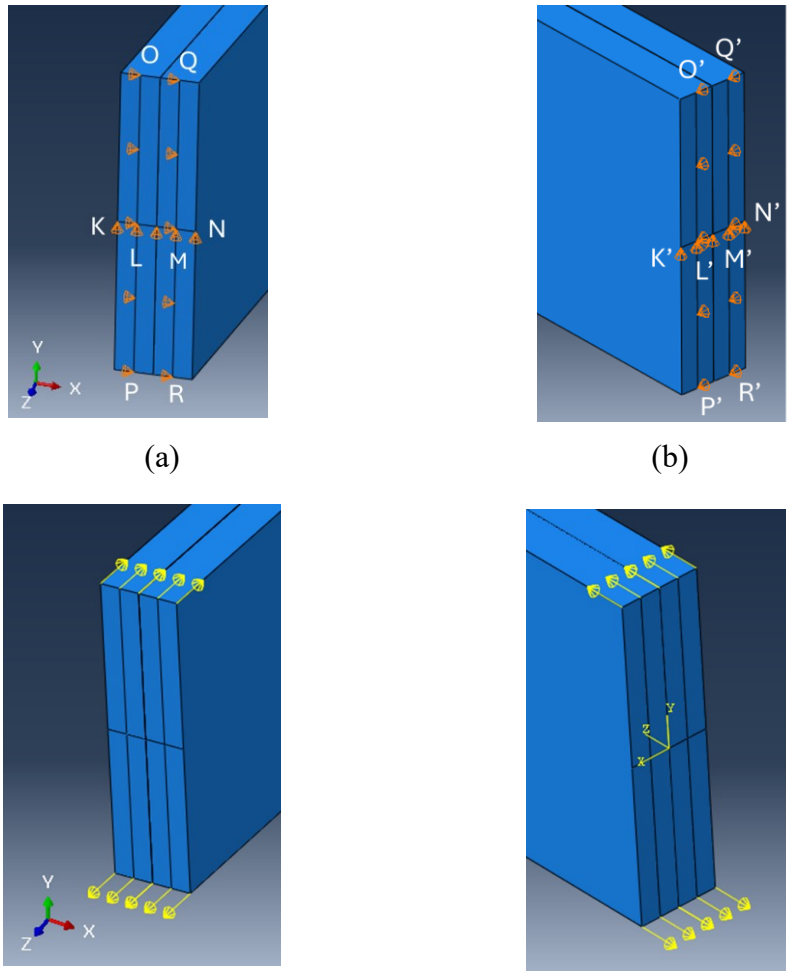

Figure 3.3 Boundary conditions for (a) left end, (b) right end, and load application for (C) left end, and (d) right end.

KLMN and K'L'M'N' and lateral restraints were provided along the vertical lines OLP, QMR, O'L'P' and Q'M'R' as shown in Figure 3.3. The shear centers L' and M' of both plies were longitudinally restrained at one end and longitudinally unrestrained at the other end. To model the interaction at the interface between both plies, the finite sliding, surface-to-surface contact was used. This feature enables the relative sliding between plies. The hard contact pressure over-closure sub-feature was used to prevent any penetration between surfaces (Figure 3.4 a).

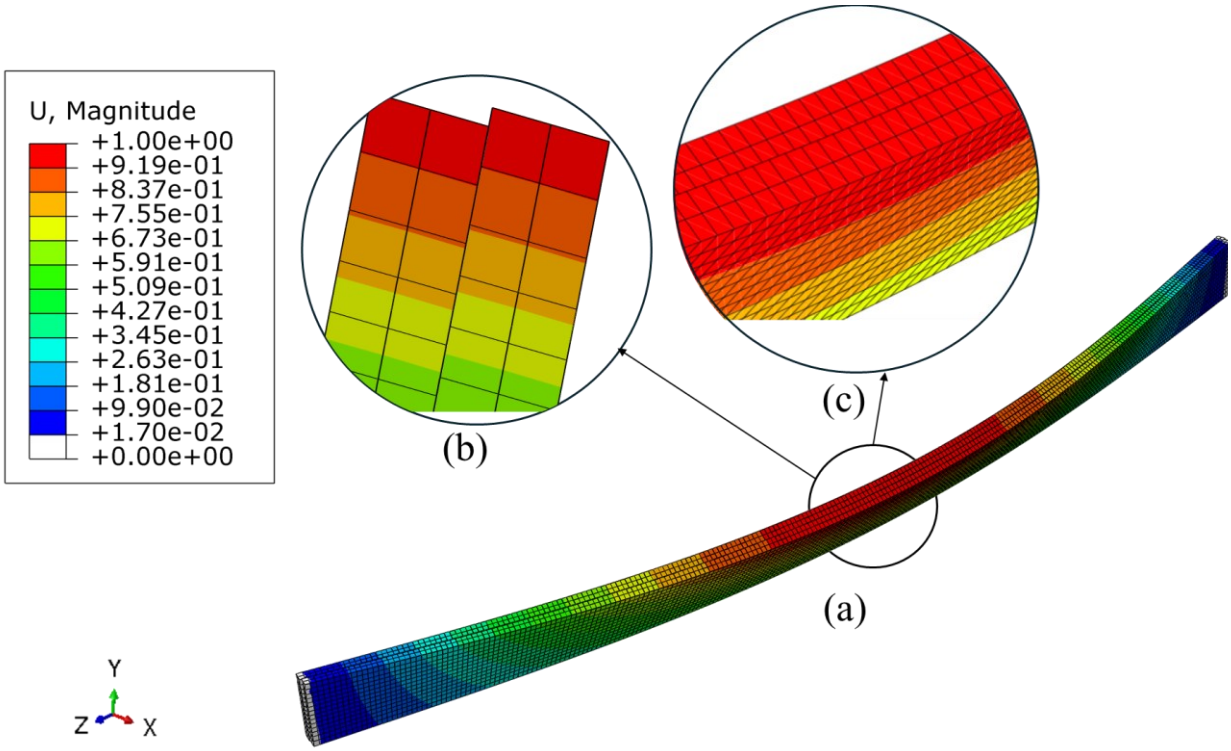

Figure 3.4 (a) Buckling mode of a built-up beam modeled with a finite sliding contact surface, (b) cross-sectional view showing relative vertical slip between both plies and (c) relative longitudinal slip between both plies looking from the top

3.7.4 Comparison

The verification study involves the predictions of the 3D FE analysis with those based on the present study regarding (a) the critical moments and (b) the modes shapes. For the reference case, the critical moment predicted by the present solution is 9.78 kNm (Column 13 in Table 3.1), while that based on 3D FEA is 9.34 kNm (Column 14). According to Eurocode 5 [3.3], the relative slenderness of the reference case $\lambda_{rel,m}$ is 1.72 > 1.4 which indicates that it is a slender beam. Eighteen additional cases were examined while varying the ply dimensions, material properties, fastener stiffness, nailing pattern, and loading type (Table 3.1). The ratios of critical moments based on the 3D FE model to that based on the present formulation are less than 1 with an average of 0.96 and a standard deviation of 0.02 (Column 15) indicating a close agreement. The minor difference is attributed to the cross-sectional distortion that is omitted in the present study

(Assumption 3) but captured in the 3D FE model. In the present model, the omission of distortional effects leads to a stiffer model which, in the present case, more than offsets the detrimental effect induced by omitting the warping stiffness (Assumption 1). A comparison of the mode shape predicted by models for the reference beam is provided (Figure 3.5). All displacements were normalized relative to the peak lateral displacement at beam mid-depth.

Table 3.1: Comparison between the critical moments obtained from 3D FE analysis (Abaqus) and the present study

Run No. (1)	Ply dimensions (mm)			Material Properties (MPa)		Fastener Stiff-ness (N/mm)	Nailing Pattern Dimensions (mm)				Load Type	Critical moment kNm		Ratio
	b (2)	d (3)	L (4)	E (5)	G (6)	k (7)	S_p (8)	S_q (9)	a (10)	e (11)	Load Type (12)	Present Study (13)	3D FEA (14)	(14)/ (13)= (15)
R1	38	286	5000	9500	594	830	294	98	148	45	UM	9.78	9.34	0.96
2	42	313	5000	9500	594	1196	294	107	148	45	UM	13.4	13.2	0.99
3	40	300	5000	9500	594	1004	294	103	148	45	UM	11.4	11.1	0.97
4	34	286	5000	11281	705	830	294	98	148	45	UM	8.13	7.90	0.97
5	38	286	5000	9500	594	1.10	294	98	148	45	UM	7.48	7.12	0.95
6	38	286	5000	9500	594	11.0	294	98	148	45	UM	7.57	7.20	0.95
7	38	286	5000	9500	594	110	294	98	148	45	UM	7.89	7.43	0.94
8	38	286	5000	9500	594	500	294	98	148	45	UM	8.81	8.58	0.97
9	38	286	5000	9500	594	1000	294	98	148	45	UM	9.85	9.65	0.98
10	38	286	5000	9500	594	1500	294	98	148	45	UM	10.5	10.4	0.99
11	38	286	5000	9500	594	2000	294	98	148	45	UM	11.2	10.9	0.97
12	38	286	5000	9500	594	830	100	98	148	45	UM	11.5	11.1	0.97
13	38	286	5000	9500	594	830	336	98	148	45	UM	9.45	9.10	0.96
14	38	286	5000	9500	594	830	600	98	148	45	UM	8.73	8.31	0.95
15	38	286	5000	9500	594	830	294	49	148	45	UM	10.5	10.1	0.96
16	38	286	5000	9500	594	830	20	20	20	20	UM	28.3	28.1	0.99
17	38	286	5000	9500	594	830	294	98	148	45	UDL	10.6	10.1	0.95
18	38	286	5000	9500	594	830	294	98	148	45	PL	12.5	11.7	0.94
19	38	286	5000	9500	594	830	294	98	148	45	2PL	10.2	9.62	0.94
									Average					0.96
									Standard deviation					0.02

Note: UM = uniform moment applied at both ends; UDL = uniformly distributed load; PL = point load applied at the midspan; and 2PL = two-point loads applied at third span points.

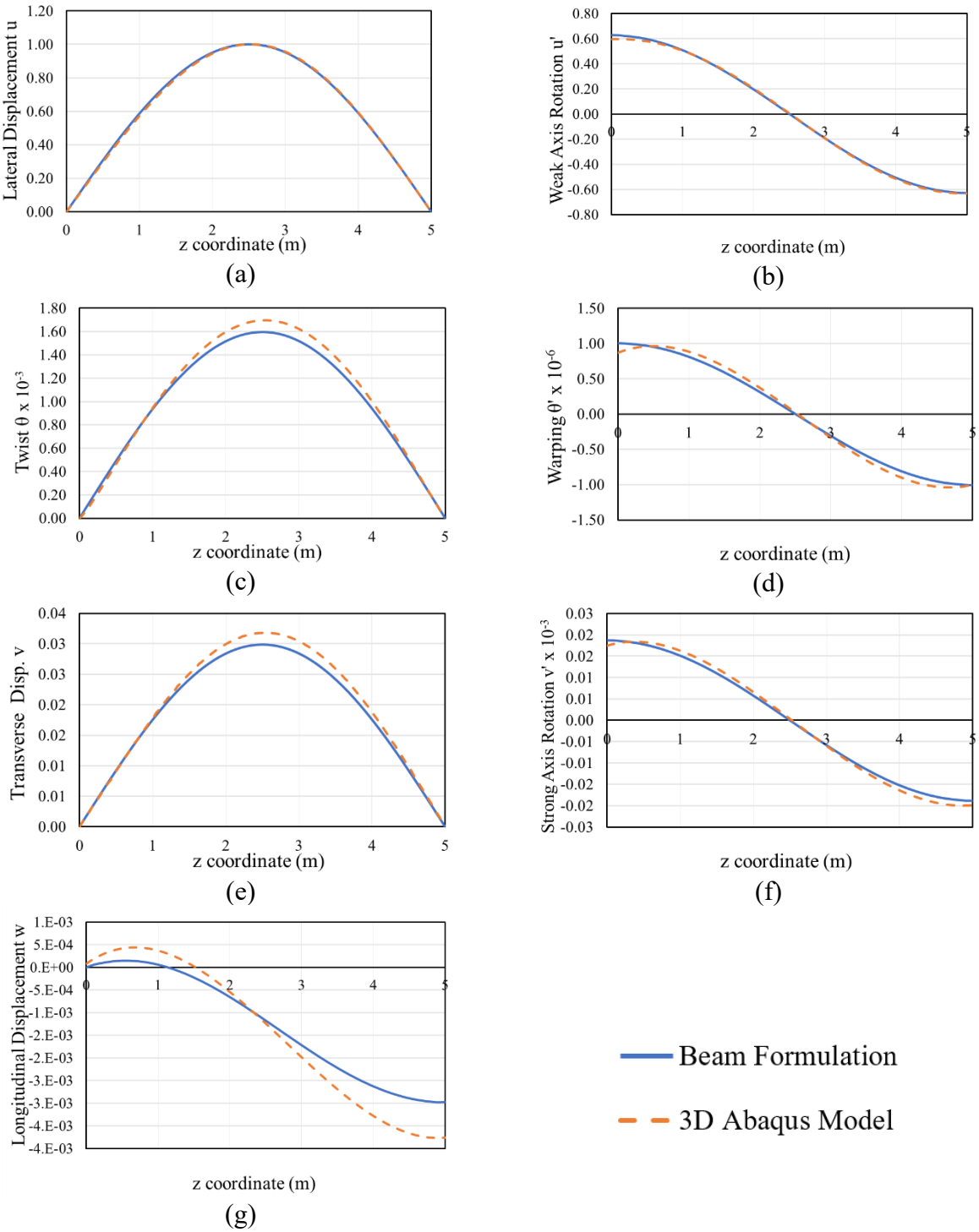

Figure 3.5 Normalized mode shape for reference beam a) lateral displacement; (b) weak-axis rotation; (c) twist; (d) warping; (e)transverse displacement; (f) strong axis rotation; and (g) longitudinal displacement (mode shapes have been normalized relative to the peak lateral displacement)

As anticipated, the 3D FE model is a bit more flexible than the present model (beam formulation) because the present model ignores cross-sectional distortion. The close agreement between the predicted mode shapes shows that the present model is able to successfully emulate the LTB behaviour predicted by the solid FEA model.

3.8 Parametric Study

A parametric study based on the present formulation was conducted. The study considered several factors that affect the behavior of built-up beams as the effect of fastener stiffness, fastener spacing, moment gradient, load height, and beam dimensions. In addition, non-uniform nail patterns were considered. While it is recognized that wood members exhibit long-term effects under sustained loading, the present study does not attempt to incorporate time-dependent behaviour on the buckling response sought.

3.8.1 Fasteners with Uniform Spacing

3.8.1.1 Effect of Fastener Stiffness

The reference case defined in the verification section was reconsidered. The longitudinal spacing $S_p = 300mm$ of the reference case represents nearly a quarter of the maximum allowed longitudinal spacing requirement to attain monolithic action ($S_p = 4d = 1144mm$) when computing the elastic LTB resistance according to CSA-O86:19 [3.1]. Specifically, Cl. 7.5.6.3.3 of CSA-O86:19 states "*For built-up beams consisting of two or more individual members of the same depth, the maximum (depth to width) ratio permitted in Clause 7.5.6.3.1 for laterally unsupported members may be based on the total width of the beam provided that the individual members are fastened together securely at intervals not exceeding four times the depth".* The standard shows that in order to

calculate the slenderness ratio $C_B = \sqrt{Ld/b^{*2}}$ which forms the basis of computation of the elastic lateral torsional buckling resistance (Cl. 7.5.6.4.4.c, and 7.5.6.5.1), one would assume that $b^* = 2b$ when both plies are fastened together "securely" at intervals not exceeding four times the depth. Yet, the Clause does not provide a basis to assess whether the plies are securely attached together. Therefore, this study assessed the capability of the fasteners to "securely" connect the plies; thus, the built-up beam reaches the monolithic case.

Four nailing patterns were investigated (Table 3.2): the maximum allowed nail spacing to reach the monolithic case as per CSA-O86:19 [3.1] ($S_p = 4d = 1144mm$), the reference spacing ($S_p = 300mm$), the minimum spacing for nails and screws as stated in CSA-O86:19 [3.1] ($S_p = 80mm$), and 20 mm spacing connection. The stiffness k for a single fastener was normalized relative to the transverse flexural stiffness of a ply, i.e., $\bar{k} = k/\left(EI_x/L^3\right)$. The fastener stiffness k was varied in the range between 0 to 2000 *N/mm* and the corresponding critical moment M_{cr} as predicted by the present formulation was obtained. The normalized critical moment ratio M_{cr}/M_{nc} versus the normalized transverse stiffness $\bar{k}$ for the four nailing patterns is plotted in Figure 3.6.*a*, in which M_{nc} is twice the critical moment of a single ply. For a single ply, one has $\left(I_y, J\right) = \left(1.31\times10^6, 4.79\times10^6\right)mm^4$, and the corresponding total critical moment of the non-composite beam is $M_{nc} = 2(\pi/L)\sqrt{EGI_yJ} = 7.47kNm$ which represents a lower bound for the LTB capacity of the system for the hypothetical case of no fastener connecting both plies. As an upper bound, the monolithic critical moment M_m is computed based on the hypothetical case of a rigid connection between both plies that prevents any slip between them. For the full monolithic cross-section, one has $\left(I_y, J\right)_m = \left(1.05\times10^7, 3.45\times10^7\right)mm^4$ and the corresponding critical moment is

$M_m = (\pi/L)\sqrt{EG(I_y J)_m} = 28.4 kNm$, i.e., $M_m / M_{nc} = 3.80$ as depicted in (Figure 3.6.a). For a typical nail stiffness $k = 830 N/mm$ which corresponds to $\bar{k} = 150$, the critical moment for the two-ply beam that complies with the limits of the nail spacing as per CSA-O86:19 ranges from 1.10 to 2.10 relative to the lower bound non-composite critical moment M_{nc}. Yet, when compared to the monolithic critical moment, M_{cr}/M_m ranges from 0.3 to 0.55. Similar observations were reported in the study of Robatmili et al. [3.22]. For the reference spacing, the critical moment with respect to the non-composite case is $M_{cr}/M_{nc} = 1.27$ which corresponds to $M_{cr}/M_m = 0.33$. Only the 20 mm spacing connection, out of the four considered cases, allows the system to reach the monolithic beam's critical moment (Figure 3.6.a); however, this spacing is impractical and significantly less than the minimum allowed longitudinal spacing for nails and screws as per CSA-O86:19. As a result, this study shows that by adhering to the spacing limits specified in the standard and adopting a stiffness within the practical ranges of nails, the monolithic status will not be attained. This is attributed to the fact that the slip at the interface between the plies is not entirely prevented by using discrete fasteners within the permitted spacings specified in the standard.

Table 3.2. Nailing patterns details

Spacing	Spacing parallel to grain S_p (mm)	End dist. parallel to grain a (mm)	Spacing normal to grain S_q (mm)	Edge distance normal to grain e (mm)	Total number of fasteners n	Stiffness range k (N/mm)	Normalized Stiffness range $\bar{k}$	Total Normalized Stiffness range $n\bar{k}$
Max spacing as per CSA-O86:19 [3.1]	1144	212	93	50	15	0 - 2000	0 - 360	0 - 5.4×10^3
Reference	300	100	93	50	51	0 - 2000	0 - 360	0 - 1.8×10^4
Min. spacing as per CSA-O86:19 [3.1]	80	60	45	30	455	0 - 2000	0 - 360	0 - 1.6×10^5
20 mm spacing	20	20	20	20	3486	0 - 2000	0 - 360	0 - 1.3×10^6

3.8.1.2 Effect of the Number of Fasteners

The four nailing patterns in sub-section 3.8.1.1 were reconsidered. In the previous sub-section, the normalized stiffness $\bar{k}$ for a single fastener was kept the same among all nailing patterns and was increasing gradually with the same value while the total normalized transverse stiffnesses $n\bar{k}$ was different because the number of fasteners n varied among different nailing patterns. In contrast, this section investigates the case where both n and $\bar{k}$ are varied while the total normalized stiffness for the fasteners $n\bar{k}$ is kept the same for all nailing patterns (Table 3.3). As depicted in Figure 3.6.b, while keeping $n\bar{k}$ constant, the normalized critical moment increases with increasing the number of fasteners used. As a result, this study indicates that increasing the number of fasteners is a more effective measure to increase the critical moment than increasing the fastener stiffness. This could be due to the interfacial shear stresses that are developed while the beam undergoes LTB and cause slippage. Having a large number of fasteners with a small stiffness ensures a more even shear flow and less slippage than the case of fewer fasteners with a larger stiffness.

Table 3.3: Total normalized stiffness of the considered nailing patterns

$n\bar{k}$	Max spacing as per CSA-O86:19 [3.1]			Ref. Spacing			Min. spacing as per CSA-O86:19 [3.1]			20 mm spacing		
	n	k	$\bar{k}$	n	k	$\bar{k}$	n	k	$\bar{k}$	n	k	$\bar{k}$
0	15	0	0.0E+0	51	0	0.00E+0	455	0	0.00E+0	3486	0	0.00E+0
150000	15	56200	1.0E+4	51	16500	2.94E+3	455	1850	3.30E+2	3486	261	4.63E+1
300000	15	112000	2.0E+4	51	33100	5.88E+3	455	3710	6.59E+2	3486	521	9.27E+1
450000	15	169000	3.0E+4	51	49600	8.82E+3	455	5560	9.89E+2	3486	782	1.39E+2
600000	15	225000	4.0E+4	51	66200	1.18E+4	455	7416	1.32E+3	3486	1040	1.85E+2

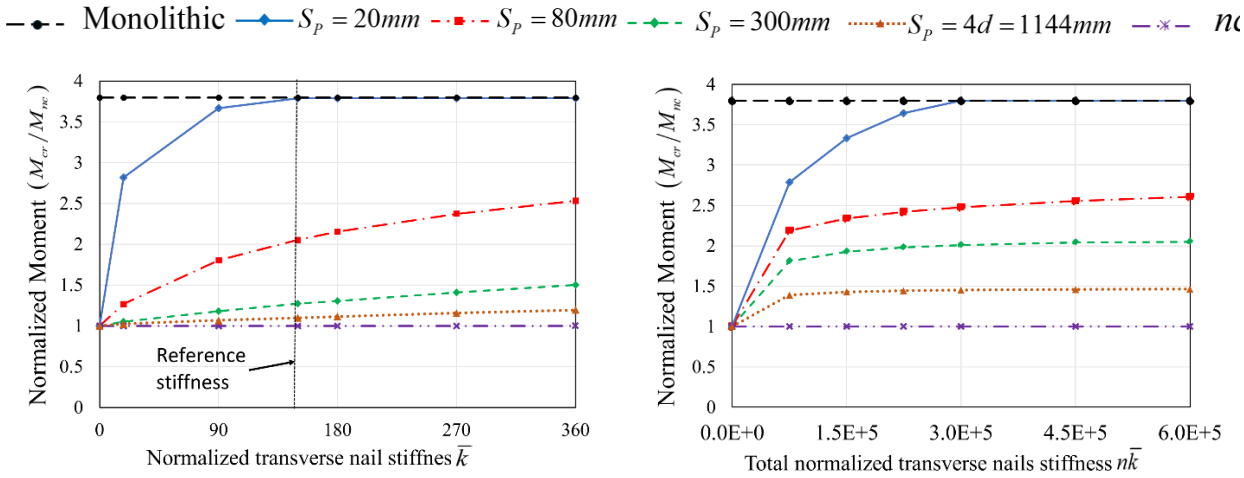

Figure 3.6 Normalized critical moment vs (a) normalized stiffness for a single fastener $\bar{k}$ (b) total normalized stiffness for all fasteners $n\bar{k}$

3.8.1.3 Loading patterns

The reference beam was reconsidered under three scenarios as shown in Table 3.4; (1) without fasteners $k_w = 0$, (2) with relatively flexible fasteners $k = 500N/mm$, and (3) with relatively stiff fasteners $k = 1500N/mm$. The studied beams are subjected to different load cases: uniformly distributed load (UDL), point load applied at the midspan (PL), two-point loads applied at third span points (2PL), and linear bending moments where the end moment ratio ψ varies from ψ = +1 to ψ = −1. Column 3 of Table 3.4 provides the moment gradient factors $C_b = M_{cr}/M_{cr,u}$ for the built-up beam as predicted by the present study, where M_{cr} is the critical moment of built up beams and $M_{cr,u}$ is the critical moment of under uniform moment. Column 4 provides the moment gradient factor for monolithic beams based on AWC-TR14 [3.33] $C_{b-AWC} = 12.5M_{\max}/(3M_a + 4M_b + 3M_c + 2.5M_{\max})$, while Column 5 is based on the study of Sahraei et al. [3.14] (also for monolithic beams). Generally, The results reveal that the moment gradient factor C_b of built-up beams decreases with the increase in fastener stiffness.

Table 3.4: Moment gradient factors for two 38×286 mm ply beams of a 5m span

Bending moment pattern (1)	k (N/mm) (2)	Moment gradient factor			Ratios	
		Present Study (3)	AWC-TR14 (4)	Sahraei Study (5)	(6) =(3)/(4)	(7) =(3)/(5)
UDL	0	1.13	1.14	1.15	0.99	0.98
Mid-PL		1.35	1.32	1.36	1.02	0.99
2-PL		1.09	1.14	1.10	0.95	0.99
ψ = 1		1.00	1.00	1.00	1.00	1.00
ψ = 0.5		1.31	1.25	1.32	1.05	0.99
ψ = 0		1.77	1.67	1.78	1.06	0.99
ψ = -0.5		2.33	2.17	2.36	1.07	0.99
ψ = -1		2.55	2.27	2.59	1.13	0.99
Average					1.03	0.99
Standard deviation					0.05	0.01
UDL	500	1.12	1.14	1.15	0.99	0.98
Mid-PL		1.33	1.32	1.36	1.01	0.98
2-PL		1.08	1.14	1.10	0.95	0.98
ψ = 1		1.00	1.00	1.00	1.00	1.00
ψ = 0.5		1.31	1.25	1.32	1.05	0.99
ψ = 0		1.73	1.67	1.78	1.04	0.97
ψ = -0.5		2.20	2.17	2.36	1.01	0.93
ψ = -1		2.30	2.27	2.59	1.01	0.89
Average					1.01	0.96
Standard deviation					0.03	0.04
UDL	1500	1.11	1.14	1.15	0.98	0.97
Mid-PL		1.30	1.32	1.36	0.99	0.96
2-PL		1.07	1.14	1.10	0.94	0.97
ψ = 1		1.00	1.00	1.00	1.00	1.00
ψ = 0.5		1.30	1.25	1.32	1.04	0.99
ψ = 0		1.69	1.67	1.78	1.01	0.95
ψ = -0.5		2.07	2.17	2.36	0.96	0.88
ψ = -1		2.09	2.27	2.59	0.92	0.81
Average					0.98	0.94
Standard deviation					0.04	0.06

The moment gradient factor C_b drops by 2.0-5.0 % with the increase in the fastener's stiffness k from 0 to 1500 *N/mm* for the studied load cases except for the case of ψ = -0.5 and ψ = -1 where the drop reaches 19.0%. Since the moment gradient coefficients in Sahraei et al. and AWC-TR14 are intended for monolithic wooden beams, using their coefficients with built-up beams would overestimate the capacity by 0-19%.

3.8.1.4 Load height effect

The reference beam was reconsidered to examine the load height effect. The beam was subjected to a top-face loading in the form of UDL, Mid-PL, 2PL at third span points, and 3PL at quarter span points. For each case, three fastener stiffnesses were examined: $k = 0$ (i.e., no connection between both plies), $k = 500$ N/mm and $1500\,N/mm$. In all cases, the load height factor C_L was computed by dividing the predicted critical moment M_{cr} for the case of top face loading by that for the beam under shear center loading M_{cr-sc}. AWC-TR14 [3.33] and Sahraei et al. study [3.14] proposed a load height coefficient in the form $C_L = \sqrt{1+\eta^2} - \eta$, in which $\eta = \left(k_A y_q / L\right)\sqrt{EI_y / GJ}$, y_q is a normalized load height as measured from the shear center and is taken as $y_q = d/2$ for top flange loading, and k_A is a load-dependent coefficient and takes the values 1.44, 1.72, 1.63, and 1.45 in [3.33] and 1.46, 1.81, 1.60, and 1.54 in [3.14], respectively, for UDL, Mid-PL, 2PL, and 3PL loading. The corresponding height effect coefficients are given in Columns 3-5 of Table 3.5. For the case $k = 0$, the present model predicts C_L values in close agreement with those based on [3.14], [3.33]. As the stiffness of the fastener increases, the load height coefficient C_L as predicted by the present model is observed to slightly decrease relative to the case of no connection. As a result, the use of the AWC-TR14 [3.33] and Sahraei et al. [3.14] load height coefficients (devised for

monolithic beams) would slightly overestimate the critical moments for two-ply beams connected with discrete fasteners by 0-3%.

Table 3.5: Effect of loading type on load height coefficient C_L for top face loading for 5m span two-ply beam with 38×286 mm per ply

Load Cases (1)	k (N/mm) (2)	Load height coefficient			Ratio	
		Present study (3)	AWC-TR-14 (4)	Sahraei Study (5)	(6)= (3)/(4)	(7)= (3)/(5)
UDL	0	0.918	0.916	0.918	1.00	1.00
Mid-PL		0.891	0.898	0.902	0.99	0.99
2-PL		0.910	0.909	0.907	1.00	1.00
3-PL		0.914	0.912	0.917	1.00	1.00
					1.00	1.00
					0.01	0.01
UDL	500	0.907	0.916	0.918	0.99	0.99
Mid-PL		0.877	0.898	0.902	0.98	0.97
2-PL		0.898	0.909	0.907	0.99	0.99
3-PL		0.902	0.912	0.917	0.99	0.98
					0.99	0.98
					0.01	0.01
UDL	1500	0.894	0.916	0.918	0.97	0.97
Mid-PL		0.860	0.898	0.902	0.96	0.95
2-PL		0.883	0.909	0.907	0.97	0.97
3-PL		0.888	0.912	0.917	0.97	0.97
Average					0.97	0.97
Standard deviation					0.01	0.01

3.8.1.5 Effect of beam dimensions

The reference case was reconsidered for investigating the effect of the beam dimensions on the critical moment of the built-up beams. The reference parameters are ply length to depth ratio $L/d = 17.42$, ply depth to width ratio $d/b = 7.53$, longitudinal fastener spacing to span ratio $S_p/L = 0.06$, transverse fastener spacing to depth $S_q/d = 0.34$, and total normalized fasteners' stiffness $n\bar{k} = 7650$

. Parametric runs were conducted by varying L/d from 16.0 to 20.0 and d/b from 7.00 to 8.50 (Figure 3.7), while maintaining the reference values for S_p/L, S_q/d and $n\bar{k}$. The normalized critical moment remains essentially unchanged, i.e., it can be considered independent of the geometric parameters L/d and d/b.

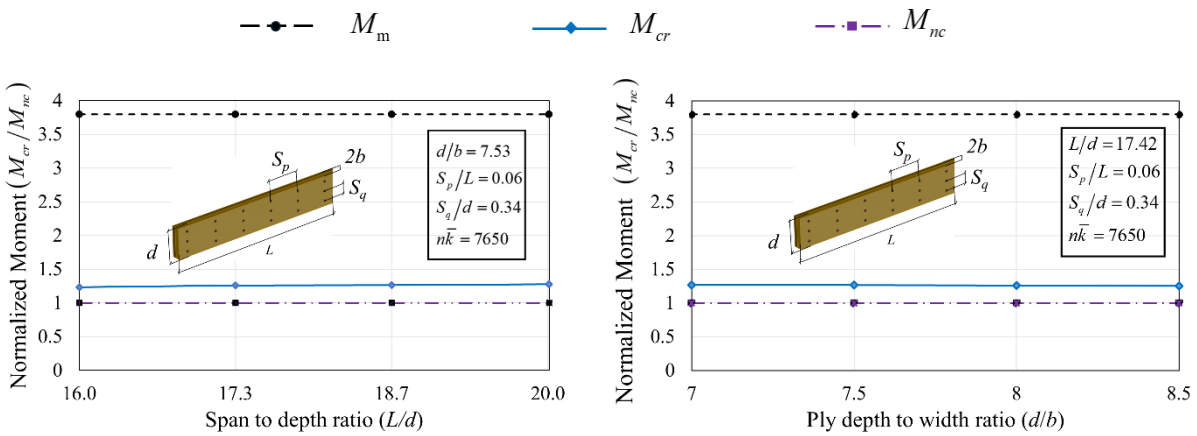

(a) (b)

Figure 3.7 Normalized Critical moment versus (a) Span to depth ratio *L/d*; and (b) depth to ply width ratio *d/b*

3.8.2 Fasteners with Non-Uniform Spacing

3.8.2.1 Non-uniform nailing patterns for a simply supported beam

In design practice, it is common to adopt a uniform fastener distribution along the member span. In this context, this section explores the possibility of attaining more favourable designs by considering the possibility of concentrating the fasteners in specific portions of the span. Toward this goal, three scenarios were considered (Figure 3.10.a): (1) fasteners concentrated near beam ends (E) within a length $L/5$ at both ends, (2) fasteners concentrated in two intermediate zones (I) over a length $L/5$, and (3) fasteners concentrated in the central $2L/5$ zone of the beam in the neighborhood of the midspan (M). In all three scenarios, the longitudinal spacing was taken as $S_p = 180mm$ within the zones of fastener concentration and $S_p = 500mm$ in the remaining portion. The

reference scenario corresponding to a uniform distribution (U) of fasteners with spacing $S_p = 300mm$ is provided as a benchmark. In all four cases, the total number of fasteners was kept constant at $n = 51$. The beams in all scenarios have the same boundary and loading conditions as the reference beam which is a simply supported beam with longitudinal restraint at the left end subjected to a uniform moment. The mode shapes of the beam are presented in Figure 3.8 while the corresponding relative displacements of the fasteners at the interface are presented in Figure 3.9. The ratio M_{cr}/M_{ref} of critical moments based on uneven fastener distribution scenarios (E, I, M) to that of the reference case that has uniform distribution (U) are 1.06, 0.99 and 0.97 respectively [Figure 3.10.b]. Scenario (E) with the dense nailing towards the end is observed to be the most effective scenario as it increases the critical moment by 6.0% above the conventional uniform distribution case (U). The effectiveness of the end-concentrating scenario stems from the fact that concentrating the fasteners near the end reduces the differential longitudinal displacements at the interface of both plies and accordingly at the shear plane of fasteners located near the end of the beam as shown in Figure 3.9.b. This in turn reduces the average shear force per fastener at the fastener shear plane. In contrast, Scenario (M) results in a reduction in the predicted critical moment, as in this case the fasteners are concentrated in the region of the least relative longitudinal displacements. While Scenario (I) almost attained the same critical moment as the uniform distribution case (U).

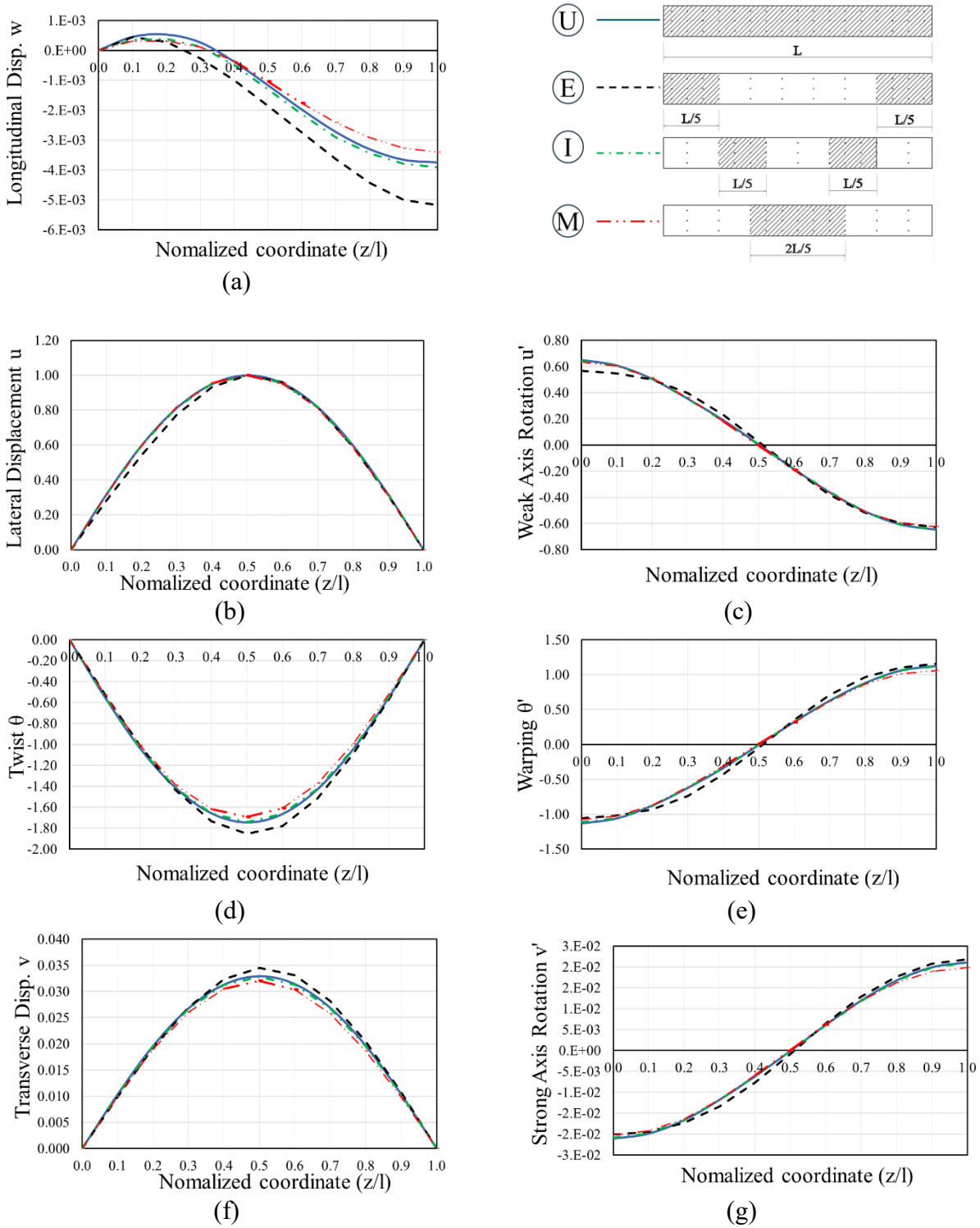

Figure 3.8 Normalized Mode Shapes for a simply supported built-up beam with uneven fastener densities: a) longitudinal displacement; (b) lateral displacement; (c) weak-axis rotation; (d) twist; (e) warping; (f) transverse displacement; and (g) strong axis rotation. (Mode shapes have been normalized relative to the peak lateral displacement).

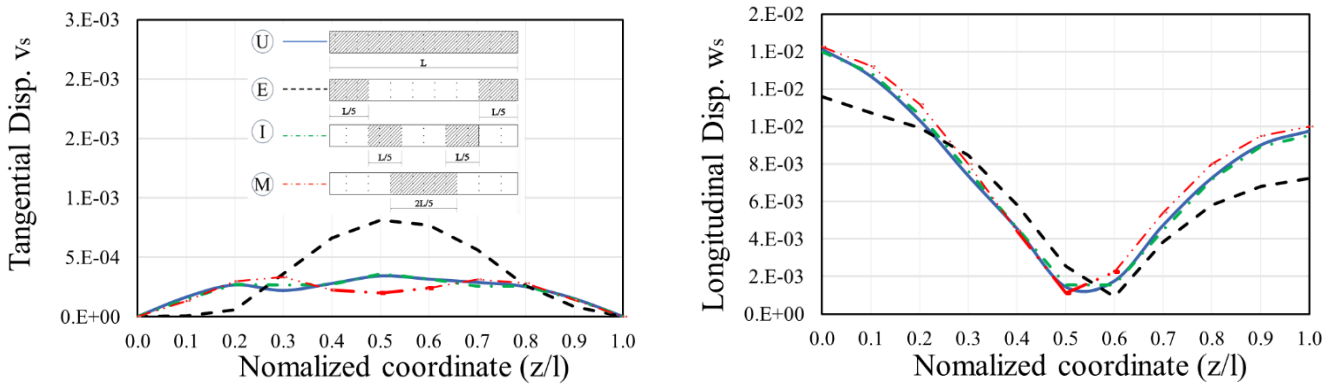

Figure 3.9 Relative displacements of fasteners of a simply supported built-up beam as extracted from the normalized buckling modes; a) transverse displacement v_s ; (b) Longitudinal displacement w_s

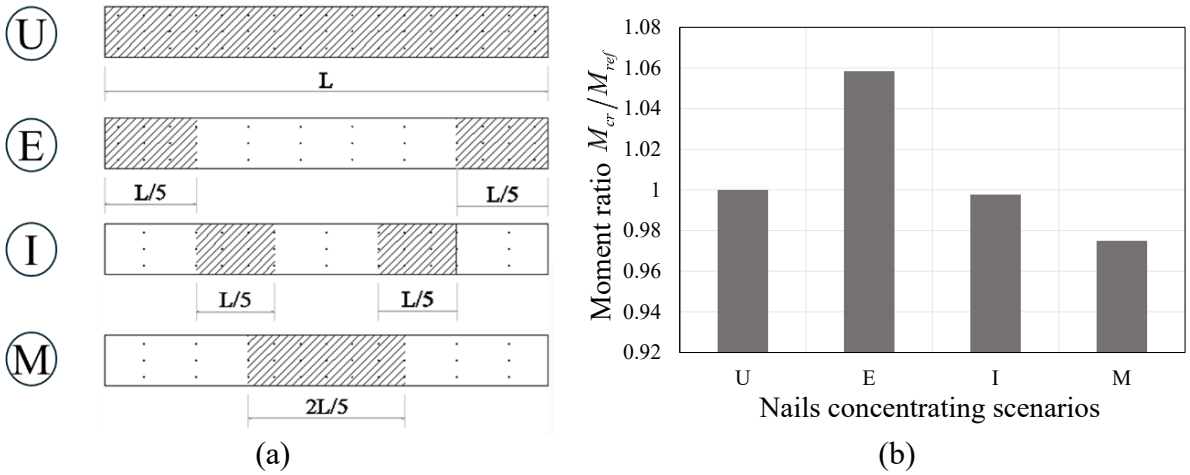

Figure 3.10 (a) Scenarios for uneven fastener density (total number of fasteners =51), (b) Attained normalized bending moment.

3.8.2.2 Effect of the Longitudinal Restraint Location

The parametric runs in the previous sub-section were based on the assumption of a longitudinal restraint at the left end. In contrast, the present section explores the effect of the location of the longitudinal restraint on the critical moment and the mode shapes. Towards this objective, the present section considers a beam that is laterally and transversely restrained at both ends and

longitudinally restrained at mid-span. In contrast to the unsymmetric mode shapes observed in Figure 3.8 and Figure 3.9, the mode shapes of the present case are observed to be perfectly symmetric/ anti-symmetric (Figure 3.11 and Figure 3.12) owing to the perfect symmetry of the boundary conditions. The critical moment for the case of a midspan longitudinal restraint is found to be marginally lower than the case of a single-end longitudinal restraint. However, restraining both ends longitudinally is observed to yield a slightly higher critical moment than that of the case of a single-end longitudinal restraint (Figure 3.13.b). Also, Scenario (E) with the dense nailing towards the end is observed to be the most effective scenario as it can maximize the critical moment more than the uniform scenario (U). In contrast, Scenario (M) reduces the critical moment, and Scenario (I) does not experience a significant difference from the case of the uniform Scenario (U).

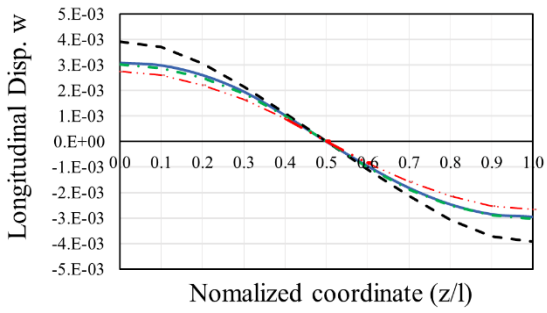

(a)

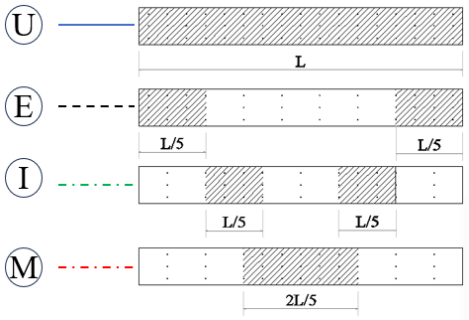

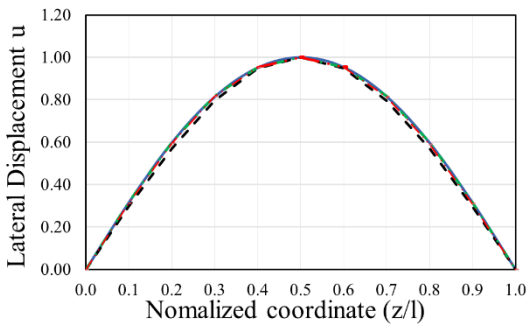

(b)

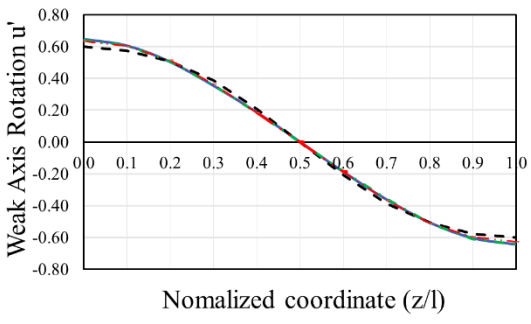

(c)

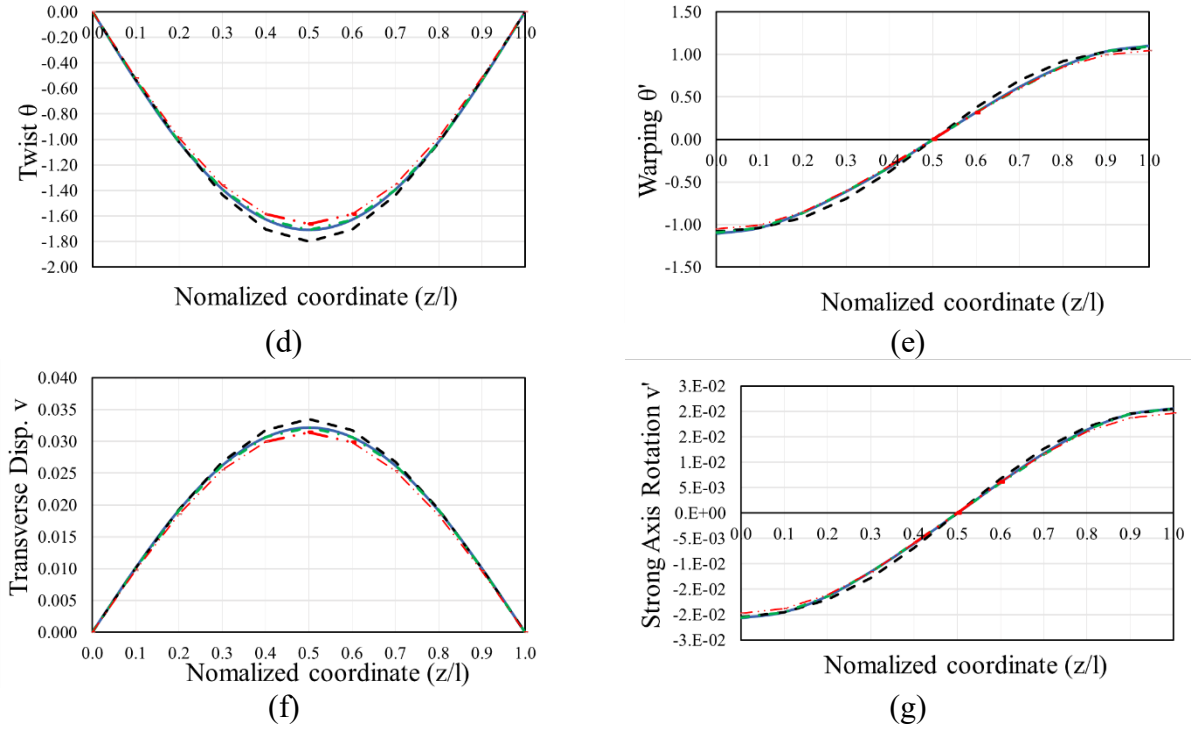

Figure 3.11 Normalized Mode Shapes for a built-up beam longitudinally restrained at the mid-span with uneven fastener densities: a) longitudinal displacement; (b) lateral displacement; (c) weak-axis rotation; (d) twist; (e) warping; (f) transverse displacement; and (g) strong axis rotation. (Mode shapes have been normalized relative to the peak lateral displacement).

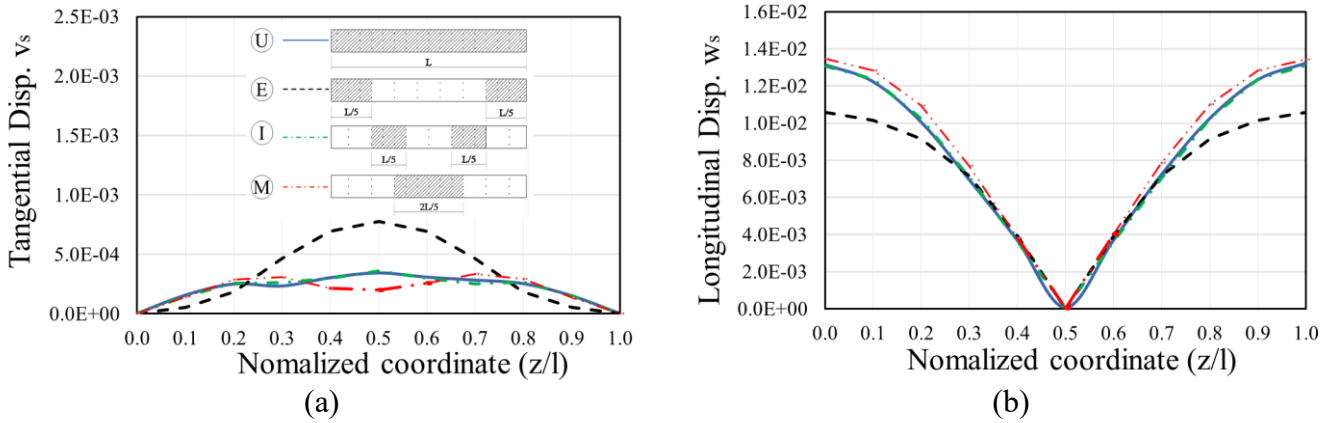

Figure 3.12 Relative displacements of fasteners of a built-up beam longitudinally restrained at the mid-span as extracted from the normalized buckling modes; a) transverse displacement v_s ; (b) Longitudinal displacement w_s

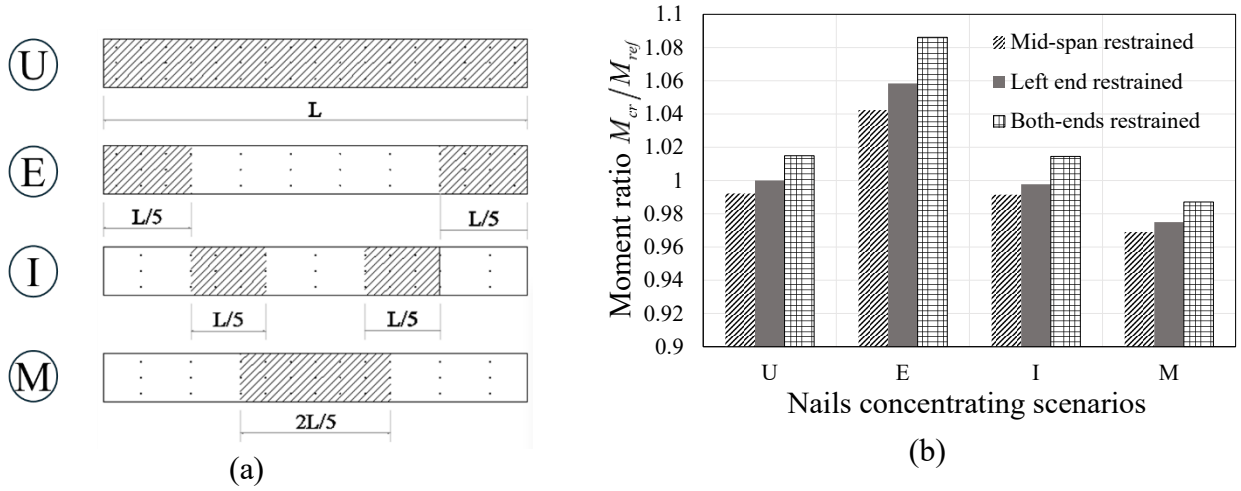

Figure 3.13 (a) Selected scenarios for the distribution of the fasteners maintaining the same total number of fasteners and (b) effect of different fasteners distribution scenarios and longitudinal restraint location on the critical moment normalized relative to the critical moment M_{ref} for the case of left end longitudinal restraint with uniform fastener distribution.

3.9 Summary and Conclusions

The present study developed a variational principle and finite element formulation to predict the elastic lateral torsional buckling capacity of built-up wooden beams consisting of two plies connected together with discrete fasteners. The formulation accounts for the shear stiffness of the fasteners and captures the effects of the moment gradient and the load height. The study considered uniform and non-uniform nail patterns. The following conclusions are drawn from the parametric runs:

1- The critical moment of built-up beams with two plies connected with discrete fasteners of common stiffness and nailing patterns based on the allowed spacing by CSA O86:19 [3.1] was found to be significantly lower than that of a monolithic beam with identical geometry.

2- For a given total fasteners' stiffness, increasing the number of fasteners while reducing the stiffness of the individual fasteners was found to be more beneficial in increasing the critical moment than increasing the stiffness per fastener and decreasing the number of fasteners.

3- As the fasteners' stiffness increases, the load height coefficient C_L and the moment gradient coefficient C_b decrease. Adopting the conventional moment gradient coefficient C_b and the load height coefficient C_L, which were originally developed for monolithic beams, in the case of built-up beams can overpredict the moment gradient coefficient by 0-19% and the load height coefficient by 0-3%. Consequently, the present study recommends applying a reduction factor to both coefficients when applied to built-up beams.

4- Adopting a denser nailing pattern near the end of simply supported beams was found to increase the critical moment when compared to the conventional uniform pattern by nearly 6%.

5- While this paper investigates the elastic LTB of built-up slender beams with two plies, future work can explore the LTB of built-up beams with more than two plies. Also, it is recommended to conduct full non-linear analyses that incorporate geometric and material imperfections.

Acknowledgments:

The authors gratefully acknowledge research funding to the Senior authors from the Natural Sciences and Engineering Research Council of Canada (NSERC) and Canadian Wood Council and Scholarship Support to the Junior author from the University of Ottawa.

References

[3.1] Canadian Standard Association (CSA), *CSA Standard O86-19 Engineering design in wood*. 2019.

[3.2] American Wood Council, *National design specification for wood construction*. Leesburg, VA, USA, 2024.

[3.3] CEN, *Eurocode 5: Design of timber structures - Part 1-1: General - Common rules and rules for buildings Eurocode*, vol. 1. 2004.

[3.4] R. . Hooley and B. Madsen, "Lateral Stability of Glued Laminated Beams," *J. Struct. Div.*, vol. 90, no. 3, 1964.

[3.5] D. P. Hindman, H. B. Manbeck, and J. J. Janowiak, "Measurement and prediction of lateral torsional buckling loads of composite wood materials: Rectangular sections," *For. Prod. J.*, vol. 55, no. 10, pp. 43–48, 2005.

[3.6] D. P. Hindman, H. B. Manbeck, and J. J. Janowiak, "Measurement and prediction of lateral torsional buckling loads of composite wood materials: I-joist sections," *For. Prod. J.*, vol. 55, no. 10, pp. 43–48, 2005.

[3.7] Q. Xiao, G. Doudak, and M. Mohareb, "Numerical and experimental investigation of lateral torsional buckling of wood beams," *Eng. Struct.*, vol. 151, pp. 85–92, 2017, doi: 10.1016/j.engstruct.2017.08.020.

[3.8] R. St-Amour and G. Doudak, "Experimental and numerical investigation of lateral torsional buckling of wood I-joists," *Can. J. Civ. Eng.*, vol. 45, no. 1, pp. 41–50, 2018, doi: 10.1139/cjce-2017-0281.

[3.9] B. Pelletier and G. Doudak, "Investigation of the lateral-torsional buckling behaviour of engineered wood I-joists with varying end conditions," *Eng. Struct.*, vol. 187, no. November 2018, pp. 329–340, 2019, doi: 10.1016/j.engstruct.2019.03.003.

[3.10] J. Töpler and U. Kuhlmann, "Lateral torsional buckling of glulam beams," in *10th International Network on Timber Engineering Research (INTER)*, Biel/Bienne,

Switzerland, 2023, pp. 6–12. doi: 10.18419/opus-13593.

[3.11] Y. Du, M. Mohareb, and G. Doudak, "Nonsway Model for Lateral Torsional Buckling of Wooden Beams under Wind Uplift," *J. Eng. Mech.*, vol. 142, no. 12, 2016.

[3.12] Y. Du, M. Mohareb, and G. Doudak, "Sway Model for the Lateral Torsional Buckling Analysis of Wooden Twin-beam-deck Systems," *Structures*, vol. 19, no. November 2018, pp. 19–29, 2019, doi: 10.1016/j.istruc.2018.11.012.

[3.13] Y. Du, G. Doudak, and M. Mohareb, "Effect of beam-deck connection flexibility on lateral torsional buckling strength of wooden twin-beams," *Eng. Struct.*, vol. 207, no. November 2019, p. 110226, 2020, doi: 10.1016/j.engstruct.2020.110226.

[3.14] A. Sahraei, P. Pezeshky, M. Mohareb, and G. Doudak, "Simplified expressions for elastic lateral torsional buckling of wooden beams," *Eng. Struct.*, vol. 174, no. February, pp. 229–241, 2018, doi: 10.1016/j.engstruct.2018.07.042.

[3.15] G. Doudak, M. Mohareb, and Y. Du, "Proposed Design Approach for Lateral Stability of Timber Beams," in *International Network on Timber Engineering Research (INTER)*, 2022, p. 55-10-1.

[3.16] R. A. S. Ribeiro and P. J. Pellicane, "Modeling load-slip behavior of nailed joints," *J. Mater. Civ. Eng.*, vol. 4, no. 26692, pp. 385–398, 1992.

[3.17] U. A. Girhammar and V. K. A. Gopu, "Composite beam-columns with interlayer slip-exact analysis," *J. Struct. Eng.*, vol. 119, no. 4, pp. 1265–1282, 1993.

[3.18] N. T. Mascia, C. L. de O. Santana, and Steven M. Cramer, "Evaluation of the Equivalent Slip Modulus of Nailed Connections for Application in Linear Analysis of Plywood Timber

Beams," *Mater. Res.*, vol. 11, no. 2, pp. 151–157, 2008.

[3.19] N. T. Mascia and C. L. de O. Santana, "Remarks on the slip modulus of nailed connections for linear analysis of plywood timber beams," *Constr. Build. Mater.*, vol. 23, no. 8, pp. 2731–2737, 2009, doi: 10.1016/j.conbuildmat.2009.02.037.

[3.20] J. F. Miller and W. M. Bulleit, "Analysis of Mechanically Laminated Timber Beams Using Shear Keys," *J. Struct. Eng.*, vol. 137, no. 1, pp. 124–132, 2011, doi: 10.1061/(asce)st.1943-541x.0000273.

[3.21] N. Challamel and U. A. Girhammar, "Lateral-torsional buckling of vertically layered composite beams with interlayer slip under uniform moment," *Eng. Struct.*, vol. 34, pp. 505–513, 2012, doi: 10.1016/j.engstruct.2011.10.004.

[3.22] G. Robatmili, Robabeh, Du, Yang and Doudak, "Effect of fastener stiffness on buckling behaviour of wooden built-up beams," *CSCE 2022 Annu. Conf. Whistler, Br. Columbia*, 2022.

[3.23] R. Robatmili, "Lateral Torsional Buckling of Timber Built-up Beams," University of Ottawa, 2022.

[3.24] Y. Hu, M. Mohareb, and G. Doudak, "Lateral Torsional Buckling of Wooden Beams with Midspan Lateral Bracing Offset from Section Midheight," *J. Eng. Mech.*, vol. 143, no. 11, pp. 1–13, 2017, doi: 10.1061/(asce)em.1943-7889.0001359.

[3.25] Y. Hu, M. Mohareb, and G. Doudak, "Effect of Eccentric Lateral Bracing Stiffness on Lateral Torsional Buckling Resistance of Wooden Beams," vol. 18, no. 02, pp. 1–34, 2018.

[3.26] Hörsting, "Zum Tragverhalten druck- und biegebeanspruchter Holzbauteile," Der

Universität Carolo-Wilhelmina zu Braunschweig, 2008.

[3.27] Q. Xiao, G. Doudak, and M. Mohareb, "Lateral torsional buckling of wood beams: Fea-modelling and sensitivity analysis," *WCTE 2014 - World Conf. Timber Eng. Proc.*, vol. 2, no. 1, 2014.

[3.28] L. A. Soltis, S. Karnasudirdja, and J. K. Little, "Angle to grain strength of dowel-type fasteners," *Wood Fiber Sci.*, vol. 19, no. 1, pp. 68–80, 1987.

[3.29] Simulia, "Abaqus/CAE," 2016, *ABAQUS analysis user's manual*.

[3.30] L. A. Winistorfer, S.G. and Soltis, "Lateral and Withdrawal Strength of Nail Connections for Manufactured Housing," *J. Struct. Eng.*, vol. 120, no. 12, pp. 3577–3594, 1994.

[3.31] FPL, *Wood Handbook*, 2010th ed. Madison, USA, 2010.

[3.32] B. J. F. Davalos, A. Member, J. R. Loferski, and V. Yadama, "Transverse Isotropy Modelling of 3-D glulam timber beams," *ASCE*, vol. 3, no. 2, pp. 125–139, 1991.

[3.33] American Wood Council, "Designing for lateral-torsional stability in wood members, AFPA Technical Report 14," Washington, D.C, USA, 2003.

3.10 Notation

The following symbols are used in this paper:

A : Cross sectional Area

a : End distance of fasteners.

b : Ply width.

c = half ply width

C_b : Moment gradient factor for built-up beams.

C_B : Slenderness ratio

C_L : Load height factor, defined as the ratio between the critical moment when loads are applied at an offset from the shear center and that when the load is applied at the shear center.

d : Ply depth.

E : Young's modulus of timber.

E_X, E_Y and E_Z : Three moduli of elasticity along the global coordinates X, Y, Z.

E_L, E_T and E_R : Three moduli of elasticity along the longitudinal L, the tangential T, and the radial R directions in Abaqus.

e : Beam finite element index.

e_d : Edge distance

G : Shear modulus of timber.

G_{XY} , G_{XZ} and G_{YZ} : Three shear moduli on the three global faces of the beam XY, XZ, YZ.

G_{LT} , G_{LR} G_{RT} : Three shear moduli on the three main faces LT, LR, RT in Abaqus.

H : Hermitian interpolation functions

$\mathbf{H}_1, \mathbf{H}_2$: Vector of cubic Hermitian polynomials.

I_x : Major-axis moment of inertia.

I_y : Minor-axis moment of inertia.

$I_{y,m}$: Minor-axis moment of inertia of monolithic section.

J : Saint-Venant torsional constant of a single ply.

J_m : Saint-Venant torsional constant for the monolithic (fully composite) section.

j : Fastener index within a fastener group.

k : Fastener stiffness.

$\overline{k}$: Normalized fastener stiffness.

$\mathbf{K}$: stiffness matrix.

L : Span of the built-up beam.

$\mathbf{L}$: Vector of Linear interpolation functions.

l_e : Length of beam finite element e

M : Bending moment of the beam.

M_1 : End bending moment at $z = 0$.

M_2 : End bending moment at $z = L$.

M_{cr} : Elastic lateral–torsional buckling critical moment.

M_{cru} : Uniform critical moment of the built-up beam

M_m : Uniform critical moment of the monolithic (fully composite) section.

M_{nc} : Uniform critical moment of the non-composite (no interaction) case.

n_i : Number of fasteners in columns i.

n_e : Beam segment between two fastener columns (groups).

S_P : Longitudinal fastener spacing (parallel to the grain).

S_q : Transverse fastener spacing (perpendicular to the grain).

q : Transverse load acting on each ply.

u : Lateral displacement of the plies during buckling.

$\mathbf{u}_e(z)$: Vector of nodal lateral displacements

v_γ :Transverse displacement of ply γ.

v_s : Transverse displacement of fasteners

$\mathbf{V}_e(z)$: Vector of nodal transverse displacements

$\mathbf{W}_e(z)$: Vector of nodal longitudinal displacements.

w_γ : Longitudinal displacement of ply γ.

w_s : Longitudinal displacement of fasteners

y_j : Vertical location of fastener $j$measured from the shear center.

y_q : Load height measured below the shear center.

z : Longitudinal coordinate along the beam axis.

z_i : Longitudinal coordinate of fastener plane i.

UDL : Uniformly distributed load.

1-PL : Mid-span point load.

2-PL : Two point loads applied at one-third points along the span.

α: Degree of interaction between plies; values near zero indicate no interaction, while a value of one denotes full interaction.

β : Parameter defining ply numbering limits depending on whether the number of plies is odd or even.

γ : Ply index.

λ : Load multiplier to be determined from the buckling analysis.

π : Total potential energy of the built-up system throughout buckling.

$\pi_{b,e}$: Total potential energy stored in the plies of beam segment e.

$\pi_{s,i}$: Internal strain energy stored in the fastener group located at fastener plane i.

ρ_m : Mean wood density.

θ : Angle of twist of the built-up beam.

$\mathbf{\theta}_e(z)$: Vector of nodal angles of twist

$\mu_{XY}, \mu_{XZ}, \mu_{YZ}$: Three major Poisson's ratios on the three global faces of the beam XY, XZ, YZ.

$\mu_{LR}, \mu_{RL}, \mu_{RT}, \mu_{TR}, \mu_{LT}$, and μ_{TL} : Six Poisson's ratios in Abaqus.

Chapter 4: Elastic Lateral Torsional Buckling of Multi-Ply Built up Timber Beams[1]

Abstract

A beam finite element formulation is developed for the elastic lateral torsional analysis of built-up timber beams consisting of multiple plies that are vertically connected by discrete fasteners. The solution captures the partial interaction between plies and its validity is demonstrated through comparisons against the predictions of 3D finite element models and full-scale lateral torsional buckling experiments. The formulation is subsequently used to generate a database of 733 parametric runs to quantify the effect of the key factors on the LTB resistance of built-up members. The database is then used to develop dimensionless regression equations to characterize the uniform critical moment, moment gradient factor, and load height factor for built-up beams. The equations are then consolidated into a simple procedure, and the use of the proposed procedure in a design context is illustrated through examples.

Keywords: Lateral torsional buckling, built-up timber beams, multiple plies, composite action, slip, finite element.

4.1 Introduction and Literature Review

Built-up wooden beams formed by connecting multiple plies of equal depth using mechanical fasteners offer an economic advantage over timber beams with monolithic cross-sections of identical size. When such built-up beams have long unbraced lengths and are subjected to major-axis flexure, they become prone to a lateral torsional buckling (LTB) mode of failure which is

[1] This chapter has been submitted to an international journal and is currently under review.

expected to dictate their flexural resistance. An upper bound for the LTB resistance of built-up beams can be obtained by assuming full composite action between plies, i.e., treating the built-up section as a monolithic entity. A lower bound for their LTB resistance can be obtained by omitting the shear interaction between plies, thus treating the built-up beam as a series of independent plies. In practice, mechanical fasteners provide partial shear interaction between plies, and the LTB resistance of built-up beams is expected to lie between the two bounds.

The previous Canadian wood design standard CSA O86:19 [4.1] enabled the adoption of the lateral-torsional buckling (LTB) capacity of an equivalent monolithic section, provided that plies are securely connected at spacing intervals not exceeding four times the beam depth. The ambiguity surrounding how to securely connect the plies prompted a shift to a more conservative approach in the most recent version of the standard, CSA O86:24 [4.2], in which the LTB capacity is taken as the sum of the individual capacities of its plies. The American Standard [3] and Eurocode [4.3], [4.4] do not provide guidance for estimating the LTB capacity of built-up beams. Within this context, the present study aims to quantify the LTB capacity of built-up beams in a manner that accounts for the degree of interaction between plies.

The following review will first survey the experimental and numerical research on the LTB of monolithic timber beams and will then review aspects related to the LTB of built-up timber beams. LTB tests on monolithic timber beams include the work of Hooley and Madsen [4.5], Xiao et al. [4.6], Capellán et al. [4.7] and Töpler and Kuhlmann [4.8], while LTB tests on timber I joists include the work of St-Amour and Doudak [4.9] and Pelletier and Doudak [4.10].

Analytical research on monolithic timber beams includes the effect of lateral bracing on the LTB, (Hu et al. [4.11], [4.12]). Finite element developments on the LTB of timber beam-deck systems under wind uplift include the work of Du et al. [4.13] on non-sway systems and Du et al. [4.14] on

sway systems. The effect of rotational flexibility of deck–beam connections on LTB systems was investigated in Du et al. [4.15]. Sahraei et al. [4.16] developed an energy-based solution that captures the effects of moment gradient, load height, pre-buckling deformations, and partial twist end restraints on LTB capacity. The LTB of multi-segment beams was investigated in Doudak et al. [4.17] and the load height effect on the LTB of continuous beams was investigated in Mansor et al. [4.18].

In built-up beams, the composite action between plies depends on the load–deformation characteristics of the fasteners along ply interfaces. In this respect, Ribeiro and Pellicane [4.19] conducted an experimental program to investigate the effect of wood density and connection geometry on load-slip behavior of nailed wood joints. Miller and Bulleit [4.20] characterized the interlayer slip in horizontally laminated beams connected with inclined and square shear keys. Mascia and Santana [4.21] carried out analytical and experimental investigations to determine the slip modulus associated with nailed plywood joints. The Eurocode 5 [4.4] provides an empirical equation to estimate the elastic stiffness of sheared fasteners as a function of the fastener diameter and the wood density. Robatmili [4.22] conducted an experimental investigation to obtain the shear stiffness for nailed and screwed assemblies.

LTB studies on multi-ply built-up beams remain limited. Challamel and Girhammar [4.23] proposed an analytical LTB solution for two-ply beams connected at their vertical interface with a continuous adhesive layer subjected to uniform moments. Robatmili et al. [4.24] numerically investigated the LTB of built-up laminated veneer lumber (LVL) beams. In a recent study, Waltz et al. [4.25] experimentally investigated the LTB of built-up LVL beams. Mansor et al. [4.26] developed a 3D finite element model and formulated a beam finite element [4.27] to determine the LTB resistance of built-up beams. Both solutions, however, were limited to two-ply built-up

systems. In this respect, this study extends previous work by formulating a generalized beam finite-element model applicable to built-up members with an arbitrary number of plies, which captures the partial composite action offered by the connections between plies. The study then uses the solution to generate a database of runs and subsequently develops a series of simplified design-oriented equations.

4.2 Statement of the Problem

A simply supported built-up wooden beam of span L consists of n_p vertical plies of equal height d and ply width b. The plies are connected through $s-1$ groups of fasteners. Each group $i=1,2...s-1$ of fasteners is arranged in a vertical plane located at a coordinate z_i along the built-up beam axis and consists of n_f fasteners stacked vertically. The $s-1$ fastener planes subdivide the beam longitudinally into s segments. Each of the fasteners $j=1,2....n_f$ is located at a height y_j relative to the shear center. Each ply is assumed to be subjected to a transverse load $q(z)$ acting at a height $y_q(z)$ below the shear center, and/or end moments M_1, M_2 acting at $z=0$ and $z=L$. It is required to determine the elastic lateral torsional buckling resistance of the built-up system.

4.3 Assumptions

The present formulation generalizes the formulation reported in [4.27]. Hence, the underlying assumptions remain similar to those in [4.27] with the difference that the current solution accommodates an arbitrary number of plies, whereas the solution in [4.27] is restricted to only two plies. The main assumptions are:

1- Warping effects within all plies are neglected. The validity of this assumption has been supported for rectangular cross-sections in past investigations (e.g., [4.6], [4.11], [4.12], [4.28]).

2- The constitutive behaviour of timber is fully characterized by the longitudinal Young's modulus and the shear modulus on the transverse plane [4.29].

3- Throughout buckling, the plies are assumed to undergo equal lateral displacement and twist, with no cross-sectional distortion (e.g., [4.11], [4.15]), while the transverse and longitudinal displacements of plies symmetrically placed relative to the vertical centreline of the assembly are equal and opposite [4.27].

4- Pre-buckling deformation effects are neglected.

5- The fasteners are assumed to possess identical stiffnesses in the transverse (y-axis) and longitudinal (z-axis) directions (e.g., [4.4]).

6- The interfacial friction is conservatively excluded from the analysis.

7- The formulation assumes small displacements and moderate rotations, i.e., the angle of twist θ satisfies the approximations $\theta \approx \sin\theta \approx \tan\theta$ and $\cos\theta \approx 1-\theta^2/2$.

4.4 Formulation

4.4.1 Notation

When the number of plies n_p is odd, the central ply is designated by $\gamma = 0$. Irrespective of whether n_p is odd or even, the plies to the left of the built-up assembly are numbered as $\gamma = -\beta,,.....-2,-1$ from left to right, while the plies to the right are numbered $\gamma = 1,2,...,\beta$, in which

$$\beta = \begin{cases} n_p/2, & n_p \text{ is even} \\ (n_p-1)/2 & n_p \text{ is odd} \end{cases} \tag{4.1}$$

Figure 4.1 depicts a built-up beam subjected to lateral torsional buckling. Stage (1) represents the unloaded beam. Under increasing transverse load, the beam undergoes transverse displacement (Stage 2). As the load continues to increase, it reaches a critical value that corresponds to the onset of buckling (Stage 3) at which the system has a natural tendency to buckle laterally to stage 4 (involving lateral displacement and twist) with no further increase in the applied load. At this stage, the angle of twist and lateral displacements for all plies are assumed to be identical, i.e., $\theta_\gamma = \theta$ and $u_\gamma = u$ while the transverse and longitudinal displacements in plies $-\gamma$ and γ are equal and opposite, i.e., $v_\gamma = -v_{-\gamma}$ and $w_\gamma = -w_{-\gamma}$ (Assumption 3).

4.4.2 Variational Principle

The total potential energy π for the built-up system consisting of s longitudinal segments and $(s-1)$ vertical planes of fasteners can be expressed as

$$\pi = \sum_{e=1}^{s} \pi_{b,e} + \sum_{i=1}^{s-1} \pi_{s,i} \tag{4.2}$$

in which the total potential energy $\pi_{b,e}$ stored in the plies of segment e is given by

$$\pi_{b,e} = (n_p/2)\int_0^{l_e} \left(EI_y u''^2 + GJ\theta'^2 + 2\lambda M \theta u'' + \lambda q y_q \theta^2 \right) dz + 1/2 \sum_{\gamma=-\beta}^{\beta} \int_0^{l_e} \left(EI_x v_\gamma''^2 + EA w_\gamma'^2 \right) dz \tag{4.3}$$

and E is Young's modulus in the longitudinal direction, G is the shear modulus on the transverse face, and J is the Saint-Venant torsional constant and I_y, I_x are the minor and major moments of inertia. It is noted that Eq. (4.3) omits warping effects (Assumption 1) and pre-buckling deformation effects (Assumption 4). The relative transverse displacement $v_{s,\gamma}(z_i)$

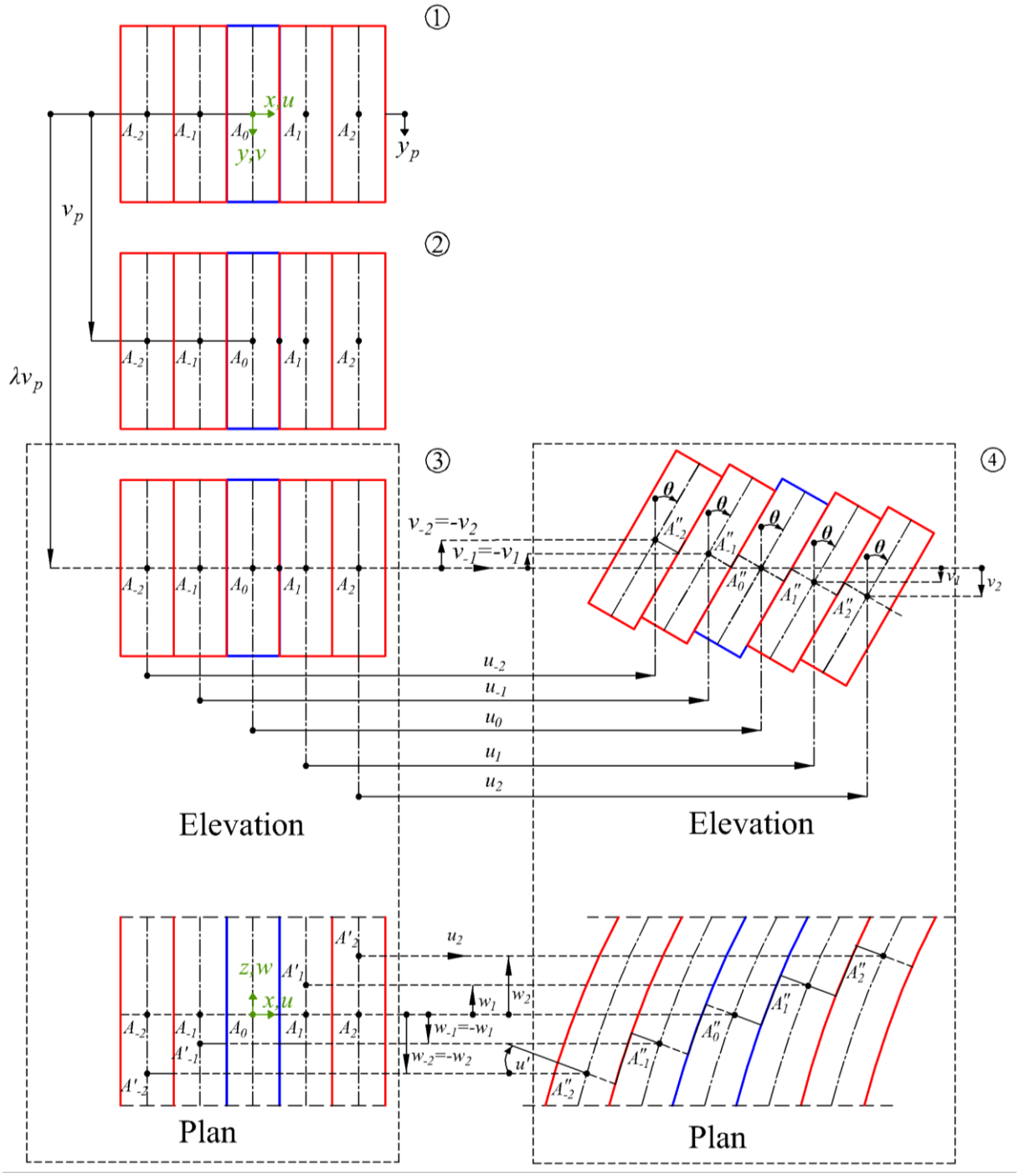

Figure 4.1 Lateral torsional Buckling kinematics for Built-up beam with five plies (1) Under no Loading (2) In a Pre-buckling state (3) At the Onset of Buckling and (4) In the Buckled Configuration

and longitudinal displacement $w_{s,\gamma}\left(y_j, z_i\right)$ of a fastener at the interface between plies γ and $\gamma+1$ are expressed in terms of the displacements of its adjacent plies as given by [4.27]:

$$\begin{aligned} v_{s,\gamma}\left(z_i\right) &= v_{\gamma+1}\left(z_i\right) - v_{\gamma}\left(z_i\right) - 2c\theta\left(z_i\right) \\ w_{s,\gamma}\left(y_j, z_i\right) &= w_{\gamma+1}\left(z_i\right) - w_{\gamma}\left(z_i\right) + 2cu'\left(z_i\right) + y_j v'_{\gamma+1}\left(z_i\right) - y_j v'_{\gamma}\left(z_i\right) \end{aligned} \tag{4.4a-b}$$

A system consisting of n_p plies, has $n_p - 1$ interfaces numbered as $-\beta, ...\beta - 1$. The internal strain energy $\pi_{s,i}$ stored in the group of fasteners located at longitudinal coordinate z_i and consisting of $j = 1, 2, ...n_f$ fasteners is the sum of the internal strain energies $U_{sv,i}$ associated with the relative transverse displacement $v_{s,\gamma}\left(z_i\right)$ and $U_{sw,i}$ related to the relative longitudinal displacement $w_{s,\gamma}\left(y_j, z_i\right)$, i.e.,

$$\pi_{s,i} = U_{sv,i} + U_{sw,i} \tag{4.5}$$

in which

$$U_{sv,i} = \frac{1}{2} n_f k \sum_{\gamma=-\beta}^{\gamma=\beta-1} v_{s,\gamma}\left(z_i\right)^2 \qquad U_{sw,i} = \frac{1}{2} k \sum_{\gamma=-\beta}^{\gamma=\beta-1} \sum_{j=1}^{j=n_f} w_{s,\gamma}\left(y_j, z_i\right)^2 \tag{4.6a-b}$$

From Eq. (4.4a-b), by substituting into Eq. (4.6a-b), one obtains

$$\begin{aligned} U_{sv,i} &= \frac{1}{2} k n_f \sum_{\gamma=-\beta}^{\gamma=\beta-1} \left[v_{\gamma+1}\left(z_i\right) - v_{\gamma}\left(z_i\right) - 2c\theta\left(z_i\right) \right]^2 \\ U_{sw,i} &= \frac{1}{2} k \sum_{\gamma=-\beta}^{\gamma=\beta-1} \sum_{j=1}^{j=n_f} \left[w_{\gamma+1}\left(z_i\right) - w_{\gamma}\left(z_i\right) + 2cu'\left(z_i\right) + y_j v'_{\gamma+1}\left(z_i\right) - y_j v'_{\gamma}\left(z_i\right) \right]^2 \end{aligned} \tag{4.7a-b}$$

4.4.3 Finite Element Formulation

For an element e of length l_e consisting of n_p plies denoted $\gamma = -\beta,....+\beta$, the lateral displacement $u_e(z)$ and angle of twist $\theta_e(z)$ for all plies are equal (Assumption 3), while the transverse displacements $v_{e,\gamma}(z)$ differ for each ply. Hermitian interpolation is used to relate the displacement fields $u_e(z)$, $\theta_e(z)$ and $v_{e,\gamma}(z)$ to the nodal displacement vectors $\mathbf{u}_e^{\mathbf{T}} = \langle u_{1,e} \quad u'_{1,e} \quad u_{2,e} \quad u'_{2,e} \rangle, \boldsymbol{\theta}_e^{\mathbf{T}} = \langle \theta_{1,e} \quad \theta'_{1,e} \quad \theta_{2,e} \quad \theta'_{2,e} \rangle$ $\tilde{\mathbf{V}}_{e,\gamma}^{\mathbf{T}} = \langle \mathbf{v}^{\mathbf{T}}{}_{e,-\beta} \quad \mathbf{v}^{\mathbf{T}}{}_{e,-\beta+1} \quad ... \quad \mathbf{v}^{\mathbf{T}}{}_{e,+\beta} \rangle_{1\times 4n_p}$

and $\mathbf{v}^{\mathbf{T}}{}_{e,\gamma} = \langle v_{1e,\gamma} \quad v'_{1,e,\gamma} \quad v_{2,e,\gamma} \quad v'_{2,e,\gamma} \rangle$, i.e.,

$$\begin{aligned} u_e(z) &= \mathbf{H_1}(z)^{\mathbf{T}}{}_{1\times 4}\, \mathbf{u}_{e4\times 1} \\ \theta_e(z) &= \mathbf{H_1}(z)^{\mathbf{T}}{}_{1\times 4}\, \boldsymbol{\theta}_{\mathbf{e}4\times 1} \\ \mathbf{V_{e,\gamma}}(z)_{n_p\times 1} &= \mathbf{B_1}(z)^{\mathbf{T}}{}_{n_p\times 4n_p}\, \tilde{\mathbf{V}}_{\mathbf{e}4n_p\times 1} \end{aligned} \tag{4.8}$$

in which

$$\begin{aligned} &\mathbf{H_1}^{\mathbf{T}}(z) = \left\langle\ 1-3\xi_e^{\,2}+2\xi_e^{\,3} \ \vdots\ \xi l(1-\xi_e)^2 \ \vdots\ 3\xi_e^{\,2}-2\xi_e^{\,3} \ \vdots\ l\xi_e^{\,2}(\xi_e-1)\right\rangle,\ \ \xi_e = z/l_e \\ &\mathbf{B_1}(z)^{\mathbf{T}} = \mathbf{Diag}\left[\mathbf{H_2}(z)^{\mathbf{T}}, \mathbf{H_2}(z)^{\mathbf{T}} .....\mathbf{H_2}(z)^{\mathbf{T}}\right]_{n_p\times 4n_p} \\ &\mathbf{H_2}^{\mathbf{T}}(z) = \left\langle\ 1-3\xi_e^{\,2}+2\xi_e^{\,3} \ \vdots\ -\xi_e l(1-\xi_e)^2 \ \vdots\ 3\xi_e^{\,2}-2\xi_e^{\,3} \ \vdots\ -l\xi_e^{\,2}(\xi_e-1)\right\rangle \end{aligned} \tag{4.9a-c}$$

Additionally, the longitudinal displacements of the plies of element e $\mathbf{w}_{e,\gamma}(z)_{n_p\times 1} = \langle w_{e,-\beta}(z) \quad w_{e,-\beta+1}(z) \quad ... \quad w_{e,+\beta}(z) \rangle^{\mathbf{T}}$ are linearly interpolated to the vector of nodal longitudinal displacements $\tilde{\mathbf{W}}_{\mathbf{e},\boldsymbol{\gamma}\ 2n_p\times 1} = \langle \mathbf{w}_{\mathbf{e},-\beta} \quad \mathbf{w}_{\mathbf{e},-\beta+1} \quad ... \quad \mathbf{w}_{\mathbf{e},\beta} \rangle^{\mathbf{T}}$ in which , $\mathbf{w}_{\mathbf{e},\boldsymbol{\gamma}} = \langle w_{1e,\gamma} \quad w_{2,e,\gamma} \rangle^{\mathbf{T}}$ through

$$\mathbf{W_{e,\gamma}}\left(z\right)_{n_p\times 1}=\mathbf{B_2}\left(z\right)^{\mathbf{T}}{}_{n_p\times 2n_p}\,\tilde{\mathbf{W}}_{\mathbf{e},\gamma\,2n_p\times 1} \tag{4.10}$$

in which

$$\mathbf{B}_2\left(z\right)^{\mathbf{T}}=\mathbf{Diag}\left[\mathbf{L}\left(z\right)^{\mathbf{T}},\mathbf{L}\left(z\right)^{\mathbf{T}}.....\mathbf{L}\left(z\right)^{\mathbf{T}}\right]_{n_p\times 2n_p},\qquad \mathbf{L}^{\mathbf{T}}=\left\langle 1-\xi_e \;\vdots\; \xi_e\right\rangle \tag{4.11a-b}$$

For beam element e, the bending moment is assumed to vary linearly between end moments M_{e0},M_{e1}. Also, the distributed load $q\left(z\right)$ is assumed to vary linearly between q_{e0},q_{e1},, i.e.,

$$M_e\left(z\right)=-M_{e0}\left(1-\xi_e\right)+M_{e1}\xi_e \qquad\qquad q_e\left(z\right)=q_{e0}\left(1-\xi_e\right)+q_{e1}\xi_e \tag{4.12a-b}$$

From Eqs. (4.8), (4.10), and (4.12a-b), by substituting into Eq. (4.3) , one obtains

$$\begin{aligned}\pi_{b,e}=&\left(n_p/2\right)\left(\mathbf{u}_e{}^{\mathbf{T}}\mathbf{K}_{\mathbf{uu},e}\mathbf{u}_e+\boldsymbol{\theta}_e{}^{\mathbf{T}}\mathbf{K}_{\boldsymbol{\theta\theta},e}\boldsymbol{\theta}_e+2\lambda\mathbf{u}_e{}^{\mathbf{T}}\mathbf{K}_{\mathbf{g1},e}\boldsymbol{\theta}_e+\lambda\boldsymbol{\theta}_e{}^{\mathbf{T}}\mathbf{K}_{\mathbf{g2},e}\boldsymbol{\theta}_e\right)\\&+1/2\sum_{\gamma=-\beta}^{\beta}\left(\mathbf{V}_{e,\gamma}{}^{\mathbf{T}}\mathbf{K}_{\mathbf{vv},e}\mathbf{V}_{e,\gamma}+\mathbf{W}_{e,\gamma}{}^{\mathbf{T}}\mathbf{K}_{\mathbf{ww},e}\mathbf{W}_{e,\gamma}\right)\end{aligned} \tag{4.13}$$

in which the following matrices have been defined as

$$\begin{aligned}\mathbf{K}_{\mathbf{uu},e}&=EI_y\int_0^{l_e}\mathbf{H}''_{\mathbf{1},e}\mathbf{H}''_{\mathbf{1},e}{}^{\mathbf{T}}dz & \mathbf{K}_{\mathbf{vv,i}}&=EI_x\int_0^{l_e}\mathbf{B}''_{\mathbf{1},e}\mathbf{B}''_{\mathbf{1},e}{}^{\mathbf{T}}dz\\ \mathbf{K}_{\boldsymbol{\theta\theta},e}&=GJ\int_0^{l_e}\mathbf{H}'_{\mathbf{1},e}\mathbf{H}'_{\mathbf{1},e}{}^{\mathbf{T}}dz & \mathbf{K}_{\mathbf{ww,i}}&=EA\int_0^{l_e}\mathbf{B}'_{\mathbf{2},e}\mathbf{B}'_{\mathbf{2},e}{}^{\mathbf{T}}dz\\ \mathbf{K}_{\mathbf{g1},e}&=\int_0^{l_e}M\left(z\right)\mathbf{H}''_{\mathbf{1},e}\mathbf{H}_{\mathbf{1},e}{}^{\mathbf{T}}dz & \mathbf{K}_{\mathbf{g}2,e}&=\int_0^{l_e}q\left(z\right)y_q\mathbf{H}_{\mathbf{1},e}\mathbf{H}_{\mathbf{1},e}{}^{\mathbf{T}}dz\end{aligned} \tag{4.14a-e}$$

From Eqs. (4.7a-b), by substituting into Eq. (4.5), one can express the terms of the internal strain energy $\pi_{s,i}=U_{sv,i}+U_{sw,i}$ stored in plane i of fasteners as

$$U_{sv,i}=\frac{1}{2}\mathbf{v}_{\mathbf{s},i}^{\mathbf{T}}\mathbf{K}_{\mathbf{sv},i}\mathbf{v}_{\mathbf{s},i} \qquad\qquad U_{sw,i}=\frac{1}{2}\mathbf{w}_{\mathbf{s},i}^{\mathbf{T}}\mathbf{K}_{\mathbf{sw},i}\mathbf{w}_{\mathbf{s},i} \tag{4.15a-e}$$

in which

$$\mathbf{v}_{\mathbf{s},i}^{\mathbf{T}} = \left\langle v_{\gamma+1}(z_i) \;\vdots\; v_{\gamma}(z_i) \;\vdots\; \theta(z_i) \right\rangle,$$

$$\mathbf{w}_{\mathbf{s},i}^{\mathbf{T}} = \left\langle w_{\gamma+1}(z_i) \;\vdots\; w_{\gamma}(z_i) \;\vdots\; u'(z_i) \;\vdots\; v'_{\gamma+1}(z_i) \;\vdots\; v'_{\gamma}(z_i) \right\rangle$$

$$\mathbf{K}_{\mathbf{sv},i} = n_f \sum_{\gamma=-\beta}^{\gamma=\beta-1} \overline{\mathbf{K}}_{\mathbf{sv},i,j} \qquad \overline{\mathbf{K}}_{\mathbf{sv},i,j} = k \left[\begin{array}{c:c:c} 1 & -1 & -2c \\ \hdashline -1 & 1 & 2c \\ \hdashline -2c & 2c & 4c^2 \end{array}\right]$$

$$\mathbf{K}_{\mathbf{sw},i} = \sum_{\gamma=-\beta}^{\gamma=\beta-1} \sum_{j=1}^{j=n_f} \overline{\mathbf{K}}_{\mathbf{sw},i,j}, \overline{\mathbf{K}}_{\mathbf{sw},i,j} = k \left[\begin{array}{c:c:c:c:c} 1 & -1 & 2c & y & -y_{i,j} \\ \hdashline -1 & 1 & -2c & -y & y_{i,j} \\ \hdashline 2c & -2c & 4c^2 & 2cy_{i,j} & -2cy_{i,j} \\ \hdashline y_{i,j} & -y_{i,j} & 2cy_{i,j} & y^2{}_{i,j} & -y^2{}_{i,j} \\ \hdashline -y_{i,j} & y_{i,j} & -2cy_{i,j} & -y^2{}_{i,j} & y^2{}_{i,j} \end{array}\right]$$

4.5 **Verification**

4.5.1 Reference Case

A 5 m span built-up beam is considered as a reference case. The beam consists of three plies, each having a 38 x 286mm cross-section. The beam is simply supported against transverse and lateral displacements as well as the angle of twist. One end of the beam is longitudinally restrained. The beam is subjected to a uniform bending moment. Ply material is SPF No.1/No.2 grade sawn lumber with a modulus of elasticity $E = 9500\, N/mm^2$ and a transverse modulus of rigidity $G = E/16 = 594 N/mm^2$ as taken from CSA-O86:24 [4.2]. The plies are connected using 3" common nails with 3.76 mm diameter. The fastener stiffness k is computed from the Eurocode 5 formula* [4.4]:

$$k = \rho_m{}^{1.5} d^{0.8} / 30 \tag{4.16}$$

* Eurocode 5 provides Eq. (4.16) to characterize the shear stiffness for the connection between the fastener and the timber component in which it is embedded. This shear stiffness is termed as the fastener stiffness in the present study.

which relates nail stiffness k in N/mm to the mean wood density ρ_m in kg/m^3, and the fastener diameter d in mm. For a nail diameter $d = 3.76mm$ embedded into a wood member with density $\rho_m = 420\ Kg/m^3$, the reference stiffness is $k = 830\ N/mm$. The nailing pattern used is chosen based on practical considerations while complying with the spacing requirements of CSA-O86:24 [4.2], i.e., the longitudinal spacing parallel to the grain is taken as $S_p = 294mm$, with an end distance $a = 148mm$, while the transverse spacing perpendicular to the grain is $S_q = 98mm$ with an edge distance $e_d = 45mm$.

4.5.2 Verification against 3D FE analysis

For the FE model based on the present formulation, a mesh sensitivity analysis showed that convergence was attained when the beam span was subdivided into 18 elements. The C3D8 brick element in Abaqus was also used to develop the 3D model for the problem [4.30]. The C3D8 is a fully integrated element with eight nodes and three translational degrees per node. The element was shown to reliably model the LTB of wooden beams in previous studies (e.g. [4.6], [4.11], [4.12]). A mesh study revealed that convergence was achieved when the element size was approximately 20 mm. The constitutive behaviour of wood was idealized as an orthotropic material. The relative spring SPRING2 element was used to simulate the effect of the fasteners at adjacent ply interfaces. At each fastener location, three relative springs were assigned between the nodes of both plies to represent the stiffness of the nails along the lateral (withdrawal), transverse, and longitudinal directions. The uniform moment was modeled by applying a compressive force

to the top edge and a tensile force to the bottom edge at both ends of the beam. To simulate the interaction between plies, the Abaqus surface-to-surface contact feature with finite sliding was employed, which enables relative sliding between plies. The hard contact with the pressure over-closure sub-feature was used to avoid surface penetration. The friction between ply interfaces was conservatively neglected in the model.

Table 4.1: Comparison of critical moments from 3D FEA and the present study

Run No.	Ply dimensions (mm)			Material Properties (MPa)		No. of plies	Fastener Stiffness (N/mm)	Fastener Pattern (mm)				Load Type	Critical moment (kNm)		Ratio
(1)	b (2)	d (3)	L (4)	E (5)	G (6)	n_p (7)	k (8)	S_p (9)	S_q (10)	a (11)	e (12)	Load Type (13)	Present Study (14)	3D FEA (15)	(15)/(14)= (16)
R1	38	286	5000	9500	594	3	830	294	98	148	45	UM	17.6	17.5	0.99
2	38	286	5000	9500	594	3	0.11	294	98	148	45	UM	11.2	10.5	0.94
3	38	286	5000	9500	594	3	110	294	98	148	45	UM	12.5	11.9	0.95
4	38	286	5000	9500	594	3	500	294	98	148	45	UM	15.8	15.4	0.97
5	38	286	5000	9500	594	3	1000	294	98	148	45	UM	18.3	18.5	1.01
6	38	286	5000	9500	594	3	1500	294	98	148	45	UM	20.3	20.8	1.02
7	38	286	5000	9500	594	4	0.11	294	98	148	45	UM	14.9	14.1	0.95
8	38	286	5000	9500	594	4	110	294	98	148	45	UM	17.8	17.0	0.96
9	38	286	5000	9500	594	4	500	294	98	148	45	UM	23.3	22.4	0.96
10	38	286	5000	9500	594	4	830	294	98	148	45	UM	26.1	25.9	0.99
11	38	286	5000	9500	594	4	1000	294	98	148	45	UM	27.3	27.4	1.00
12	38	286	5000	9500	594	4	1500	294	98	148	45	UM	30.7	31.4	1.02
13	38	286	5000	9500	594	5	0.11	294	98	148	45	UM	18.7	17.7	0.95
14	38	286	5000	9500	594	5	110	294	98	148	45	UM	23.0	22.0	0.96
15	38	286	5000	9500	594	5	500	294	98	148	45	UM	31.0	29.7	0.96
16	38	286	5000	9500	594	5	830	294	98	148	45	UM	35.1	34.6	0.99
17	38	286	5000	9500	594	5	1000	294	98	148	45	UM	36.5	36.8	1.01
18	38	286	5000	9500	594	5	1500	294	98	148	45	UM	41.2	42.4	1.03
19	44	286	5000	9500	594	3	830	294	98	148	45	UM	26.3	26	0.99
20	44	333	5000	9500	594	3	830	294	98	148	45	UM	30.2	29.8	0.99
21	38	286	5000	12000	750	3	830	294	98	148	45	UM	21.1	20.8	0.99
22	38	286	5000	9500	594	3	830	588	98	148	45	UM	16.2	16.6	1.02
23	38	286	5000	9500	594	3	830	196	98	148	45	UM	19.6	19.9	1.02
24	38	286	5000	9500	594	3	830	294	98	148	45	1PL	22.5	23.0	1.02
25	38	286	5000	9500	594	3	830	294	98	148	45	2PL	18.7	19.3	1.03
													Average		0.99
													Standard deviation		0.03

Note: UM: Uniform moment, 1PL: Mid-span point load, and 2PL: Two-point loads applied at one-third points along the span

For the reference case, the critical moment predicted by the present solution is found to be 17.6 kNm (Column 14 in Table 4.1), which compares to 17.5 kNm as predicted by the 3D finite element

model (Column 15). Twenty-four additional cases were examined, in which ply dimensions, fastener stiffness, number of plies, nailing pattern, material properties, and loading type were varied (Table 4.1). The ratios of critical moments predictions by the 3D FE model to those based on the present formulation averaged 0.99 with a standard deviation of 0.03 (Column 16), indicating close agreement.

4.5.3 Experimental Validation

Waltz et al. [4.25] conducted a recent experimental investigation on the LTB capacity of built-up wooden beams. Each of the three built-up beams (C3, C6, D3) consists of two plies made of Douglas-fir LVL were tested under two-point loading. The beams were restrained against transverse and lateral displacements as well as twist at both ends. Additional lateral and torsional restraints were provided at the points of load application. The details of the tested specimens are provided in Table 4.2. Duplex nails of dimensions 4.11 × 76.2 mm (0.162 × 3.0 in) were used to connect plies. The stiffness of the fasteners as predicted by Eq. (4.16) is $k = 1150 N/mm$. All three beams were reported to have failed in a lateral torsional buckling mode. The experimentally measured critical moments reported in the study were compared against the predictions of the present finite element formulation and those of 3D FEA models based on the C3D8 element in Abaqus. The mesh specifics of both models are similar to those provided under Section 4.5.2. The ratios of buckling moments as predicted by the present formulation (Column 13) to test-measured values (Column 11) are observed to range between 0.92 and 0.95. Comparatively, the predictions of the 3D FEA model (Column 12) to test results ranged from 0.91 to 0.97. The difference between the test results and those of both FEA models can partly be attributed to the friction between plies, which is present in the tests but omitted in both models.

Table 4.2: Experimental verification

Specimen (1)	Ply dimensions [1] (mm)			Nail Stiffness (N/mm)	Nailing Pattern Dimensions (mm)				Load Location [2]	Critical moments (kNm)			Ratios		
	b (2)	d (3)	L (4)	k (5)	S_p (6)	S_q (7)	a (8)	e (9)	Location (10)	Test (11)	3D FEA (12)	Present study (13)	(13)/(11) = (14)	(12)/(11) = (15)	(13)/(12) = (16)
C3	44.5	457	14630	1150	488	119	239	50	L/4	44.4	40.9	41.2	0.93	0.92	1.01
C6	44.5	302	10060	1150	546	101	389	50	L/4	38.4	35.5	35.1	0.91	0.92	0.99
D3	44.5	457	14630	1150	488	119	239	50	L/3	53.1	50.7	51.3	0.97	0.95	1.01
											Average		0.94	0.93	1.00

[1] All beams have lateral and torsional restraints at both ends, and the load application points

[2] All beams are subjected to two-point loads

4.6 Parametric Study

A parametric study* is conducted using the present model to investigate the effects of various parameters on the LTB capacity of built-up beams. A one-factor-at-a-time approach is adopted, in which each dimensionless parameter is varied individually while keeping the others constant. The starting point for the parametric study is the reference case described in the previous section which has a normalized fastener stiffness $\bar{k} = k/\left(EI_x/L^3\right)$ = 147, a longitudinal spacing to span ratio S_p/L = 0.059, a transverse spacing to ply depth ratio S_q/d = 0.343, a span to depth ratio L/d =17.5 and depth to width ratio d/b = 7.53. The number of plies n_p is varied from 2 to 5.

4.6.1 Effect of Connection Stiffness

Two nailing patterns are considered: (1) a reference spacing that matches the nailing pattern of the reference case, in which the spacing parallel to the grain is $S_p = 294mm$ and that perpendicular to the grain is $S_q = 98mm$, and (2) minimum spacing as per CSA-O86:24 [4.2], in which

* A summary of parametric results is provided in Appendix B

$S_p = 80mm$ and $S_q = 42mm$. The stiffness for a typical 3" common nail is $k = 830\,N/mm$ as predicted based on Eq. (4.16) . Yet, the fastener stiffness is varied from 0.1 to $10^6\ N/mm$. An upper bound for the uniform critical moment of the system is obtained by assuming full interaction between plies, leading to a monolithic beam with a total width $n_p b$. The critical moment corresponding to the monolithic case is $M_m = (\pi/L)\sqrt{EGI_{y,,m}J_m}$ in which the minor moment of inertia is $I_{y,m} = d(n_p b)^3/12$ and the Saint-Venant torsional constant is $J_m = \omega d(n_p b)^3$ where ω is a constant that depends on the cross-section aspect ratio [4.31]. A lower bound for the uniform critical moment is obtained by completely omitting any interaction between plies. In this case, the critical moment of the resulting non-composite system is $M_{nc} = n_p(\pi/L)\sqrt{EGI_y J}$ in which I_y and J are the minor moment of inertia and Saint-Venant torsional constant for a single ply. The uniform critical moment predicted by the present study to that of the non-composite scenario M_{cru}/M_{nc} is plotted against the normalized fastener stiffness $\bar{k} = k/(EI_x/L^3)$ (Figure 4.2). Overlaid on the figure are four horizontal lines showing the ratio of the critical moment of the monolithic system to that based on the non-composite system M_m/M_{nc} for built-up beams consisting of 2 to 5 plies. The results show that while M_{cru}/M_{nc} is always larger than unity, it is significantly lower than M_{cru}/M_m , i.e., the elastic LTB capacity of built-up beams is significantly lower than that of the monolithic case.

As shown in Table 4.3, the ratio of the critical moment M_{cru} of built-up beams as predicted by the present model to that of the non-composite case (Column 12) increases with the number of plies. In contrast, the ratio between M_{cru} to that of the monolithic case decreases with the number of plies

(Column 13). In general, the uniform critical moment M_{cru} lies between that of the monolithic case M_m and that of the non-composite case M_{nc}, i.e.,

$$M_{cru} = (1-\alpha)M_{nc} + \alpha M_m \tag{4.17}$$

in which α represents the degree of interaction between plies: values near zero indicate negligible interaction, while a value of unity denotes full interaction. For the parametric cases considered in Table 4.3 α ranged from 0.04 to 0.40 (Column 14). The results show that as the number of plies increases, the degree of interaction between plies as characterized by α decreases.

4.6.2 Effect of longitudinal spacing

The normalized longitudinal spacing S_p/L is varied from 0.016 to 0.22 which corresponds to the minimum spacing specified in CSA-O86:24 [4.2] of $S_p = 80mm$ to a maximum spacing of $S_p = 1144mm$, while keeping all parameters $\bar{k} = k/(EI_x/L^3)$, S_q/d, L/d and d/b equal to those

Table 4.3: Critical moments and interaction ratios for built-up beams with fasteners at reference and minimum spacing according to CSA-O86

Run No. (1)	No. of Plies (2)	Nailing Pattern (*mm*)				Fastener Stiff. (*N/mm*)	Critical Moments (*kNm*)			Ratios			
		S_p (3)	S_q (4)	a (5)	e (6)	k (7)	M_{nc} (8)	M_m (9)	M_{cru} (10)	$\frac{M_m}{M_{nc}}$ (11)	$\frac{M_{cru}}{M_{nc}}$ (12)	$\frac{M_{cru}}{M_m}$ (13)	α (14)
Reference Spacing													
1	2	294	98	148	45	830	7.47	28.5	9.78	3.81	1.31	0.34	0.11
2	3	294	98	148	45	830	11.2	91.2	19.2	8.14	1.71	0.21	0.10
3	4	294	98	148	45	830	14.9	204	26.1	13.6	1.75	0.13	0.06
4	5	294	98	148	45	830	18.7	374	35.0	20.0	1.87	0.09	0.04
Minimum Spacing													
5	2	80	42	60	38	830	7.47	28.5	16.8	3.81	2.25	0.59	0.44
6	3	80	42	60	38	830	11.2	91.2	35.1	8.14	3.13	0.39	0.30
7	4	80	42	60	38	830	14.9	204	54.6	13.6	3.65	0.27	0.21
8	5	80	42	60	38	830	18.6	374	75.3	20.0	4.03	0.20	0.16

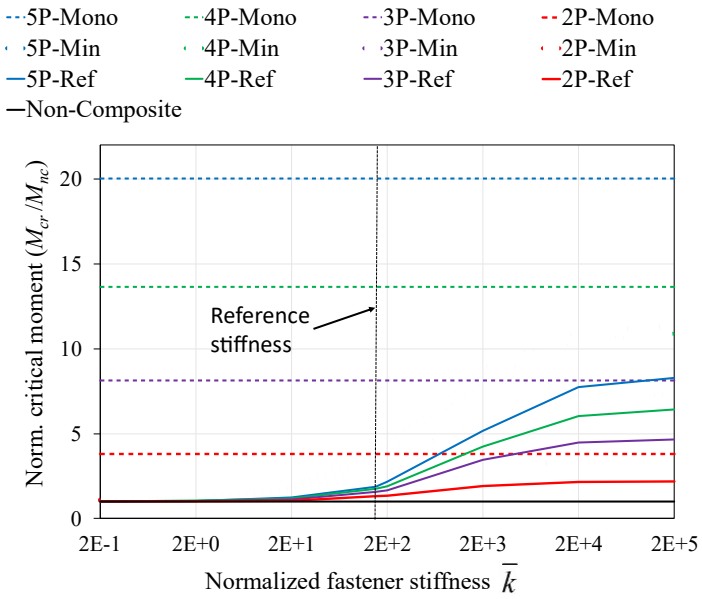

Figure 4.2 Normalized critical moment vs Normalized fastener stiffness

of the reference case. Figure 4.3a shows that the normalized critical moment ratio increases as the normalized longitudinal spacing reduces and as the number of plies increases.

4.6.3 Effect of transverse spacing

The spacing S_q is varied from the minimum value $S_q = 10d_F \approx 40mm$, d_F being the fastener diameter, as specified in CSA-O86:24 [4.2] up to $S_q = 130mm$, i.e., the corresponding normalized spacing ranged from $S_q/d = 0.15$ to 0.45 while keeping all $\bar{k} = k/\left(EI_x/L^3\right)$, S_p/L, L/d and d/b equal to the reference values. The normalized critical moment ratio M_{cru}/M_{nc} is observed to increase as the normalized transverse spacing S_q/d decreases and as the number of plies increases (Figure 4.3.b).

4.6.4 Effect of beam geometry

The effect of beam geometry on the critical moment is investigated by keeping constant all dimensionless geometric parameters at their reference values while varying one geometric parameter at a time. Firstly, the reference span to depth ratio of L/d is varied from 15.0 to 21.0. (Figure 4.3.c). Secondly, the reference ply depth to width ratio of d/b is varied from 6.5 to 9.0. (Figure 4.3.d). Both figures show a mild increase in the normalized critical moment ratio M_{cru}/M_{nc} with L/d and with d/b.

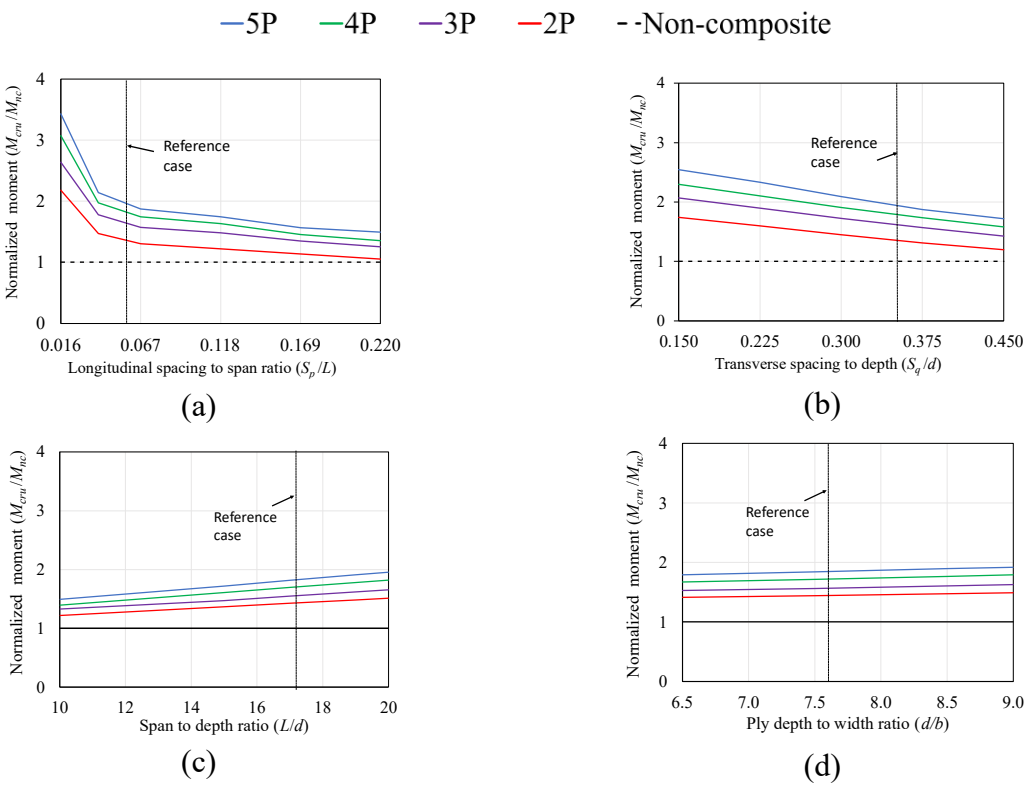

Figure 4.3 Normalized critical moment vs (a) spacing parallel to the grain to span ratio $\left(S_p/L\right)$, (b) spacing perpendicular to the grain to span ratio $\left(S_q/d\right)$, (c) ply length to depth ratio $\left(L/d\right)$, (d) ply depth to width ratio $\left(d/b\right)$

4.6.5 Factors affecting the moment gradient coefficient

Three loading patterns are investigated: uniformly distributed load (UDL), mid-span Point load (1-PL), and 2-point loads applied at third span points (2-PL). The moment gradient factor $C_b = M_{cr}/M_{cru}$ is the ratio of the critical moment M_{cr} of a built-up beam under a given loading pattern to the critical moment M_{cru} of the same beam under a uniform moment. Figure 4.4 illustrates the moment gradient factor C_b versus the normalized fastener stiffness, transverse spacing to depth ratio, longitudinal spacing to span ratio, span to depth ratio, and depth to width ratio. The normalized fastener stiffness $\bar{k} = k/\left(EI_x/L^3\right)$ is varied from 0 to 360, which corresponds to a fastener stiffness k ranging from 0 to 2000 N/mm. The transverse spacing S_q/d is varied from 0.15 to 0.45, corresponding to two to six rows of fasteners over the cross-section depth. The longitudinal spacing S_p/L is varied from 0.016 to 0.220, which corresponds to the minimum spacing $S_p = 80mm$ specified in [4.2] to $S_p = 1144mm$. The span to depth ratio L/d is varied from 15.0 to 21.0 and the reference ply depth to width ratio of d/b is varied from 6.5 to 9.0. Figure 4.4 shows that the moment gradient factor C_b decreases with the normalized fastener stiffness, the number of plies, mildly decreases with the span to depth and depth to width ratios, and increases with the normalized transverse spacing and the longitudinal spacing.

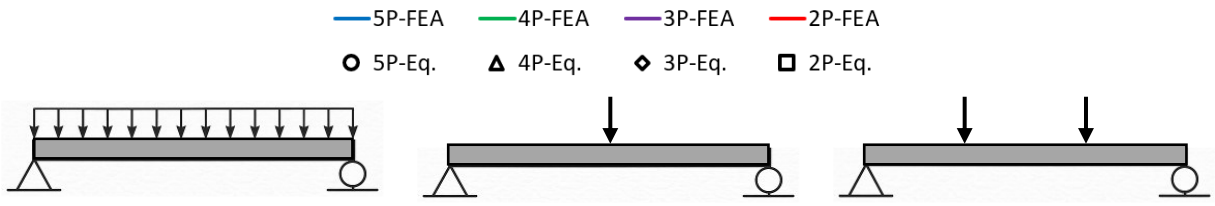

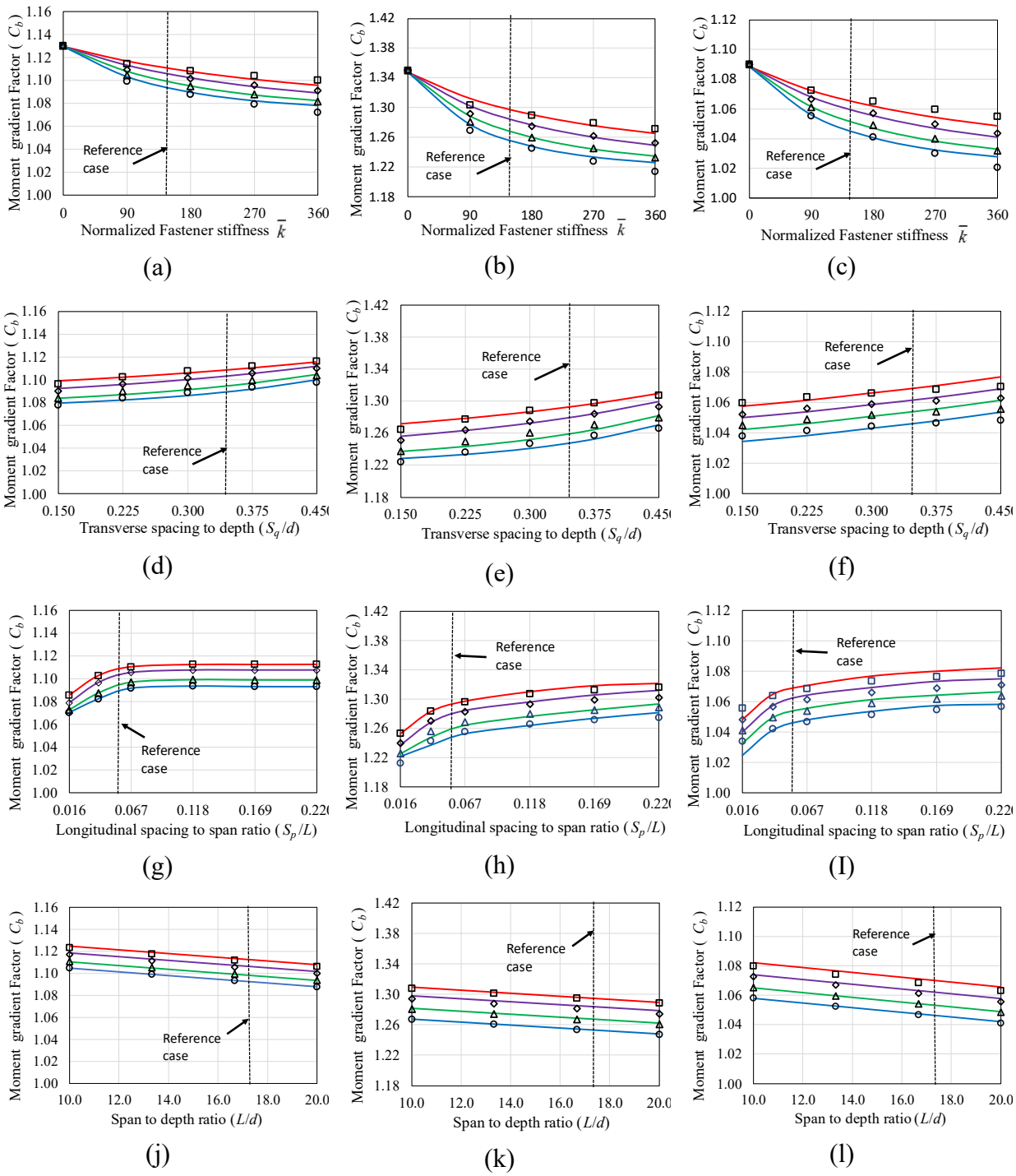
Moment gradient Factor (C_b)
Normalized Fastener stiffness $\bar{k}$
Transverse spacing to depth (S_q/d)
Longitudinal spacing to span ratio (S_p/L)
Span to depth ratio (L/d)
Reference case
(a)
(b)
(c)
(d)
(e)
(f)
(g)
(h)
(I)
(j)
(k)
(l)

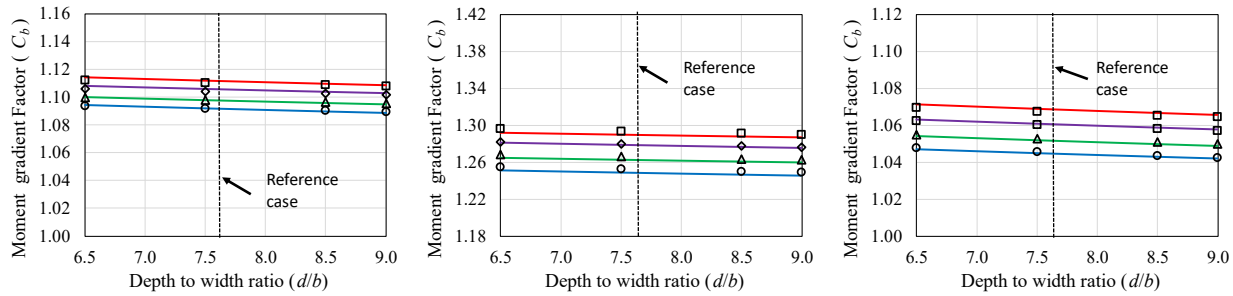

Figure 4.4 Moment gradient factor C_b vs (a-c) normalized fastener stiffness $\left(\overline{k}\right)$; (d-f) transverse spacing to depth ratio $\left(S_q/d\right)$; (g-I) longitudinal spacing to span ratio $\left(S_p/L\right)$ $\left(S_p/L\right)$; (j-l) span to depth ratio $\left(L/d\right)$; (m-o) depth to width ratio $\left(d/b\right)$ for uniformly distributed load, 1-point load and 2-point load

4.6.6 Factors influencing load height coefficient

The load height factor is defined as the ratio between the critical moment of the beam when the loads are offset from the shear center to that of the case where the load is applied at the shear center. The load height effect is investigated by subjecting the beam to the three load configurations UDL, 1-PL and 2-PL. In the current study, the load is applied at the top edge, as it represents the worst-case scenario for the beam stability. As shown in Figure 4.5, the results show that the load height factor decreases as the normalized fastener stiffness, number of plies, and depth to width ratio increase. Conversely, the load height factor is observed to increase as the span to depth, the normalized transverse and longitudinal spacings increase.

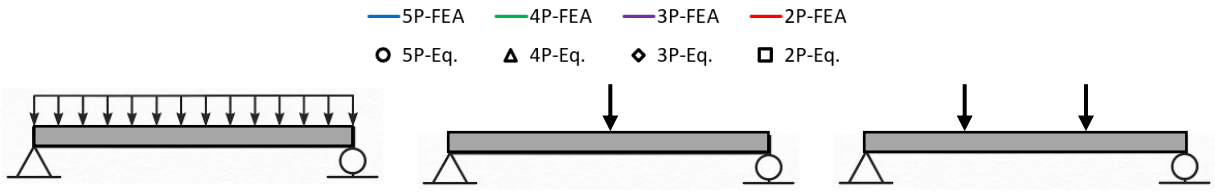

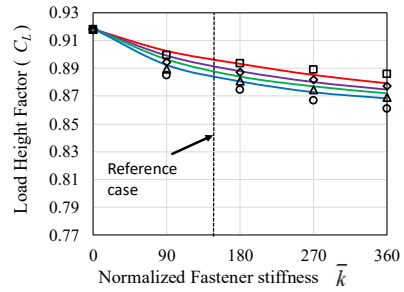

(a)

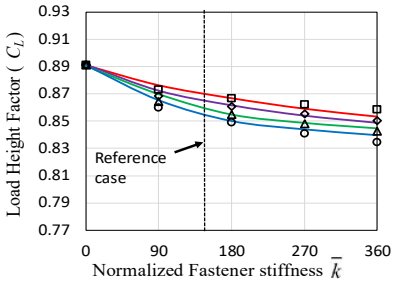

(b)

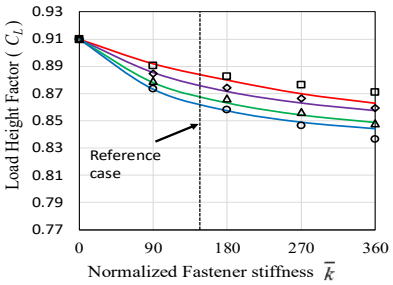

(c)

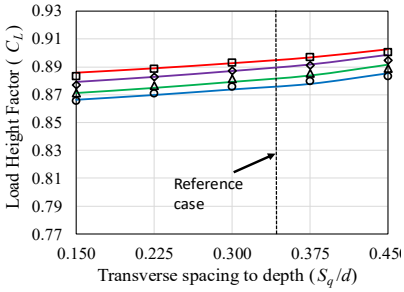

(d)

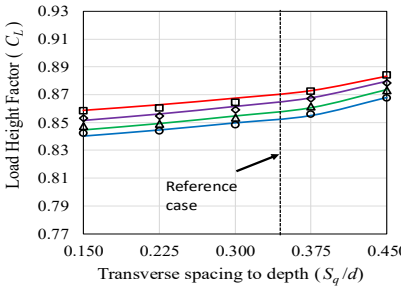

(e)

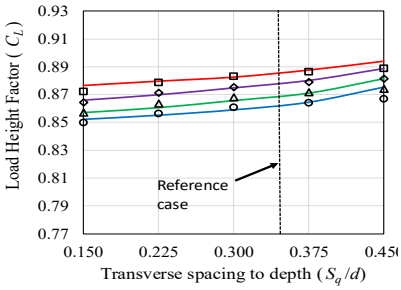

(f)

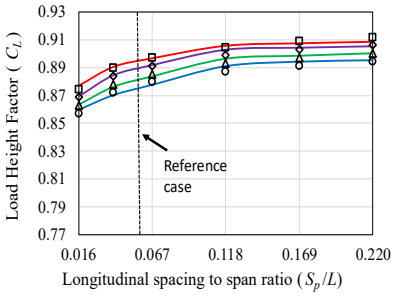

(g)

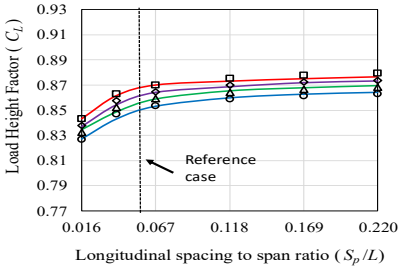

(h)

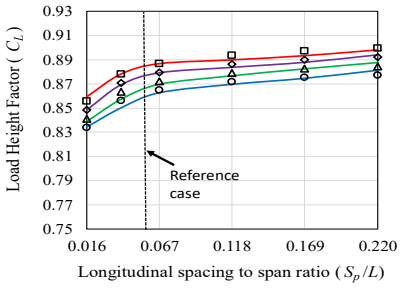

(i)

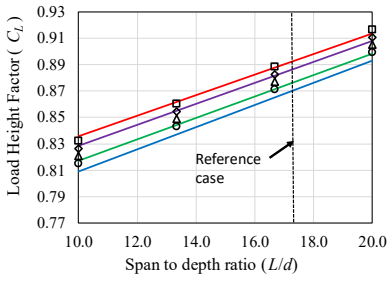

(j)

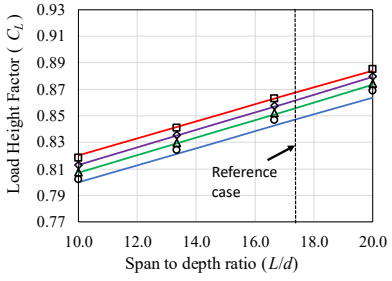

(k)

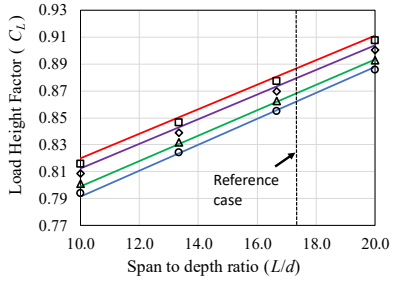

(l)

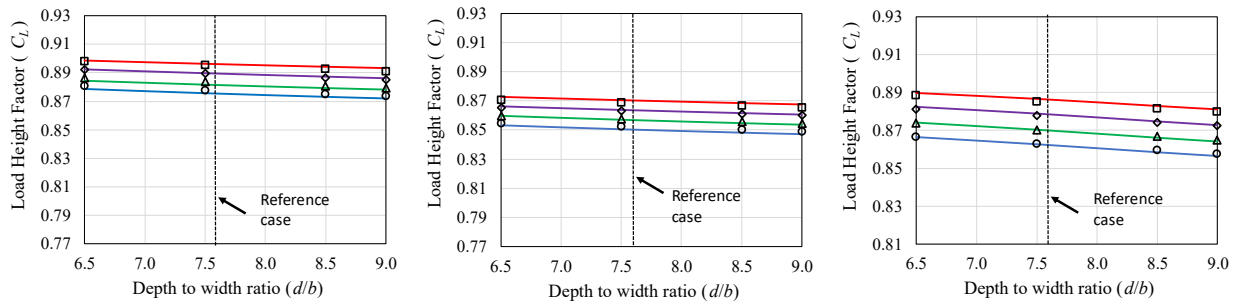

Figure 4.5 Load height factor (C_L) vs (a-c) normalized fastener stiffness $\bar{k}$; (d-f) transverse spacing to depth ratio S_q/d ; (g-i) longitudinal spacing to span ratio S_p/L ; (j-l) length to depth ratio L/d ; (m-o) depth to width ratio d/b for uniformly distributed load, 1-point load and 2-point load

4.7 Simplified Design Procedure

The present section aims to establish simplified design equations for predicting the elastic critical moment of built-up beams. This objective is accomplished by developing three equations: (1) an equation that predicts the moment ratio $m = M_{cru}/M_{nc}$, defined as the elastic critical moment of the built-up beam subjected to uniform bending relative to that of the non-composite case; (2) an equation that determines the moment gradient factor C_b for common loading conditions; and (3) an equation that characterizes the load height factor C_L .

A symbolic regression analysis is carried out based on the database of 733 parametric runs developed in the previous section using PySR [4.32], a Python library for symbolic regression, to predict the moment ratio $m = M_{cru}/M_{nc}$ in terms of the normalized stiffness $\bar{k}$, number of plies n_p , normalized longitudinal spacing S_p/L , normalized transverse spacing S_q/d , ply span to depth L/d , and ply depth to width d/b ratios. The regression yielded the equation

$$m = \frac{M_{cru}}{M_{nc}} = 1.0 + \bar{k}^{d_0}\left[c_1 n_p + \frac{c_2}{\left(S_p/L\right)^{d_1}} + \frac{c_3}{e_0 + \left(S_q/d\right)^{d_2}} + c_4\frac{L}{d} + c_5\frac{d}{b}\right] \le \frac{M_m}{M_{nc}} \qquad (4.18)$$

in which the regression coefficients $c_1 - c_5, d_0 - d_2$ and e_0 are presented in Table 4.4 for the case of uniform moment. The corresponding coefficient of determination is found to be $R^2 = 0.94$. A comparison between the predictions of the regression Eq. (4.18) and FE predictions is provided in Figure 4.6.

Similarly, the moment gradient factor C_b and load height factor C_L are approximated by

$$C_b = c_0 - \bar{k}^{d_0}\left[c_1 n_p + \frac{c_2}{\left(S_p/L\right)^{d_1}} + \frac{c_3}{e_0 + \left(S_q/d\right)^{d_2}} + c_4\frac{L}{d} + c_5\frac{d}{b}\right] \geq 1 \tag{4.19}$$

$$C_L = c_0 - \bar{k}^{d_0}\left[c_1 n_p + \frac{c_2}{\left(S_p/L\right)^{d_1}} + \frac{c_3}{e_0 + \left(S_q/d\right)^{d_2}} + c_4\frac{L}{d} + c_5\frac{d}{b}\right] \leq 1 \tag{4.20}$$

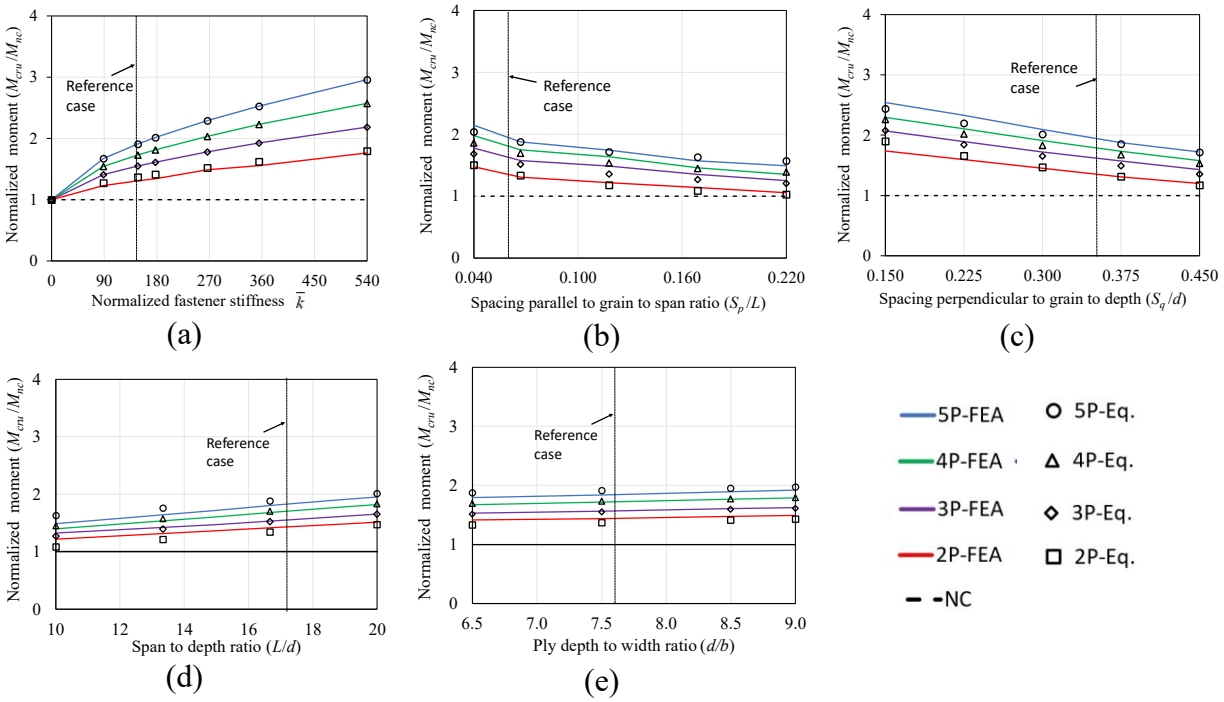

Figure 4.6 Normalized critical moment vs (a) Normalized fastener stiffness (b) spacing parallel to the grain (S_p /L) (c) spacing perpendicular to the grain (S_q /d) (d) ply length to depth ratio (L/d), (e) ply depth to width ratio (d/b) using FEA based on the formulation and the simplified solution

in which the corresponding regression coefficients and coefficients of determination are presented in Table 4.4. Comparisons between the predictions from the regression [Eqs. (4.19) and (4.20)] and the FE predictions based on the present study are provided in Figure 4.4 and Figure 4.5.

Table 4.4: Regression coefficients for the simplified solutions

Eq.	Load type	R^2	Regression Coefficients									
			c_0	c_1 x10^{-4}	c_2 x10^{-3}	c_3 x10^{-3}	c_4 x10^{-4}	c_5 x10^{-4}	e_0	d_0	d_1	d_2
Eq. (4.18)	UM	0.94	-	95.8	30.00	−160	20.4	21.5	0	0.59	0.265	−0.34
Eq. (4.19)	UDL	0.95	1.13	6.33	0.0032	−7.00	1.76	1.73	0	0.46	1.64	−0.53
	1-PL	0.95	1.35	20.9	2.220	−21.5	3.00	3.71	0	0.38	0.44	−0.59
	2-PL	0.94	1.09	6.00	9.200	−15.0	1.40	1.70	0	0.50	0.065	−0.06
Eq. (4.20)	UDL	0.94	0.92	8.20	0.646	9.61	−11.9	3.89	0.79	0.39	0.18	1.00
	1-PL	0.96	0.89	6.57	0.336	1.62	−8.00	2.54	0.13	0.42	0.66	3.95
	2-PL	0.96	0.91	6.07	0.501	0.832	−7.56	2.93	0	0.50	0.54	0.13

In summary, the critical moment M_{cr} can be estimated using the equation

$$M_{cr} = mC_L C_b M_{nc} \tag{4.21}$$

in which ratios m, C_b and C_L are given by Eqs. (4.18), (4.19) and (4.20) respectively. The use of Eq. (4.21) in a design context* is illustrated in the following section.

4.8 Design Examples

4.8.1 Design Example 1

A 6.1m span built-up LVL beam is made of 4-plies. Ply dimensions are 44.5×457mm. Material is Douglas-Fir No.1/No.2 with $E = 11{,}000 MPa$**, $E/G = 16$. The plies are mechanically fastened using four rows of M6-1.0×120mm screws*** spaced at 300 mm longitudinally and 115 mm transversely. Lateral and torsional restraints are provided at beam ends so that its unbraced length is equal to the span. The beam is subjected to a uniformly distributed load at its top face. It is required to determine the elastic LTB capacity of the member.

Solution: Cross-sectional properties are $I_x = bd^3/12 = 354\times10^6 mm^4$, $I_y = db^3/12 = 3.36\times10^6 mm^4$, $J = k_1 db^3 = 0.313\times457\times44.5^3 = 1.26\times10^7 mm^4$. The uniform critical moment assuming non-composite action is $M_{nc} = n_p(\pi/L)\sqrt{EGI_yJ} = 36.9kNm$. The fastener stiffness is $k = \rho_m^{1.5} d^{0.8}/30 = 1516\,N/mm$ which corresponds to a normalized value $\bar{k} = kL^3/EI_x = 88.4$. The normalized longitudinal spacing is $S_p/L = 1/20$, the normalized transverse spacing is $S_q/d = 1/4$, the length to depth ratio is $L/d = 13.4$, and the span to depth ratio is $d/b = 10.27$. Given the dimensionless parameters n, $\bar{k}$, S_p/L, S_q/d, L/d and d/b, by substituting into Eq. (4.18), one obtains a uniform critical moment ratio $m = 1.71$. By substituting in Eq. (4.19), one obtains $C_b = 1.10$ and from Eq. (4.20), one obtains $C_L = 0.85$. The critical moment as given by the Eq. (4.21) is $M_{cr} = mC_LC_bM_{cru} = 1.71\times1.10\times0.85\times36.9 = 58.9kNm$. This value compares with $61.5kNm$ as predicted by the present finite element formulation and $61.9kNm$ as predicted by the 3D FEA, corresponding to a difference of less than 5%. A comparison between the predictions of the regression equations, the present formulation, and the 3D FEA model is presented in Table 4.5.

[*] Appendix C demonstrates the integration of current study's findings to the existing design framework of CSA-O86:24
[**] Based on the average value of modulus of elasticity for LVL as published in NRC-CNRC Evaluation Report CCMC 13310-R, "RigidLam® LVL".
[***] As published in the Fast-Rite International, Technical Specifications Guide for Fasteners, 2018.

Table 4.5: Critical moments comparison for design example 1

	Proposed equations (1)	Present Formulation (2)	3D FEA (3)	(1)/ (2) (4)	(1)/ (3) (5)
Moment gradient factor C_b	1.10	1.10	1.11	1.000	0.991
Load height factor C_L	0.85	0.84	0.83	1.012	1.024
Critical moment M_{cr} (kNm)	58.9	61.5	61.9	0.958	0.952

4.8.2 Design Example 2

A 3-ply built-up beam has an unbraced length of 4.9m. Ply dimensions are 38×286mm. Material is sawn lumber SPF No.1/No.2 with $E = 9500MPa,\ E/G = 16$. The plies are connected using three rows of 10d common nails at 350 mm longitudinal spacing and 96 mm transverse spacing. The beam is subjected to a midspan point load acting at the top edge. It is required to determine the elastic LTB capacity of the member.

Solution: Cross-sectional properties are $I_x = bd^3/12 = 74.08\times10^6\,mm^4$, $I_y = db^3/12 = 1.31\times10^6\,mm^4$, $J = k_1 db^3 = 0.305\times286\times38^3 = 4.786\times10^6\,mm^4$ The uniform critical moment assuming non-composite action is $M_{nc} = n_p(\pi/L)\sqrt{EGI_yJ} = 11.4kNm$. The fastener stiffness is $k = \rho_m^{1.5}d^{0.8}/30 = 830\,N/mm$ and the corresponding normalized value is $\bar{k} = kL^3/EI_x = 138.75$. The normalized longitudinal spacing is $S_p/L = 1/14$, the normalized transverse spacing is $S_q/d = 1/3$, the length to depth ratio is $L/d = 17.13$ and the length to depth ratio is $d/b = 7.53$. By substituting into Eq. (4.18), one obtains a uniform critical moment ratio $m = 1.48$. By substituting in Eq. (4.19), one obtains $C_b = 1.29$ and from Eq. (4.20), one obtains the load height factor is found to be $C_L = 0.87$. The critical moment as determined from Eq. (4.21) is $M_{cr} = mC_LC_bM_{cru} = 1.48\times1.29\times0.86\times11.4 = 18.8kNm$. This value compares with $18.9kNm$ as predicted by the present finite element model and $18.7kNm$ as predicted by the 3D FEA model, with a difference of less than 1%. A comparison between the predictions of the regression equations, the present finite element model and the 3D FEA model is presented in **Table 4.6**.

Table 4.6: Critical moment comparisons for design example 2

	Proposed equations (1)	Present Formulation (2)	3D FEA (3)	(1)/ (2) (4)	(1)/ (3) (5)
Moment gradient factor C_b	1.29	1.27	1.29	1.016	1.000
Load height factor C_L	0.86	0.88	0.86	0.977	1.000
Critical moment $M_{cr}(kNm)$	18.8	18.9	18.7	0.995	1.005

4.9 Summary and Conclusions

1. The present study develops a beam finite element formulation for the elastic lateral torsional buckling analysis of built-up wooden beams with an arbitrary number of plies, connected using discrete fasteners. The formulation captures the partial composite action between plies.
2. The validity of the formulation is established through comparisons against the experimental results of full-scale experiments and against the predictions of 3D FE models.
3. The model provides a basis to quantify the degree of interaction provided between plies offered by the connecting fasteners. While partial interactions between plies are shown to increase the LTB resistance of built-up beams compared to the hypothetical lower bound case of no interaction, the resistance gain attained remains well below the monolithic upper bound.
4. The formulation developed is used to conduct a parametric investigation consisting of 733 runs to quantify the effects of different factors on the achieved composite actions. The results show that the uniform critical moment of built-up beams increases with the fastener normalized stiffness, number of plies, span to depth and depth to width ratios and reduces with normalized longitudinal and transverse spacings.
5. Unlike monolithic simply supported beams in which the moment gradient factor depends solely on the moment distribution, the moment gradient factor for built-up beams is shown to depend on several factors. It increases with the normalized longitudinal and transverse

spacings and reduces as the normalized fastener stiffness, number of plies, span to depth and depth to width ratios.

6. The load height factor is shown to increase with the span to depth ratio and normalized longitudinal and transverse spacings and to reduce with the normalized stiffness of the fasteners, number of plies, and depth to width ratio.
7. The results of the database of runs are used in conjunction with symbolic regression, to develop simplified design equations to predict the normalized elastic uniform critical moment, moment gradient and load height factors for a wide range of built-up beams.
8. The developed equations are consolidated into a unified procedure for quantifying the elastic lateral torsional buckling capacity of built-up wooden beams.

4.10 Acknowledgments

The senior authors acknowledge with appreciation the financial support provided by the Natural Sciences and Engineering Research Council of Canada (NSERC) and the Canadian Wood Council. The junior author also acknowledges scholarship funding from the University of Ottawa.

4.11 References

[4.1] Canadian Standard Association (CSA), *CSA Standard O86-19 Engineering design in wood*. 2019.

[4.2] Canadian Standard Association (CSA), *CSA Standard O86-24 Engineering design in wood*, vol. 1, no. 1. 2024.

[4.3] American Wood Council, *National design specification for wood construction*. Leesburg, VA, USA, 2024.

[4.4] CEN, *Eurocode 5: Design of timber structures - Part 1-1: General - Common rules and rules for buildings Eurocode*, vol. 1. 2004.

[4.5] R. . Hooley and B. Madsen, "Lateral Stability of Glued Laminated Beams," *J. Struct. Div.*, vol. 90, no. 3, 1964.

[4.6] Q. Xiao, G. Doudak, and M. Mohareb, "Numerical and experimental investigation of lateral torsional buckling of wood beams," *Eng. Struct.*, vol. 151, pp. 85–92, 2017, doi: 10.1016/j.engstruct.2017.08.020.

[4.7] G. Capellán, J. Sánchez-Haro, P. de Celis, and A. B. Ramos-Gavilán, "Theoretical, experimental and numerical study of lateral buckling in glued laminated timber beams," *Eng. Struct.*, vol. 338, no. December 2024, 2025, doi: 10.1016/j.engstruct.2025.120558.

[4.8] J. Töpler and U. Kuhlmann, "Lateral torsional buckling of glulam beams," in *10th International Network on Timber Engineering Research (INTER)*, Biel/Bienne,

Switzerland, 2023, pp. 6–12. doi: 10.18419/opus-13593.

[4.9] R. St-Amour and G. Doudak, "Experimental and numerical investigation of lateral torsional buckling of wood I-joists," *Can. J. Civ. Eng.*, vol. 45, no. 1, pp. 41–50, 2018, doi: 10.1139/cjce-2017-0281.

[4.10] B. Pelletier and G. Doudak, "Investigation of the lateral-torsional buckling behaviour of engineered wood I-joists with varying end conditions," *Eng. Struct.*, vol. 187, no. November 2018, pp. 329–340, 2019, doi: 10.1016/j.engstruct.2019.03.003.

[4.11] Y. Hu, M. Mohareb, and G. Doudak, "Lateral Torsional Buckling of Wooden Beams with Midspan Lateral Bracing Offset from Section Midheight," *J. Eng. Mech.*, vol. 143, no. 11, pp. 1–13, 2017, doi: 10.1061/(asce)em.1943-7889.0001359.

[4.12] Y. Hu, M. Mohareb, and G. Doudak, "Effect of Eccentric Lateral Bracing Stiffness on Lateral Torsional Buckling Resistance of Wooden Beams," vol. 18, no. 02, pp. 1–34, 2018.

[4.13] Y. Du, M. Mohareb, and G. Doudak, "Nonsway Model for Lateral Torsional Buckling of Wooden Beams under Wind Uplift," *J. Eng. Mech.*, vol. 142, no. 12, 2016.

[4.14] Y. Du, M. Mohareb, and G. Doudak, "Sway Model for the Lateral Torsional Buckling Analysis of Wooden Twin-beam-deck Systems," *Structures*, vol. 19, no. November 2018, pp. 19–29, 2019, doi: 10.1016/j.istruc.2018.11.012.

[4.15] Y. Du, G. Doudak, and M. Mohareb, "Effect of beam-deck connection flexibility on lateral torsional buckling strength of wooden twin-beams," *Eng. Struct.*, vol. 207, no. November 2019, p. 110226, 2020, doi: 10.1016/j.engstruct.2020.110226.

[4.16] A. Sahraei, P. Pezeshky, M. Mohareb, and G. Doudak, "Simplified expressions for elastic lateral torsional buckling of wooden beams," *Eng. Struct.*, vol. 174, no. February, pp. 229–241, 2018, doi: 10.1016/j.engstruct.2018.07.042.

[4.17] G. Doudak, M. Mohareb, and Y. Du, "Proposed Design Approach for Lateral Stability of Timber Beams," in *International Network on Timber Engineering Research (INTER)*, 2022, p. 55-10-1.

[4.18] M. Mansor, M. Mohareb, and G. Doudak, "Load Height Effect on the Lateral Torsional Buckling Resistance of Continuous Wooden Beams," in *CSCE 2024 Annual Conference, Niagara Falls, ON, Canada*, Niagara Falls, ON, Canada: Canadian Society for Civil Engineering, 2024.

[4.19] R. A. S. Ribeiro and P. J. Pellicane, "Modeling load-slip behavior of nailed joints," *J. Mater. Civ. Eng.*, vol. 4, no. 26692, pp. 385–398, 1992.

[4.20] J. F. Miller and W. M. Bulleit, "Analysis of Mechanically Laminated Timber Beams Using Shear Keys," *J. Struct. Eng.*, vol. 137, no. 1, pp. 124–132, 2011, doi: 10.1061/(asce)st.1943-541x.0000273.

[4.21] N. T. Mascia, C. L. de O. Santana, and Steven M. Cramer, "Evaluation of the Equivalent Slip Modulus of Nailed Connections for Application in Linear Analysis of Plywood Timber Beams," *Mater. Res.*, vol. 11, no. 2, pp. 151–157, 2008.

[4.22] R. Robatmili, "Lateral Torsional Buckling of Timber Built-up Beams," University of Ottawa, 2022.

[4.23] N. Challamel and U. A. Girhammar, "Lateral-torsional buckling of vertically layered composite beams with interlayer slip under uniform moment," *Eng. Struct.*, vol. 34, pp. 505–513, 2012, doi: 10.1016/j.engstruct.2011.10.004.

[4.24] G. Robatmili, Robabeh, Du, Yang and Doudak, "Effect of fastener stiffness on buckling behaviour of wooden built-up beams," *CSCE 2022 Annu. Conf. Whistler, Br. Columbia*, 2022.

[4.25] N. Waltz, M. O. Amini, and B. Douglas, "Lateral Torsional Buckling Design for Multi-Ply Structural Composite Lumber Beams," *J. Struct. Eng.*, vol. 151, no. 4, 2025, doi: 10.1061/jsendh.steng-13649.

[4.26] M. Mansor, M. Mohareb, and G. Doudak, "Numerical Investigation of Elastic Lateral Torsional Buckling Behaviour of Two-Ply Built-up Wooden Beams," in *CSCE 2024 Annual Conference, Niagara Falls, ON, Canada*, Niagara Falls, ON, Canada: Canadian Society for Civil Engineering, 2024.

[4.27] M. Mansor, M. Mohareb, and G. Doudak, "Elastic lateral torsional buckling of two-ply built-up wooden beams connected with discrete fasteners," *Eng. Struct.*, vol. 331, no. January, 2025, doi: 10.1016/j.engstruct.2025.119944.

[4.28] Hörsting, "Zum Tragverhalten druck- und biegebeanspruchter Holzbauteile," Der Universität Carolo-Wilhelmina zu Braunschweig, 2008.

[4.29] Q. Xiao, G. Doudak, and M. Mohareb, "Lateral torsional buckling of wood beams: Fea-modelling and sensitivity analysis," *WCTE 2014 - World Conf. Timber Eng. Proc.*, vol. 2, no. 1, 2014.

[4.30] Simulia, "Abaqus/CAE," 2016, *ABAQUS analysis user's manual*.

[4.31] A. P. BORESI and R. J. SCHMIDT, *Advanced Mechanics of Materials*, 6th Ed. New York: Wiley, 2003.

[4.32] M. Cranmer, "Interpretable Machine Learning for Science with PySR and SymbolicRegression.jl," *arXiv*, 2023, [Online]. Available: http://arxiv.org/abs/2305.01582

4.12 Notation

The following symbols are used in this paper:

A: Cross sectional Area

a : End distance of fasteners.

$\mathbf{B_1}, \mathbf{B_2}$: A diagonal vector that includes $\mathbf{H}_2$ and $\mathbf{L}$ vectors respectively for all plies.

b : Ply width.

C_b : Moment gradient factor for built-up beams.

C_L : Load height factor, defined as the ratio between the critical moment when loads are applied at an offset from the shear center and that when the load is applied at the shear center.

$c_1 - c_5$: Regression coefficients.

d : Ply depth.

$d_0 - d_2$: Regression coefficients.

E : Young's modulus of timber.

e : Beam finite element index.

e_d : Edge distance

e_0 : Regression coefficient.

G : Shear modulus of timber.

H : Hermitian interpolation functions

$\mathbf{H}_1, \mathbf{H}_2$: Vector of cubic Hermitian polynomials.

I_x : Major-axis moment of inertia.

I_y : Minor-axis moment of inertia.

$I_{y,m}$: Minor-axis moment of inertia of monolithic section.

J : Saint-Venant torsional constant of a single ply.

J_m : Saint-Venant torsional constant for the monolithic (fully composite) section.

j : Fastener index within a fastener group.

k : Fastener stiffness.

$\overline{k}$: Normalized fastener stiffness.

$\mathbf{K}$: stiffness matrix.

L : Span of the built-up beam.

$\mathbf{L}$: Vector of Linear interpolation functions.

l_e : Length of beam finite element e

M : Bending moment of the beam.

M_1 : End bending moment at $z = 0$.

M_2 : End bending moment at $z = L$.

M_{cr} : Elastic lateral–torsional buckling critical moment.

M_{cru} : Uniform critical moment of the built-up beam

M_m: Uniform critical moment of the monolithic (fully composite) section.

M_{nc}: Uniform critical moment of the non-composite (no interaction) case.

m: The elastic uniform critical moment of the built-up beam under uniform bending relative to that of the non-composite case.

n_p: Number of plies in the built-up beam.

n_f: Number of fasteners stacked vertically within a fastener group.

S_P: Longitudinal fastener spacing (parallel to the grain).

S_q: Transverse fastener spacing (perpendicular to the grain).

s: Beam segment between two fastener columns (groups).

q: Transverse load acting on each ply.

u: Lateral displacement of the plies during buckling.

$\mathbf{u}_e(z)$: Vector of nodal lateral displacements

v_γ: Transverse displacement of ply γ.

$\mathbf{V}_e(z)$: Vector of nodal transverse displacements

$\mathbf{W}_e(z)$: Vector of nodal longitudinal displacements.

w_γ: Longitudinal displacement of ply γ.

y_j: Vertical location of fastener $j$measured from the shear center.

y_q : Load height measured below the shear center.

z : Longitudinal coordinate along the beam axis.

z_i : Longitudinal coordinate of fastener plane i.

UDL : Uniformly distributed load.

1-PL : Mid-span point load.

2-PL : Two point loads applied at one-third points along the span.

α: Degree of interaction between plies; values near zero indicate no interaction, while a value of one denotes full interaction.

β : Parameter defining ply numbering limits depending on whether the number of plies is odd or even.

γ : Ply index.

λ : Load multiplier to be determined from the buckling analysis.

π : Total potential energy of the built-up system throughout buckling.

$\pi_{b,e}$: Total potential energy stored in the plies of beam segment e .

$\pi_{s,i}$: Internal strain energy stored in the fastener group located at fastener plane i.

ρ_m : Mean wood density.

θ : Angle of twist of the built-up beam.

$\boldsymbol{\theta}_e(z)$: Vector of nodal angles of twist

ω: Constant depending on the cross-sectional aspect ratio used in torsional constant expressions.

Chapter 5: Summary, Conclusions and Recommendations

5.1 Summary

The present study contributed to the advancement of the state of knowledge of the LTB of built-up wooden beams consisting of multiple plies with the same depth connected through discrete mechanical fasteners through three contributions.

The first contribution developed a 3D finite-element model to numerically evaluate the elastic LTB resistance of two-ply built-up beams based on an eigenvalue analysis. The model adopts an orthotropic model to idealize the timber material behaviour and treats the fasteners as relatively elastic springs with a specified shear stiffness representative of their load deformation behaviour. The study examined the effect of fastener stiffness and spacing on the elastic LTB resistance.

The second contribution developed a variational principle and a finite element formulation for the LTB analysis of two-ply beams, leading to an eigenvalue problem. A parametric investigation was conducted to determine the effect of fastener stiffness and arrangement, moment gradient, load height effect, and beam geometry on the LTB capacity. The investigation also examined the potential of adopting non-uniform fastener distributions as a means of optimizing the design of built-up beams.

The third contribution extended the variational formulation and finite element analysis to LTB of multi-ply built-up beams. The predictions of the developed finite element formulation were verified against a 3D finite element model and an experimental study. The formulation employs a two-node beam element per ply with seven degrees of freedom (DOFs) per node. The nodal lateral displacement u, angle of twist θ, and their derivatives u', θ' are taken as common to all plies while the longitudinal displacement w, transverse displacement v and bending rotation, v' and are

assigned independently for each ply. For a built-up beam consisting of n_p plies that is discretized into n_e elements, the total number of buckling DOFs in the system is $(n_e+1)(4+3n_p)$. For example, the three-ply reference beam analyzed in Chapter 4, which was discretized into 18 longitudinal elements involved only 247 DOFs, which corresponds to less than 0.5% of the 49,005 DOFs required in C3D8 Abaqus model for the same problem. The computational advantage realized becomes even more pronounced as the number of plies increases. This feature enabled the generation of a large database of parametric study comprising 733 runs to investigate the effect of number of plies, fastener stiffness, spacing, number of plies, and the beam geometry on the critical moment. Using the resulting database, design-oriented dimensionless equations were developed through symbolic regression to predict the normalized critical moments, moment-gradient factor for common loading conditions, and load height effects.

5.2 Conclusions

The main conclusions of the study are summarized in the following:

5.2.1 Two-ply beams

1. The elastic critical moment of two-ply built-up beams connected by discrete fasteners with typical stiffness values and nailing layouts was found to be significantly lower than that of a monolithic beam with the same geometry.
2. For a target total fastener stiffness, reducing the spacing between fasteners (i.e., increasing the number of fasteners) was found to be a more effective measure to increase the lateral torsional buckling capacity than increasing the stiffness of the individual fasteners.

3. Adopting a denser nailing pattern near the supports of simply supported beams was shown to marginally enhance the elastic critical moment (by approximately 6%) relative to the conventional uniform nailing pattern.

5.2.2 Multi-Ply beams

1. The validity of the formulation developed in the present study was verified through comparisons with full-scale experimental results and with 3D-finite element models' predictions.
2. The parametric study conducted indicates that the uniform elastic critical moment increases with fastener normalized stiffness, number of plies, span-to-depth ratio, and depth-to-width ratio, while it decreases with normalized longitudinal and transverse fastener spacings.
3. In contrast to monolithic simply supported beams, for which the moment gradient factor depends solely on the bending moment distribution, moment gradient factors for built-up beams were shown to depend on additional parameters. It increases with normalized longitudinal and transverse spacings and decreases with the normalized fastener stiffness, number of plies, span-to-depth ratio, and depth-to-width ratio.
4. The load height factor was found to increase with the span-to-depth ratio and with the normalized longitudinal and transverse spacings, while it decreases with the normalized fastener stiffness, number of plies, and depth-to-width ratio.

5.3 Recommendations for future research

1. The proposed beam formulation can be extended to account for pre-buckling deformation effects as well as partial end restraint conditions, both of which are known to influence the elastic lateral–torsional buckling response of beams.

2. The present framework has been based on an eigenvalue-type buckling analysis. It is of interest to develop nonlinear beam and three-dimensional finite element models that capture material and geometric nonlinear effects, thus enabling the investigation of post-buckling behaviour.
3. The analysis conducted herein is restricted to aligned (non-staggered) fastener arrangements. Future studies may examine the effect of staggered fastener configurations on the degree of composite action and the resulting lateral–torsional buckling resistance.
4. The present work concentrates on conventional mechanical connectors, such as nails and screws, for joining plies. Alternative connection systems, such as bolts and split-ring connectors, can be investigated, as they are expected to provide substantially higher shear stiffness and subsequently higher LTB capacity.
5. Full-scale experimental testing of built-up beams with varying nailing patterns—including uniform, non-uniform, and staggered arrangements—and different numbers of plies would provide further experimental verification.
6. The use of inclined fasteners, particularly self-tapping screws, to connect plies is a promising idea to improve the interaction between plies. Engaging such fasteners in withdrawal is expected to improve connection stiffness and may lead to measurable gains in buckling resistance. Further investigations in this respect are recommended.
7. The design-oriented equations developed in this study are limited to uniformly distributed loads, single-point loads, and two-point loading configurations. Extending the analysis to additional loading scenarios would broaden the applicability of the solution.

Appendix A: Mesh sensitivity analysis

This appendix presents the mesh sensitivity analysis performed for the reference case established in Chapters 2 and 3. Table A.1 outlines the mesh sensitivity analysis for the 3D finite element model for the reference case in Chapters 2 and 3. Columns 2 to 4 specify the number of elements in lateral, transverse and longitudinal directions respectively. Columns 5 to 7 list the element size in the three directions and Column 8 presents the critical moment. Table A.2 provides the mesh sensitivity analysis for the present model based on the formulation presented in Chapter 3. Table A.2 shows that convergence was achieved by using 18 elements along the beam length.

Table A.1: Mesh sensitivity analysis for 3D FE model

Case No. (1)	Nx Lateral Direction (2)	Ny Transverse Direction (3)	Nz Longitudinal Direction (4)	Dimension of element (mm)			Critical moment (kN·m) (8)
				x- direction (5)	y-direction (6)	z-direction (7)	
1	2	4	63	19	80	80	11.08
2	2	5	84	19	60	60	10.32
3	2	7	125	19	40	40	10.10
4	2	7	125	19	40	40	9.99
5	2	15	250	19	20	20	9.34
6	2	28	500	10	10	10	9.32

Table A.2: Mesh sensitivity analysis for present model

Case No. (1)	No. of elements (2)	Element size (mm) (3)	Critical moment (kN·m) (4)
1	18	278	9.78
2	36	139	9.78
3	54	93	9.78
4	72	69	9.78

Appendix B: Results of Parametric Study

This appendix presents the numerical results obtained from the parametric study described in Chapter 4. The study comprises a total of 733 runs. For each run, the input parameters $b, d, L, k, S_p, S_q, n_p$ and load type are provided in columns 2-9, followed by the dimensionless parameters $\bar{k}, S_p/L, S_q/L, L/d, d/b$ in columns 10-14. The predictions are organized into three tables.

Table B.1 summarizes the cases of beams subjected to a uniform bending moment and provides the critical moment ratio M_{cru}/M_{nc} as predicted by the finite element model in Column 15 and the critical moment ratio as predicted by the proposed design equations in Eq. 4.18 in Column 16.

Table B.2 presents the results for beams under non-uniform moments corresponding to loads applied at the shear center, including uniformly distributed load (UDL), mid-span point load (1-PL), and two-point loading (2-PL) applied at the third span points and provides the moment gradient ratio C_b as predicted by the finite element model in Column 15 and that predicted by Eq. 4.19 in Column 16.

Table B.3 provides the results for beams under non-uniform moments for the same loading cases as in Table B.2, when applied at the top face of the beam. The table provides the load height factor C_L as predicted by the finite element model in Column 15 and that predicted by Eq. 4.19 in Column 16.

Table B.1: Results for built-up beams subjected to uniform moment

Run No. (1)	Ply dimensions (mm)			Fastener			Load Type	Dimensionless Parameters						Present Study	Eq. (4.18)
				Stiffness (N/mm)	Pattern (mm)										
	b (2)	d (3)	L (4)	k (5)	S_p (6)	S_q (7)	Load Type (8)	n_p (9)	$\bar{k}$ (10)	$\frac{S_p}{L}$ (11)	$\frac{S_q}{d}$ (12)	$\frac{L}{d}$ (13)	$\frac{d}{b}$ (14)	$\frac{M_{cru}}{M_{nc}}$ (15)	$\frac{M_{cru}}{M_{nc}}$ (16)
1	38	286	5000	0	294	98	UM	2	0.0	0.059	0.343	17.5	7.5	1.00	1.00
2	38	286	5000	500	294	98	UM	2	88.8	0.059	0.343	17.5	7.5	1.18	1.28
3	38	286	5000	830	294	98	UM	2	147.4	0.059	0.343	17.5	7.5	1.31	1.37
4	38	286	5000	1104	294	98	UM	2	196.1	0.059	0.343	17.5	7.5	1.34	1.44
5	38	286	5000	1500	294	98	UM	2	266.4	0.059	0.343	17.5	7.5	1.39	1.53
6	38	286	5000	2000	294	98	UM	2	355.2	0.059	0.343	17.5	7.5	1.46	1.62
7	38	286	5000	3001	294	98	UM	2	532.9	0.059	0.343	17.5	7.5	1.57	1.79
8	38	286	5000	830	294	43	UM	2	147.4	0.059	0.149	17.5	7.5	1.74	1.90
9	38	286	5000	830	294	64	UM	2	147.4	0.059	0.224	17.5	7.5	1.60	1.66
10	38	286	5000	830	294	85	UM	2	147.4	0.059	0.298	17.5	7.5	1.45	1.47
11	38	286	5000	830	294	106	UM	2	147.4	0.059	0.372	17.5	7.5	1.31	1.31
12	38	286	5000	830	294	128	UM	2	147.4	0.059	0.447	17.5	7.5	1.20	1.17
13	38	286	5000	830	200	98	UM	2	147.4	0.040	0.343	17.5	7.5	1.47	1.50
14	38	286	5000	830	349	98	UM	2	147.4	0.070	0.343	17.5	7.5	1.30	1.32
15	38	286	5000	830	599	98	UM	2	147.4	0.120	0.343	17.5	7.5	1.22	1.17
16	38	286	5000	830	849	98	UM	2	147.4	0.170	0.343	17.5	7.5	1.14	1.08
17	38	286	5000	830	1098	98	UM	2	147.4	0.220	0.343	17.5	7.5	1.05	1.03
18	38	286	5000	0	294	98	UM	3	0.0	0.059	0.343	17.5	7.5	1.00	1.00
19	38	286	5000	500	294	98	UM	3	88.8	0.059	0.343	17.5	7.5	1.41	1.41
20	38	286	5000	830	294	98	UM	3	147.4	0.059	0.343	17.5	7.5	1.56	1.55
21	38	286	5000	1000	294	98	UM	3	177.6	0.059	0.343	17.5	7.5	1.65	1.62
22	38	286	5000	1500	294	98	UM	3	266.4	0.059	0.343	17.5	7.5	1.86	1.78
23	38	286	5000	2000	294	98	UM	3	355.2	0.059	0.343	17.5	7.5	2.02	1.93
24	38	286	5000	3001	294	98	UM	3	532.9	0.059	0.343	17.5	7.5	2.28	2.18
25	38	286	5000	830	294	43	UM	3	147.4	0.059	0.149	17.5	7.5	2.07	2.08
26	38	286	5000	830	294	64	UM	3	147.4	0.059	0.224	17.5	7.5	1.89	1.84
27	38	286	5000	830	294	85	UM	3	147.4	0.059	0.298	17.5	7.5	1.72	1.65
28	38	286	5000	830	294	106	UM	3	147.4	0.059	0.372	17.5	7.5	1.57	1.49
29	38	286	5000	830	294	128	UM	3	147.4	0.059	0.447	17.5	7.5	1.43	1.35
30	38	286	5000	830	200	98	UM	3	147.4	0.040	0.343	17.5	7.5	1.77	1.68
31	38	286	5000	830	334	98	UM	3	147.4	0.067	0.343	17.5	7.5	1.57	1.51
32	38	286	5000	830	589	98	UM	3	147.4	0.118	0.343	17.5	7.5	1.48	1.36
33	38	286	5000	830	844	98	UM	3	147.4	0.169	0.343	17.5	7.5	1.35	1.27
34	38	286	5000	830	1098	98	UM	3	147.4	0.220	0.343	17.5	7.5	1.25	1.21
35	38	286	5000	0	294	98	UM	4	0.0	0.059	0.343	17.5	7.5	1.00	1.00
36	38	286	5000	500	294	98	UM	4	88.8	0.059	0.343	17.5	7.5	1.56	1.54
37	38	286	5000	830	294	98	UM	4	147.4	0.059	0.343	17.5	7.5	1.75	1.73
38	38	286	5000	1000	294	98	UM	4	177.6	0.059	0.343	17.5	7.5	1.87	1.82

Run No. (1)	Ply dimensions (mm)			Fastener Stiffness (N/mm)	Fastener Pattern (mm)		Load Type	Dimensionless Parameters						Present Study	Eq. (4.18)
	b (2)	d (3)	L (4)	k (5)	S_p (6)	S_q (7)	Load Type (8)	n_p (9)	$\bar{k}$ (10)	$\frac{S_p}{L}$ (11)	$\frac{S_q}{d}$ (12)	$\frac{L}{d}$ (13)	$\frac{d}{b}$ (14)	$\frac{M_{cru}}{M_{nc}}$ (15)	$\frac{M_{cru}}{M_{nc}}$ (16)
39	38	286	5000	1500	294	98	UM	4	266.4	0.059	0.343	17.5	7.5	2.10	2.04
40	38	286	5000	2000	294	98	UM	4	355.2	0.059	0.343	17.5	7.5	2.32	2.23
41	38	286	5000	3001	294	98	UM	4	532.9	0.059	0.343	17.5	7.5	2.67	2.56
42	38	286	5000	830	294	43	UM	4	147.4	0.059	0.149	17.5	7.5	2.29	2.26
43	38	286	5000	830	294	64	UM	4	147.4	0.059	0.224	17.5	7.5	2.10	2.02
44	38	286	5000	830	294	85	UM	4	147.4	0.059	0.298	17.5	7.5	1.91	1.83
45	38	286	5000	830	294	106	UM	4	147.4	0.059	0.372	17.5	7.5	1.73	1.67
46	38	286	5000	830	294	128	UM	4	147.4	0.059	0.447	17.5	7.5	1.58	1.53
47	38	286	5000	830	200	98	UM	4	147.4	0.040	0.343	17.5	7.5	1.97	1.86
48	38	286	5000	830	334	98	UM	4	147.4	0.067	0.343	17.5	7.5	1.75	1.69
49	38	286	5000	830	589	98	UM	4	147.4	0.118	0.343	17.5	7.5	1.64	1.54
50	38	286	5000	830	844	98	UM	4	147.4	0.169	0.343	17.5	7.5	1.46	1.45
51	38	286	5000	830	1098	98	UM	4	147.4	0.220	0.343	17.5	7.5	1.35	1.39
52	38	286	5000	0	294	98	UM	5	0.0	0.059	0.343	17.5	7.5	1.00	1.00
53	38	286	5000	500	294	98	UM	5	88.8	0.059	0.343	17.5	7.5	1.66	1.68
54	38	286	5000	830	294	98	UM	5	147.4	0.059	0.343	17.5	7.5	1.87	1.91
55	38	286	5000	1000	294	98	UM	5	177.6	0.059	0.343	17.5	7.5	1.97	2.02
56	38	286	5000	1500	294	98	UM	5	266.4	0.059	0.343	17.5	7.5	2.27	2.29
57	38	286	5000	2000	294	98	UM	5	355.2	0.059	0.343	17.5	7.5	2.53	2.53
58	38	286	5000	3001	294	98	UM	5	532.9	0.059	0.343	17.5	7.5	2.94	2.94
59	38	286	5000	830	294	43	UM	5	147.4	0.059	0.149	17.5	7.5	2.54	2.44
60	38	286	5000	830	294	64	UM	5	147.4	0.059	0.224	17.5	7.5	2.33	2.20
61	38	286	5000	830	294	85	UM	5	147.4	0.059	0.298	17.5	7.5	2.09	2.01
62	38	286	5000	830	294	106	UM	5	147.4	0.059	0.372	17.5	7.5	1.87	1.85
63	38	286	5000	830	294	128	UM	5	147.4	0.059	0.447	17.5	7.5	1.72	1.71
64	38	286	5000	830	200	98	UM	5	147.4	0.040	0.343	17.5	7.5	2.14	2.04
65	38	286	5000	830	334	98	UM	5	147.4	0.067	0.343	17.5	7.5	1.87	1.87
66	38	286	5000	830	589	98	UM	5	147.4	0.118	0.343	17.5	7.5	1.74	1.72
67	38	286	5000	830	844	98	UM	5	147.4	0.169	0.343	17.5	7.5	1.57	1.63
68	38	286	5000	830	1098	98	UM	5	147.4	0.220	0.343	17.5	7.5	1.49	1.57
69	65	500	5000	830	294	98	UM	2	147.4	0.059	0.343	10.0	7.5	1.22	1.09
70	44	333	5000	830	294	98	UM	2	147.4	0.059	0.343	15.0	7.5	1.37	1.28
71	38	294	5000	830	294	98	UM	2	147.4	0.059	0.343	17.0	7.5	1.43	1.35
72	34	263	5000	830	294	98	UM	2	147.4	0.059	0.343	19.0	7.5	1.48	1.43
73	31	238	5000	830	294	98	UM	2	147.4	0.059	0.343	21.0	7.5	1.54	1.51
74	43	286	5000	830	294	98	UM	2	147.4	0.059	0.343	17.5	6.5	1.41	1.33
75	37	286	5000	830	294	98	UM	2	147.4	0.059	0.343	17.5	7.5	1.44	1.37
76	33	286	5000	830	294	98	UM	2	147.4	0.059	0.343	17.5	8.5	1.47	1.41
77	31	286	5000	830	294	98	UM	2	147.4	0.059	0.343	17.5	9.0	1.49	1.43
78	65	500	5000	830	294	98	UM	3	147.4	0.059	0.343	10.0	7.5	1.33	1.27
79	44	333	5000	830	294	98	UM	3	147.4	0.059	0.343	15.0	7.5	1.47	1.46

Run No. (1)	Ply dimensions (mm)			Fastener Stiffness (N/mm)	Fastener Pattern (mm)		Load Type	Dimensionless Parameters						Present Study	Eq. (4.18)
	b (2)	d (3)	L (4)	k (5)	S_p (6)	S_q (7)	Load Type (8)	n_p (9)	$\bar{k}$ (10)	$\frac{S_p}{L}$ (11)	$\frac{S_q}{d}$ (12)	$\frac{L}{d}$ (13)	$\frac{d}{b}$ (14)	$\frac{M_{cru}}{M_{nc}}$ (15)	$\frac{M_{cru}}{M_{nc}}$ (16)
80	38	294	5000	830	294	98	UM	3	147.4	0.059	0.343	17.0	7.5	1.55	1.54
81	34	263	5000	830	294	98	UM	3	147.4	0.059	0.343	19.0	7.5	1.62	1.61
82	31	238	5000	830	294	98	UM	3	147.4	0.059	0.343	21.0	7.5	1.69	1.69
83	43	286	5000	830	294	98	UM	3	147.4	0.059	0.343	17.5	6.5	1.53	1.51
84	38	286	5000	830	294	98	UM	3	147.4	0.059	0.343	17.5	7.5	1.56	1.55
85	33	286	5000	830	294	98	UM	3	147.4	0.059	0.343	17.5	8.5	1.61	1.59
86	31	286	5000	830	294	98	UM	3	147.4	0.059	0.343	17.5	9.0	1.63	1.61
87	65	500	5000	830	294	98	UM	4	147.4	0.059	0.343	10.0	7.5	1.40	1.45
88	44	333	5000	830	294	98	UM	4	147.4	0.059	0.343	15.0	7.5	1.61	1.64
89	38	294	5000	830	294	98	UM	4	147.4	0.059	0.343	17.0	7.5	1.70	1.72
90	34	263	5000	830	294	98	UM	4	147.4	0.059	0.343	19.0	7.5	1.78	1.79
91	31	238	5000	830	294	98	UM	4	147.4	0.059	0.343	21.0	7.5	1.86	1.87
92	43	286	5000	830	294	98	UM	4	147.4	0.059	0.343	17.5	6.5	1.67	1.69
93	38	286	5000	830	294	98	UM	4	147.4	0.059	0.343	17.5	7.5	1.72	1.73
94	33	286	5000	830	294	98	UM	4	147.4	0.059	0.343	17.5	8.5	1.77	1.77
95	31	286	5000	830	294	98	UM	4	147.4	0.059	0.343	17.5	9.0	1.79	1.79
96	65	500	5000	830	294	98	UM	5	147.4	0.059	0.343	10.0	7.5	1.49	1.63
97	44	333	5000	830	294	98	UM	5	147.4	0.059	0.343	15.0	7.5	1.72	1.82
98	38	294	5000	830	294	98	UM	5	147.4	0.059	0.343	17.0	7.5	1.82	1.90
99	34	263	5000	830	294	98	UM	5	147.4	0.059	0.343	19.0	7.5	1.91	1.97
100	31	238	5000	830	294	98	UM	5	147.4	0.059	0.343	21.0	7.5	2.00	2.05
101	36	238	5000	2027	80	129	UM	3	360.0	0.016	0.450	21.0	6.5	2.82	2.56
102	36	238	5000	0	80	43	UM	3	0.0	0.016	0.150	21.0	6.5	1.00	1.00
103	76	500	5000	2027	1098	43	UM	3	360.0	0.220	0.150	10.0	6.5	1.34	1.67
104	76	500	5000	0	80	43	UM	3	0.0	0.016	0.150	10.0	6.5	1.00	1.00
105	55	500	5000	2027	1098	43	UM	3	360.0	0.220	0.150	10.0	9.0	1.69	1.85
106	55	500	5000	2027	80	129	UM	3	360.0	0.016	0.450	10.0	9.0	2.40	2.02
107	36	238	5000	2027	1098	43	UM	3	360.0	0.220	0.15	21.0	6.5	2.05	2.39

Table B.2: Results for built-up beams subjected to uniform distributed load, Mid-span point load and two-point load applied at the shear center

Run No. (1)	Ply dimensions (mm)			Fastener Stiffness (N/mm)	Fastener Pattern (mm)		Load Type	Dimensionless Pramaeters						Present Study	Eq. (4.19)
	(2)	d (3)	L (4)	k (5)	S_p (6)	S_q (7)	Load Type (8)	n_p (9)	$\bar{k}$ (10)	$\frac{S_p}{L}$ (11)	$\frac{S_q}{d}$ (12)	$\frac{L}{d}$ (13)	$\frac{d}{b}$ (14)	C_b (15)	C_b (16)
108	38	286	5000	0	294	98	UDL	2	0.0	0.059	0.343	17.5	7.5	1.13	1.13
109	38	286	5000	507	294	98	UDL	2	90.0	0.059	0.343	17.5	7.5	1.12	1.11
110	38	286	5000	1013	294	98	UDL	2	180.0	0.059	0.343	17.5	7.5	1.11	1.11
111	38	286	5000	1520	294	98	UDL	2	270.0	0.059	0.343	17.5	7.5	1.10	1.10
112	38	286	5000	2027	294	98	UDL	2	360.0	0.059	0.343	17.5	7.5	1.10	1.10
113	38	286	5000	0	294	98	UDL	3	0.0	0.059	0.343	17.5	7.5	1.13	1.13
114	38	286	5000	507	294	98	UDL	3	90.0	0.059	0.343	17.5	7.5	1.11	1.11
115	38	286	5000	1013	294	98	UDL	3	180.0	0.059	0.343	17.5	7.5	1.10	1.10
116	38	286	5000	1520	294	98	UDL	3	270.0	0.059	0.343	17.5	7.5	1.09	1.10
117	38	286	5000	2027	294	98	UDL	3	360.0	0.059	0.343	17.5	7.5	1.09	1.09
118	38	286	5000	0	294	98	UDL	4	0.0	0.059	0.343	17.5	7.5	1.13	1.13
119	38	286	5000	507	294	98	UDL	4	90.0	0.059	0.343	17.5	7.5	1.11	1.10
120	38	286	5000	1013	294	98	UDL	4	180.0	0.059	0.343	17.5	7.5	1.10	1.09
121	38	286	5000	1520	294	98	UDL	4	270.0	0.059	0.343	17.5	7.5	1.09	1.09
122	38	286	5000	2027	294	98	UDL	4	360.0	0.059	0.343	17.5	7.5	1.08	1.08
123	38	286	5000	0	294	98	UDL	5	0.0	0.059	0.343	17.5	7.5	1.13	1.13
124	38	286	5000	507	294	98	UDL	5	90.0	0.059	0.343	17.5	7.5	1.10	1.10
125	38	286	5000	1013	294	98	UDL	5	180.0	0.059	0.343	17.5	7.5	1.09	1.09
126	38	286	5000	1520	294	98	UDL	5	270.0	0.059	0.343	17.5	7.5	1.08	1.08
127	38	286	5000	2027	294	98	UDL	5	360.0	0.059	0.343	17.5	7.5	1.08	1.07
128	38	286	5000	830	294	129	UDL	2	147.4	0.059	0.450	17.5	7.5	1.12	1.12
129	38	286	5000	830	294	107	UDL	2	147.4	0.059	0.375	17.5	7.5	1.11	1.11
130	38	286	5000	830	294	86	UDL	2	147.4	0.059	0.300	17.5	7.5	1.11	1.11
131	38	286	5000	830	294	64	UDL	2	147.4	0.059	0.225	17.5	7.5	1.10	1.10
132	38	286	5000	830	294	43	UDL	2	147.4	0.059	0.150	17.5	7.5	1.10	1.10
133	38	286	5000	830	80	98	UDL	2	147.4	0.016	0.343	17.5	7.5	1.09	1.09
134	38	286	5000	830	200	98	UDL	2	147.4	0.040	0.343	17.5	7.5	1.10	1.11
135	38	286	5000	830	334	98	UDL	2	147.4	0.067	0.343	17.5	7.5	1.11	1.11
136	38	286	5000	830	589	98	UDL	2	147.4	0.118	0.343	17.5	7.5	1.11	1.11
137	38	286	5000	830	844	98	UDL	2	147.4	0.169	0.343	17.5	7.5	1.11	1.11
138	38	286	5000	830	1098	98	UDL	2	147.4	0.220	0.343	17.5	7.5	1.11	1.11
139	38	286	5000	830	294	129	UDL	3	147.4	0.059	0.450	17.5	7.5	1.11	1.11
140	38	286	5000	830	294	107	UDL	3	147.4	0.059	0.375	17.5	7.5	1.11	1.11
141	38	286	5000	830	294	86	UDL	3	147.4	0.059	0.300	17.5	7.5	1.10	1.10
142	38	286	5000	830	294	64	UDL	3	147.4	0.059	0.225	17.5	7.5	1.10	1.10
143	38	286	5000	830	294	43	UDL	3	147.4	0.059	0.150	17.5	7.5	1.09	1.09

Run No. (1)	Ply dimensions (mm)			Fastener Stiffness (N/mm)	Fastener Pattern (mm)		Load Type	Dimensionless Pramaeters						Present Study	Eq. (4.19)
	(2)	d (3)	L (4)	k (5)	S_p (6)	S_q (7)	Load Type (8)	n_p (9)	$\bar{k}$ (10)	$\frac{S_p}{L}$ (11)	$\frac{S_q}{d}$ (12)	$\frac{L}{d}$ (13)	$\frac{d}{b}$ (14)	C_b (15)	C_b (16)
144	38	286	5000	830	80	98	UDL	3	147.4	0.016	0.343	17.5	7.5	1.08	1.08
145	38	286	5000	830	200	98	UDL	3	147.4	0.040	0.343	17.5	7.5	1.10	1.10
146	38	286	5000	830	334	98	UDL	3	147.4	0.067	0.343	17.5	7.5	1.11	1.10
147	38	286	5000	830	589	98	UDL	3	147.4	0.118	0.343	17.5	7.5	1.11	1.11
148	38	286	5000	830	844	98	UDL	3	147.4	0.169	0.343	17.5	7.5	1.11	1.11
149	38	286	5000	830	1098	98	UDL	3	147.4	0.220	0.343	17.5	7.5	1.11	1.11
150	38	286	5000	830	294	129	UDL	4	147.4	0.059	0.450	17.5	7.5	1.10	1.10
151	38	286	5000	830	294	107	UDL	4	147.4	0.059	0.375	17.5	7.5	1.10	1.10
152	38	286	5000	830	294	86	UDL	4	147.4	0.059	0.300	17.5	7.5	1.09	1.10
153	38	286	5000	830	294	64	UDL	4	147.4	0.059	0.225	17.5	7.5	1.09	1.09
154	38	286	5000	830	294	43	UDL	4	147.4	0.059	0.150	17.5	7.5	1.08	1.08
155	38	286	5000	830	80	98	UDL	4	147.4	0.016	0.343	17.5	7.5	1.07	1.07
156	38	286	5000	830	200	98	UDL	4	147.4	0.040	0.343	17.5	7.5	1.09	1.09
157	38	286	5000	830	334	98	UDL	4	147.4	0.067	0.343	17.5	7.5	1.10	1.10
158	38	286	5000	830	589	98	UDL	4	147.4	0.118	0.343	17.5	7.5	1.10	1.10
159	38	286	5000	830	844	98	UDL	4	147.4	0.169	0.343	17.5	7.5	1.10	1.10
160	38	286	5000	830	1098	98	UDL	4	147.4	0.220	0.343	17.5	7.5	1.10	1.10
161	38	286	5000	830	294	129	UDL	5	147.4	0.059	0.450	17.5	7.5	1.10	1.10
162	38	286	5000	830	294	107	UDL	5	147.4	0.059	0.375	17.5	7.5	1.09	1.09
163	38	286	5000	830	294	86	UDL	5	147.4	0.059	0.300	17.5	7.5	1.09	1.09
164	38	286	5000	830	294	64	UDL	5	147.4	0.059	0.225	17.5	7.5	1.08	1.08
165	38	286	5000	830	294	43	UDL	5	147.4	0.059	0.150	17.5	7.5	1.08	1.08
166	38	286	5000	830	80	98	UDL	5	147.4	0.016	0.343	17.5	7.5	1.07	1.07
167	38	286	5000	830	200	98	UDL	5	147.4	0.040	0.343	17.5	7.5	1.08	1.09
168	38	286	5000	830	334	98	UDL	5	147.4	0.067	0.343	17.5	7.5	1.09	1.09
169	38	286	5000	830	589	98	UDL	5	147.4	0.118	0.343	17.5	7.5	1.09	1.09
170	38	286	5000	830	844	98	UDL	5	147.4	0.169	0.343	17.5	7.5	1.09	1.09
171	38	286	5000	830	1098	98	UDL	5	147.4	0.220	0.343	17.5	7.5	1.09	1.09
172	65	500	5000	830	294	98	UDL	2	147.4	0.059	0.343	10.0	7.5	1.12	1.12
173	44	333	5000	830	294	98	UDL	2	147.4	0.059	0.343	15.0	7.5	1.12	1.11
174	38	294	5000	830	294	98	UDL	2	147.4	0.059	0.343	17.0	7.5	1.11	1.11
175	34	263	5000	830	294	98	UDL	2	147.4	0.059	0.343	19.0	7.5	1.11	1.11
176	31	238	5000	830	294	98	UDL	2	147.4	0.059	0.343	21.0	7.5	1.11	1.10
177	43	286	5000	830	294	98	UDL	2	147.4	0.059	0.343	17.5	6.5	1.11	1.11
178	37	286	5000	830	294	98	UDL	2	147.4	0.059	0.343	17.5	7.5	1.11	1.11
179	33	286	5000	830	294	98	UDL	2	147.4	0.059	0.343	17.5	8.5	1.11	1.11
180	31	286	5000	830	294	98	UDL	2	147.4	0.059	0.343	17.5	9.0	1.11	1.11
181	65	500	5000	830	294	98	UDL	3	147.4	0.059	0.343	10.0	7.5	1.12	1.12
182	44	333	5000	830	294	98	UDL	3	147.4	0.059	0.343	15.0	7.5	1.11	1.11

Run No. (1)	Ply dimensions (mm)			Fastener Stiffness (N/mm)	Fastener Pattern (mm)		Load Type	Dimensionless Pramaeters						Present Study	Eq. (4.19)
	(2)	d (3)	L (4)	k (5)	S_p (6)	S_q (7)	Load Type (8)	n_p (9)	$\bar{k}$ (10)	$\frac{S_p}{L}$ (11)	$\frac{S_q}{d}$ (12)	$\frac{L}{d}$ (13)	$\frac{d}{b}$ (14)	C_b (15)	C_b (16)
183	38	294	5000	830	294	98	UDL	3	147.4	0.059	0.343	17.0	7.5	1.11	1.10
184	34	263	5000	830	294	98	UDL	3	147.4	0.059	0.343	19.0	7.5	1.10	1.10
185	31	238	5000	830	294	98	UDL	3	147.4	0.059	0.343	21.0	7.5	1.10	1.10
186	43	286	5000	830	294	98	UDL	3	147.4	0.059	0.343	17.5	6.5	1.11	1.11
187	38	286	5000	830	294	98	UDL	3	147.4	0.059	0.343	17.5	7.5	1.11	1.10
188	33	286	5000	830	294	98	UDL	3	147.4	0.059	0.343	17.5	8.5	1.10	1.10
189	31	286	5000	830	294	98	UDL	3	147.4	0.059	0.343	17.5	9.0	1.10	1.10
190	65	500	5000	830	294	98	UDL	4	147.4	0.059	0.343	10.0	7.5	1.11	1.11
191	44	333	5000	830	294	98	UDL	4	147.4	0.059	0.343	15.0	7.5	1.10	1.10
192	38	294	5000	830	294	98	UDL	4	147.4	0.059	0.343	17.0	7.5	1.10	1.10
193	34	263	5000	830	294	98	UDL	4	147.4	0.059	0.343	19.0	7.5	1.10	1.10
194	31	238	5000	830	294	98	UDL	4	147.4	0.059	0.343	21.0	7.5	1.09	1.09
195	43	286	5000	830	294	98	UDL	4	147.4	0.059	0.343	17.5	6.5	1.10	1.10
196	38	286	5000	830	294	98	UDL	4	147.4	0.059	0.343	17.5	7.5	1.10	1.10
197	33	286	5000	830	294	98	UDL	4	147.4	0.059	0.343	17.5	8.5	1.10	1.10
198	31	286	5000	830	294	98	UDL	4	147.4	0.059	0.343	17.5	9.0	1.09	1.10
199	65	500	5000	830	294	98	UDL	5	147.4	0.059	0.343	10.0	7.5	1.10	1.10
200	44	333	5000	830	294	98	UDL	5	147.4	0.059	0.343	15.0	7.5	1.10	1.10
201	38	294	5000	830	294	98	UDL	5	147.4	0.059	0.343	17.0	7.5	1.09	1.09
202	34	263	5000	830	294	98	UDL	5	147.4	0.059	0.343	19.0	7.5	1.09	1.09
203	31	238	5000	830	294	98	UDL	5	147.4	0.059	0.343	21.0	7.5	1.09	1.09
204	43	286	5000	830	294	98	UDL	5	147.4	0.059	0.343	17.5	6.5	1.09	1.09
205	38	286	5000	830	294	98	UDL	5	147.4	0.059	0.343	17.5	7.5	1.09	1.09
206	33	286	5000	830	294	98	UDL	5	147.4	0.059	0.343	17.5	8.5	1.09	1.09
207	31	286	5000	830	294	98	UDL	5	147.4	0.059	0.343	17.5	9.0	1.09	1.09
208	36	238	5000	2027	80	129	UDL	3	360.0	0.016	0.450	21.0	6.5	1.07	1.06
209	36	238	5000	0	80	43	UDL	3	0.0	0.016	0.150	21.0	6.5	1.13	1.13
210	76	500	5000	2027	1098	43	UDL	3	360.0	0.220	0.150	10.0	6.5	1.11	1.10
211	76	500	5000	0	80	43	UDL	3	0.0	0.016	0.150	10.0	6.5	1.13	1.13
212	55	500	5000	2027	1098	43	UDL	3	360.0	0.220	0.150	10.0	9.0	1.10	1.09
213	55	500	5000	2027	80	129	UDL	3	360.0	0.016	0.450	10.0	9.0	1.08	1.08
214	36	238	5000	2027	1098	43	UDL	3	360.0	0.220	0.15	21.0	6.5	1.08	1.07
215	38	286	5000	0	294	98	1-PL	2	0.0	0.059	0.343	17.5	7.5	1.35	1.35
216	38	286	5000	507	294	98	1-PL	2	90.0	0.059	0.343	17.5	7.5	1.31	1.30
217	38	286	5000	1013	294	98	1-PL	2	180.0	0.059	0.343	17.5	7.5	1.29	1.29
218	38	286	5000	1520	294	98	1-PL	2	270.0	0.059	0.343	17.5	7.5	1.28	1.28
219	38	286	5000	2027	294	98	1-PL	2	360.0	0.059	0.343	17.5	7.5	1.26	1.27
220	38	286	5000	0	294	98	1-PL	3	0.0	0.059	0.343	17.5	7.5	1.35	1.35
221	38	286	5000	507	294	98	1-PL	3	90.0	0.059	0.343	17.5	7.5	1.30	1.29

Run No. (1)	Ply dimensions (mm)			Fastener Stiffness (N/mm)	Fastener Pattern (mm)		Load Type	Dimensionless Pramaeters						Present Study	Eq. (4.19)
	(2)	d (3)	L (4)	k (5)	S_p (6)	S_q (7)	Load Type (8)	n_p (9)	$\bar{k}$ (10)	$\frac{S_p}{L}$ (11)	$\frac{S_q}{d}$ (12)	$\frac{L}{d}$ (13)	$\frac{d}{b}$ (14)	C_b (15)	C_b (16)
222	38	286	5000	1013	294	98	1-PL	3	180.0	0.059	0.343	17.5	7.5	1.28	1.27
223	38	286	5000	1520	294	98	1-PL	3	270.0	0.059	0.343	17.5	7.5	1.26	1.26
224	38	286	5000	2027	294	98	1-PL	3	360.0	0.059	0.343	17.5	7.5	1.25	1.25
225	38	286	5000	0	294	98	1-PL	4	0.0	0.059	0.343	17.5	7.5	1.35	1.35
226	38	286	5000	507	294	98	1-PL	4	90.0	0.059	0.343	17.5	7.5	1.29	1.28
227	38	286	5000	1013	294	98	1-PL	4	180.0	0.059	0.343	17.5	7.5	1.26	1.26
228	38	286	5000	1520	294	98	1-PL	4	270.0	0.059	0.343	17.5	7.5	1.24	1.24
229	38	286	5000	2027	294	98	1-PL	4	360.0	0.059	0.343	17.5	7.5	1.23	1.23
230	38	286	5000	0	294	98	1-PL	5	0.0	0.059	0.343	17.5	7.5	1.35	1.35
231	38	286	5000	507	294	98	1-PL	5	90.0	0.059	0.343	17.5	7.5	1.28	1.27
232	38	286	5000	1013	294	98	1-PL	5	180.0	0.059	0.343	17.5	7.5	1.25	1.24
233	38	286	5000	1520	294	98	1-PL	5	270.0	0.059	0.343	17.5	7.5	1.23	1.23
234	38	286	5000	2027	294	98	1-PL	5	360.0	0.059	0.343	17.5	7.5	1.23	1.21
235	38	286	5000	830	294	129	1-PL	2	147.4	0.059	0.450	17.5	7.5	1.31	1.31
236	38	286	5000	830	294	107	1-PL	2	147.4	0.059	0.375	17.5	7.5	1.30	1.30
237	38	286	5000	830	294	86	1-PL	2	147.4	0.059	0.300	17.5	7.5	1.29	1.29
238	38	286	5000	830	294	64	1-PL	2	147.4	0.059	0.225	17.5	7.5	1.28	1.28
239	38	286	5000	830	294	43	1-PL	2	147.4	0.059	0.150	17.5	7.5	1.27	1.26
240	38	286	5000	830	80	98	1-PL	2	147.4	0.016	0.343	17.5	7.5	1.25	1.25
241	38	286	5000	830	200	98	1-PL	2	147.4	0.040	0.343	17.5	7.5	1.28	1.28
242	38	286	5000	830	334	98	1-PL	2	147.4	0.067	0.343	17.5	7.5	1.30	1.30
243	38	286	5000	830	589	98	1-PL	2	147.4	0.118	0.343	17.5	7.5	1.31	1.31
244	38	286	5000	830	844	98	1-PL	2	147.4	0.169	0.343	17.5	7.5	1.31	1.31
245	38	286	5000	830	1098	98	1-PL	2	147.4	0.220	0.343	17.5	7.5	1.32	1.32
246	38	286	5000	830	294	129	1-PL	3	147.4	0.059	0.450	17.5	7.5	1.30	1.29
247	38	286	5000	830	294	107	1-PL	3	147.4	0.059	0.375	17.5	7.5	1.28	1.28
248	38	286	5000	830	294	86	1-PL	3	147.4	0.059	0.300	17.5	7.5	1.27	1.27
249	38	286	5000	830	294	64	1-PL	3	147.4	0.059	0.225	17.5	7.5	1.26	1.26
250	38	286	5000	830	294	43	1-PL	3	147.4	0.059	0.150	17.5	7.5	1.26	1.25
251	38	286	5000	830	80	98	1-PL	3	147.4	0.016	0.343	17.5	7.5	1.24	1.24
252	38	286	5000	830	200	98	1-PL	3	147.4	0.040	0.343	17.5	7.5	1.27	1.27
253	38	286	5000	830	334	98	1-PL	3	147.4	0.067	0.343	17.5	7.5	1.28	1.28
254	38	286	5000	830	589	98	1-PL	3	147.4	0.118	0.343	17.5	7.5	1.30	1.29
255	38	286	5000	830	844	98	1-PL	3	147.4	0.169	0.343	17.5	7.5	1.30	1.30
256	38	286	5000	830	1098	98	1-PL	3	147.4	0.220	0.343	17.5	7.5	1.31	1.30
257	38	286	5000	830	294	129	1-PL	4	147.4	0.059	0.450	17.5	7.5	1.28	1.28
258	38	286	5000	830	294	107	1-PL	4	147.4	0.059	0.375	17.5	7.5	1.26	1.27
259	38	286	5000	830	294	86	1-PL	4	147.4	0.059	0.300	17.5	7.5	1.25	1.26
260	38	286	5000	830	294	64	1-PL	4	147.4	0.059	0.225	17.5	7.5	1.24	1.25

Run No. (1)	Ply dimensions (mm)			Fastener Stiffness (N/mm)	Fastener Pattern (mm)		Load Type	Dimensionless Pramaeters						Present Study	Eq. (4.19)
	(2)	d (3)	L (4)	k (5)	S_p (6)	S_q (7)	Load Type (8)	n_p (9)	$\bar{k}$ (10)	$\frac{S_p}{L}$ (11)	$\frac{S_q}{d}$ (12)	$\frac{L}{d}$ (13)	$\frac{d}{b}$ (14)	C_b (15)	C_b (16)
261	38	286	5000	830	294	43	1-PL	4	147.4	0.059	0.150	17.5	7.5	1.24	1.24
262	38	286	5000	830	80	98	1-PL	4	147.4	0.016	0.343	17.5	7.5	1.23	1.23
263	38	286	5000	830	200	98	1-PL	4	147.4	0.040	0.343	17.5	7.5	1.25	1.26
264	38	286	5000	830	334	98	1-PL	4	147.4	0.067	0.343	17.5	7.5	1.26	1.27
265	38	286	5000	830	589	98	1-PL	4	147.4	0.118	0.343	17.5	7.5	1.28	1.28
266	38	286	5000	830	844	98	1-PL	4	147.4	0.169	0.343	17.5	7.5	1.28	1.29
267	38	286	5000	830	1098	98	1-PL	4	147.4	0.220	0.343	17.5	7.5	1.29	1.29
268	38	286	5000	830	294	129	1-PL	5	147.4	0.059	0.450	17.5	7.5	1.27	1.27
269	38	286	5000	830	294	107	1-PL	5	147.4	0.059	0.375	17.5	7.5	1.25	1.26
270	38	286	5000	830	294	86	1-PL	5	147.4	0.059	0.300	17.5	7.5	1.24	1.25
271	38	286	5000	830	294	64	1-PL	5	147.4	0.059	0.225	17.5	7.5	1.23	1.24
272	38	286	5000	830	294	43	1-PL	5	147.4	0.059	0.150	17.5	7.5	1.23	1.22
273	38	286	5000	830	80	98	1-PL	5	147.4	0.016	0.343	17.5	7.5	1.22	1.21
274	38	286	5000	830	200	98	1-PL	5	147.4	0.040	0.343	17.5	7.5	1.24	1.24
275	38	286	5000	830	334	98	1-PL	5	147.4	0.067	0.343	17.5	7.5	1.25	1.26
276	38	286	5000	830	589	98	1-PL	5	147.4	0.118	0.343	17.5	7.5	1.26	1.27
277	38	286	5000	830	844	98	1-PL	5	147.4	0.169	0.343	17.5	7.5	1.26	1.27
278	38	286	5000	830	1098	98	1-PL	5	147.4	0.220	0.343	17.5	7.5	1.28	1.28
279	65	500	5000	830	294	98	1-PL	2	147.4	0.059	0.343	10.0	7.5	1.31	1.31
280	44	333	5000	830	294	98	1-PL	2	147.4	0.059	0.343	15.0	7.5	1.30	1.30
281	38	294	5000	830	294	98	1-PL	2	147.4	0.059	0.343	17.0	7.5	1.30	1.29
282	34	263	5000	830	294	98	1-PL	2	147.4	0.059	0.343	19.0	7.5	1.29	1.29
283	31	238	5000	830	294	98	1-PL	2	147.4	0.059	0.343	21.0	7.5	1.29	1.29
284	43	286	5000	830	294	98	1-PL	2	147.4	0.059	0.343	17.5	6.5	1.29	1.30
285	37	286	5000	830	294	98	1-PL	2	147.4	0.059	0.343	17.5	7.5	1.29	1.29
286	33	286	5000	830	294	98	1-PL	2	147.4	0.059	0.343	17.5	8.5	1.29	1.29
287	31	286	5000	830	294	98	1-PL	2	147.4	0.059	0.343	17.5	9.0	1.29	1.29
288	65	500	5000	830	294	98	1-PL	3	147.4	0.059	0.343	10.0	7.5	1.30	1.29
289	44	333	5000	830	294	98	1-PL	3	147.4	0.059	0.343	15.0	7.5	1.29	1.28
290	38	294	5000	830	294	98	1-PL	3	147.4	0.059	0.343	17.0	7.5	1.28	1.28
291	34	263	5000	830	294	98	1-PL	3	147.4	0.059	0.343	19.0	7.5	1.28	1.28
292	31	238	5000	830	294	98	1-PL	3	147.4	0.059	0.343	21.0	7.5	1.28	1.27
293	43	286	5000	830	294	98	1-PL	3	147.4	0.059	0.343	17.5	6.5	1.28	1.28
294	38	286	5000	830	294	98	1-PL	3	147.4	0.059	0.343	17.5	7.5	1.28	1.28
295	33	286	5000	830	294	98	1-PL	3	147.4	0.059	0.343	17.5	8.5	1.28	1.28
296	31	286	5000	830	294	98	1-PL	3	147.4	0.059	0.343	17.5	9.0	1.28	1.28
297	65	500	5000	830	294	98	1-PL	4	147.4	0.059	0.343	10.0	7.5	1.28	1.28
298	44	333	5000	830	294	98	1-PL	4	147.4	0.059	0.343	15.0	7.5	1.27	1.27
299	38	294	5000	830	294	98	1-PL	4	147.4	0.059	0.343	17.0	7.5	1.27	1.27

Run No. (1)	Ply dimensions (mm)			Fastener Stiffness (N/mm)	Fastener Pattern (mm)		Load Type	Dimensionless Pramaeters						Present Study	Eq. (4.19)
	(2)	d (3)	L (4)	k (5)	S_p (6)	S_q (7)	Load Type (8)	n_p (9)	$\bar{k}$ (10)	$\frac{S_p}{L}$ (11)	$\frac{S_q}{d}$ (12)	$\frac{L}{d}$ (13)	$\frac{d}{b}$ (14)	C_b (15)	C_b (16)
300	34	263	5000	830	294	98	1-PL	4	147.4	0.059	0.343	19.0	7.5	1.26	1.26
301	31	238	5000	830	294	98	1-PL	4	147.4	0.059	0.343	21.0	7.5	1.26	1.26
302	43	286	5000	830	294	98	1-PL	4	147.4	0.059	0.343	17.5	6.5	1.27	1.27
303	38	286	5000	830	294	98	1-PL	4	147.4	0.059	0.343	17.5	7.5	1.26	1.27
304	33	286	5000	830	294	98	1-PL	4	147.4	0.059	0.343	17.5	8.5	1.26	1.26
305	31	286	5000	830	294	98	1-PL	4	147.4	0.059	0.343	17.5	9.0	1.26	1.26
306	65	500	5000	830	294	98	1-PL	5	147.4	0.059	0.343	10.0	7.5	1.27	1.27
307	44	333	5000	830	294	98	1-PL	5	147.4	0.059	0.343	15.0	7.5	1.26	1.26
308	38	294	5000	830	294	98	1-PL	5	147.4	0.059	0.343	17.0	7.5	1.25	1.25
309	34	263	5000	830	294	98	1-PL	5	147.4	0.059	0.343	19.0	7.5	1.25	1.25
310	31	238	5000	830	294	98	1-PL	5	147.4	0.059	0.343	21.0	7.5	1.25	1.25
311	43	286	5000	830	294	98	1-PL	5	147.4	0.059	0.343	17.5	6.5	1.25	1.25
312	38	286	5000	830	294	98	1-PL	5	147.4	0.059	0.343	17.5	7.5	1.25	1.25
313	33	286	5000	830	294	98	1-PL	5	147.4	0.059	0.343	17.5	8.5	1.25	1.25
314	31	286	5000	830	294	98	1-PL	5	147.4	0.059	0.343	17.5	9.0	1.25	1.25
315	36	238	5000	2027	80	129	1-PL	3	360.0	0.016	0.450	21.0	6.5	1.24	1.21
316	36	238	5000	0	80	43	1-PL	3	0.0	0.016	0.150	21.0	6.5	1.35	1.35
317	76	500	5000	2027	1098	43	1-PL	3	360.0	0.220	0.150	10.0	6.5	1.30	1.27
318	76	500	5000	0	80	43	1-PL	3	0.0	0.016	0.150	10.0	6.5	1.35	1.35
319	55	500	5000	2027	1098	43	1-PL	3	360.0	0.220	0.15	10.0	9.0	1.28	1.26
320	55	500	5000	2027	1098	129	1-PL	3	360.0	0.016	0.45	10.0	9.0	1.21	1.23
321	36	238	5000	2027	1098	43	1-PL	3	360.0	0.220	0.15	21.0	6.5	1.23	1.24
322	38	286	5000	0	294	98	2-PL	2	0.0	0.059	0.343	17.5	7.5	1.09	1.09
323	38	286	5000	507	294	98	2-PL	2	90.0	0.059	0.343	17.5	7.5	1.07	1.07
324	38	286	5000	1013	294	98	2-PL	2	180.0	0.059	0.343	17.5	7.5	1.06	1.07
325	38	286	5000	1520	294	98	2-PL	2	270.0	0.059	0.343	17.5	7.5	1.05	1.06
326	38	286	5000	2027	294	98	2-PL	2	360.0	0.059	0.343	17.5	7.5	1.05	1.05
327	38	286	5000	0	294	98	2-PL	3	0.0	0.059	0.343	17.5	7.5	1.09	1.09
328	38	286	5000	507	294	98	2-PL	3	90.0	0.059	0.343	17.5	7.5	1.07	1.07
329	38	286	5000	1013	294	98	2-PL	3	180.0	0.059	0.343	17.5	7.5	1.06	1.06
330	38	286	5000	1520	294	98	2-PL	3	270.0	0.059	0.343	17.5	7.5	1.05	1.05
331	38	286	5000	2027	294	98	2-PL	3	360.0	0.059	0.343	17.5	7.5	1.04	1.04
332	38	286	5000	0	294	98	2-PL	4	0.0	0.059	0.343	17.5	7.5	1.09	1.09
333	38	286	5000	507	294	98	2-PL	4	90.0	0.059	0.343	17.5	7.5	1.06	1.06
334	38	286	5000	1013	294	98	2-PL	4	180.0	0.059	0.343	17.5	7.5	1.05	1.05
335	38	286	5000	1520	294	98	2-PL	4	270.0	0.059	0.343	17.5	7.5	1.04	1.04
336	38	286	5000	2027	294	98	2-PL	4	360.0	0.059	0.343	17.5	7.5	1.03	1.03
337	38	286	5000	0	294	98	2-PL	5	0.0	0.059	0.343	17.5	7.5	1.09	1.09
338	38	286	5000	507	294	98	2-PL	5	90.0	0.059	0.343	17.5	7.5	1.06	1.06

Run No. (1)	Ply dimensions (mm)			Fastener Stiffness (N/mm)	Fastener Pattern (mm)		Load Type	Dimensionless Pramaeters						Present Study	Eq. (4.19)
	(2)	d (3)	L (4)	k (5)	S_p (6)	S_q (7)	Load Type (8)	n_p (9)	$\bar{k}$ (10)	$\frac{S_p}{L}$ (11)	$\frac{S_q}{d}$ (12)	$\frac{L}{d}$ (13)	$\frac{d}{b}$ (14)	C_b (15)	C_b (16)
339	38	286	5000	1013	294	98	2-PL	5	180.0	0.059	0.343	17.5	7.5	1.04	1.04
340	38	286	5000	1520	294	98	2-PL	5	270.0	0.059	0.343	17.5	7.5	1.03	1.03
341	38	286	5000	2027	294	98	2-PL	5	360.0	0.059	0.343	17.5	7.5	1.03	1.02
342	38	286	5000	830	294	129	2-PL	2	147.4	0.059	0.450	17.5	7.5	1.08	1.07
343	38	286	5000	830	294	107	2-PL	2	147.4	0.059	0.375	17.5	7.5	1.07	1.07
344	38	286	5000	830	294	64	2-PL	2	147.4	0.059	0.225	17.5	7.5	1.07	1.06
345	38	286	5000	830	294	43	2-PL	2	147.4	0.059	0.150	17.5	7.5	1.06	1.06
346	38	286	5000	830	80	98	2-PL	2	147.4	0.016	0.343	17.5	7.5	1.06	1.06
347	38	286	5000	830	200	98	2-PL	2	147.4	0.040	0.343	17.5	7.5	1.06	1.06
348	38	286	5000	830	334	98	2-PL	2	147.4	0.067	0.343	17.5	7.5	1.06	1.07
349	38	286	5000	830	589	98	2-PL	2	147.4	0.118	0.343	17.5	7.5	1.07	1.07
350	38	286	5000	830	844	98	2-PL	2	147.4	0.169	0.343	17.5	7.5	1.08	1.08
351	38	286	5000	830	1098	98	2-PL	2	147.4	0.220	0.343	17.5	7.5	1.08	1.08
352	38	286	5000	830	294	129	2-PL	3	147.4	0.059	0.450	17.5	7.5	1.07	1.06
353	38	286	5000	830	294	107	2-PL	3	147.4	0.059	0.375	17.5	7.5	1.06	1.06
354	38	286	5000	830	294	64	2-PL	3	147.4	0.059	0.225	17.5	7.5	1.06	1.06
355	38	286	5000	830	294	43	2-PL	3	147.4	0.059	0.150	17.5	7.5	1.05	1.05
356	38	286	5000	830	80	98	2-PL	3	147.4	0.016	0.343	17.5	7.5	1.05	1.05
357	38	286	5000	830	200	98	2-PL	3	147.4	0.040	0.343	17.5	7.5	1.05	1.06
358	38	286	5000	830	334	98	2-PL	3	147.4	0.067	0.343	17.5	7.5	1.06	1.06
359	38	286	5000	830	589	98	2-PL	3	147.4	0.118	0.343	17.5	7.5	1.06	1.07
360	38	286	5000	830	844	98	2-PL	3	147.4	0.169	0.343	17.5	7.5	1.07	1.07
361	38	286	5000	830	1098	98	2-PL	3	147.4	0.220	0.343	17.5	7.5	1.07	1.07
362	38	286	5000	830	294	129	2-PL	4	147.4	0.059	0.450	17.5	7.5	1.06	1.06
363	38	286	5000	830	294	107	2-PL	4	147.4	0.059	0.375	17.5	7.5	1.06	1.05
364	38	286	5000	830	294	64	2-PL	4	147.4	0.059	0.225	17.5	7.5	1.05	1.05
365	38	286	5000	830	294	43	2-PL	4	147.4	0.059	0.150	17.5	7.5	1.05	1.04
366	38	286	5000	830	80	98	2-PL	4	147.4	0.016	0.343	17.5	7.5	1.04	1.04
367	38	286	5000	830	200	98	2-PL	4	147.4	0.040	0.343	17.5	7.5	1.04	1.05
368	38	286	5000	830	334	98	2-PL	4	147.4	0.067	0.343	17.5	7.5	1.05	1.05
369	38	286	5000	830	589	98	2-PL	4	147.4	0.118	0.343	17.5	7.5	1.06	1.06
370	38	286	5000	830	844	98	2-PL	4	147.4	0.169	0.343	17.5	7.5	1.06	1.06
371	38	286	5000	830	1098	98	2-PL	4	147.4	0.220	0.343	17.5	7.5	1.06	1.06
372	38	286	5000	830	294	129	2-PL	5	147.4	0.059	0.450	17.5	7.5	1.05	1.05
373	38	286	5000	830	294	107	2-PL	5	147.4	0.059	0.375	17.5	7.5	1.05	1.05
374	38	286	5000	830	294	64	2-PL	5	147.4	0.059	0.225	17.5	7.5	1.04	1.04
375	38	286	5000	830	294	43	2-PL	5	147.4	0.059	0.150	17.5	7.5	1.04	1.04
376	38	286	5000	830	80	98	2-PL	5	147.4	0.016	0.343	17.5	7.5	1.03	1.03
377	38	286	5000	830	200	98	2-PL	5	147.4	0.040	0.343	17.5	7.5	1.03	1.04

Run No. (1)	Ply dimensions (mm)			Fastener Stiffness (N/mm)	Fastener Pattern (mm)		Load Type	Dimensionless Pramaeters						Present Study	Eq. (4.19)
	(2)	d (3)	L (4)	k (5)	S_p (6)	S_q (7)	Load Type (8)	n_p (9)	$\bar{k}$ (10)	$\frac{S_p}{L}$ (11)	$\frac{S_q}{d}$ (12)	$\frac{L}{d}$ (13)	$\frac{d}{b}$ (14)	C_b (15)	C_b (16)
378	38	286	5000	830	334	98	2-PL	5	147.4	0.067	0.343	17.5	7.5	1.04	1.05
379	38	286	5000	830	589	98	2-PL	5	147.4	0.118	0.343	17.5	7.5	1.05	1.05
380	38	286	5000	830	844	98	2-PL	5	147.4	0.169	0.343	17.5	7.5	1.05	1.05
381	38	286	5000	830	1098	98	2-PL	5	147.4	0.220	0.343	17.5	7.5	1.06	1.06
382	65	500	5000	830	294	98	2-PL	2	147.4	0.059	0.343	10.0	7.5	1.08	1.08
383	44	333	5000	830	294	98	2-PL	2	147.4	0.059	0.343	15.0	7.5	1.07	1.07
384	38	294	5000	830	294	98	2-PL	2	147.4	0.059	0.343	17.0	7.5	1.07	1.07
385	34	263	5000	830	294	98	2-PL	2	147.4	0.059	0.343	19.0	7.5	1.07	1.06
386	31	238	5000	830	294	98	2-PL	2	147.4	0.059	0.343	21.0	7.5	1.06	1.06
387	43	286	5000	830	294	98	2-PL	2	147.4	0.059	0.343	17.5	6.5	1.07	1.07
388	37	286	5000	830	294	98	2-PL	2	147.4	0.059	0.343	17.5	7.5	1.07	1.07
389	33	286	5000	830	294	98	2-PL	2	147.4	0.059	0.343	17.5	8.5	1.07	1.07
390	31	286	5000	830	294	98	2-PL	2	147.4	0.059	0.343	17.5	9.0	1.07	1.06
391	65	500	5000	830	294	98	2-PL	3	147.4	0.059	0.343	10.0	7.5	1.07	1.07
392	44	333	5000	830	294	98	2-PL	3	147.4	0.059	0.343	15.0	7.5	1.07	1.06
393	38	294	5000	830	294	98	2-PL	3	147.4	0.059	0.343	17.0	7.5	1.06	1.06
394	34	263	5000	830	294	98	2-PL	3	147.4	0.059	0.343	19.0	7.5	1.06	1.06
395	31	238	5000	830	294	98	2-PL	3	147.4	0.059	0.343	21.0	7.5	1.06	1.05
396	43	286	5000	830	294	98	2-PL	3	147.4	0.059	0.343	17.5	6.5	1.06	1.06
397	38	286	5000	830	294	98	2-PL	3	147.4	0.059	0.343	17.5	7.5	1.06	1.06
398	33	286	5000	830	294	98	2-PL	3	147.4	0.059	0.343	17.5	8.5	1.06	1.06
399	31	286	5000	830	294	98	2-PL	3	147.4	0.059	0.343	17.5	9.0	1.06	1.06
400	65	500	5000	830	294	98	2-PL	4	147.4	0.059	0.343	10.0	7.5	1.07	1.07
401	44	333	5000	830	294	98	2-PL	4	147.4	0.059	0.343	15.0	7.5	1.06	1.06
402	38	294	5000	830	294	98	2-PL	4	147.4	0.059	0.343	17.0	7.5	1.05	1.05
403	34	263	5000	830	294	98	2-PL	4	147.4	0.059	0.343	19.0	7.5	1.05	1.05
404	31	238	5000	830	294	98	2-PL	4	147.4	0.059	0.343	21.0	7.5	1.05	1.05
405	43	286	5000	830	294	98	2-PL	4	147.4	0.059	0.343	17.5	6.5	1.05	1.05
406	38	286	5000	830	294	98	2-PL	4	147.4	0.059	0.343	17.5	7.5	1.05	1.05
407	33	286	5000	830	294	98	2-PL	4	147.4	0.059	0.343	17.5	8.5	1.05	1.05
408	31	286	5000	830	294	98	2-PL	4	147.4	0.059	0.343	17.5	9.0	1.05	1.05
409	65	500	5000	830	294	98	2-PL	5	147.4	0.059	0.343	10.0	7.5	1.06	1.06
410	44	333	5000	830	294	98	2-PL	5	147.4	0.059	0.343	15.0	7.5	1.05	1.05
411	38	294	5000	830	294	98	2-PL	5	147.4	0.059	0.343	17.0	7.5	1.05	1.05
412	34	263	5000	830	294	98	2-PL	5	147.4	0.059	0.343	19.0	7.5	1.04	1.04
413	31	238	5000	830	294	98	2-PL	5	147.4	0.059	0.343	21.0	7.5	1.04	1.04
414	43	286	5000	830	294	98	2-PL	5	147.4	0.059	0.343	17.5	6.5	1.05	1.05
415	38	286	5000	830	294	98	2-PL	5	147.4	0.059	0.343	17.5	7.5	1.05	1.05
416	33	286	5000	830	294	98	2-PL	5	147.4	0.059	0.343	17.5	8.5	1.04	1.04

Run No. (1)	Ply dimensions (mm)			Fastener Stiffness (N/mm)	Fastener Pattern (mm)		Load Type	Dimensionless Pramaeters						Present Study	Eq. (4.19)
	(2)	d (3)	L (4)	k (5)	S_p (6)	S_q (7)	Load Type (8)	n_p (9)	$\bar{k}$ (10)	$\frac{S_p}{L}$ (11)	$\frac{S_q}{d}$ (12)	$\frac{L}{d}$ (13)	$\frac{d}{b}$ (14)	C_b (15)	C_b (16)
417	31	286	5000	830	294	98	2-PL	5	147.4	0.059	0.343	17.5	9.0	1.04	1.04
418	36	238	5000	2027	80	129	2-PL	3	360.0	0.016	0.450	21.0	6.5	1.03	1.02
419	36	238	5000	0	80	43	2-PL	3	0.0	0.016	0.150	21.0	6.5	1.10	1.09
420	76	500	5000	2027	1098	43	2-PL	3	360.0	0.220	0.150	10.0	6.5	1.08	1.07
421	76	500	5000	0	80	43	2-PL	3	0.0	0.016	0.150	10.0	6.5	1.10	1.09
422	55	500	5000	2027	1098	43	2-PL	3	360.0	0.220	0.150	10.0	9.0	1.07	1.06
423	55	500	5000	2027	80	129	2-PL	3	360.0	0.016	0.450	10.0	9.0	1.04	1.04
424	36	238	5000	2027	1098	43	2-PL	3	360.0	0.220	0.15	21.0	6.5	1.06	1.04

Table B.3: Results for built-up beams subjected to uniform distributed load, Mid-span point load and two-point load applied at the top edge

Run No. (1)	Ply dimensions (mm)			Fastener			Load Type	Dimensionless Parameters						Present Study	Eq. (4.20)
				Stiffness (N/mm)	Pattern (mm)										
	b (2)	d (3)	L (4)	k (5)	S_p (6)	S_q (7)	Load Type (8)	n_p (9)	$\bar{k}$ (10)	$\frac{S_p}{L}$ (11)	$\frac{S_q}{d}$ (12)	$\frac{L}{d}$ (13)	$\frac{d}{b}$ (14)	C_L (15)	C_L (16)
425	38	286	5000	0	294	98	UDL-T	2	0	0.06	0.34	17.5	7.5	0.918	0.918
426	38	286	5000	507	294	98	UDL-T	2	90	0.06	0.34	17.5	7.5	0.906	0.899
427	38	286	5000	1013	294	98	UDL-T	2	180	0.06	0.34	17.5	7.5	0.893	0.894
428	38	286	5000	1520	294	98	UDL-T	2	270	0.06	0.34	17.5	7.5	0.885	0.889
429	38	286	5000	2027	294	98	UDL-T	2	360	0.06	0.34	17.5	7.5	0.879	0.886
430	38	286	5000	0	294	98	UDL-T	3	0	0.06	0.34	17.5	7.5	0.918	0.918
431	38	286	5000	507	294	98	UDL-T	3	90	0.06	0.34	17.5	7.5	0.901	0.895
432	38	286	5000	1013	294	98	UDL-T	3	180	0.06	0.34	17.5	7.5	0.888	0.887
433	38	286	5000	1520	294	98	UDL-T	3	270	0.06	0.34	17.5	7.5	0.880	0.882
434	38	286	5000	2027	294	98	UDL-T	3	360	0.06	0.34	17.5	7.5	0.875	0.878
435	38	286	5000	0	294	98	UDL-T	4	0	0.06	0.34	17.5	7.5	0.918	0.918
436	38	286	5000	507	294	98	UDL-T	4	90	0.06	0.34	17.5	7.5	0.898	0.890
437	38	286	5000	1013	294	98	UDL-T	4	180	0.06	0.34	17.5	7.5	0.884	0.881
438	38	286	5000	1520	294	98	UDL-T	4	270	0.06	0.34	17.5	7.5	0.877	0.875
439	38	286	5000	2027	294	98	UDL-T	4	360	0.06	0.34	17.5	7.5	0.872	0.869
440	38	286	5000	0	294	98	UDL-T	5	0	0.06	0.34	17.5	7.5	0.918	0.918
441	38	286	5000	507	294	98	UDL-T	5	90	0.06	0.34	17.5	7.5	0.895	0.885
442	38	286	5000	1013	294	98	UDL-T	5	180	0.06	0.34	17.5	7.5	0.881	0.875
443	38	286	5000	1520	294	98	UDL-T	5	270	0.06	0.34	17.5	7.5	0.873	0.867
444	38	286	5000	2027	294	98	UDL-T	5	360	0.06	0.34	17.5	7.5	0.869	0.861
445	38	286	5000	830	294	129	UDL-T	2	147	0.06	0.45	17.5	7.5	0.903	0.901
446	38	286	5000	830	294	107	UDL-T	2	147	0.06	0.38	17.5	7.5	0.897	0.897
447	38	286	5000	830	294	86	UDL-T	2	147	0.06	0.30	17.5	7.5	0.893	0.893
448	38	286	5000	830	294	64	UDL-T	2	147	0.06	0.23	17.5	7.5	0.889	0.888
449	38	286	5000	830	294	43	UDL-T	2	147	0.06	0.15	17.5	7.5	0.886	0.883
450	38	286	5000	830	80	98	UDL-T	2	147	0.02	0.34	17.5	7.5	0.877	0.875
451	38	286	5000	830	200	98	UDL-T	2	147	0.04	0.34	17.5	7.5	0.891	0.890
452	38	286	5000	830	334	98	UDL-T	2	147	0.07	0.34	17.5	7.5	0.897	0.897
453	38	286	5000	830	589	98	UDL-T	2	147	0.12	0.34	17.5	7.5	0.906	0.905
454	38	286	5000	830	844	98	UDL-T	2	147	0.17	0.34	17.5	7.5	0.908	0.909
455	38	286	5000	830	1098	98	UDL-T	2	147	0.22	0.34	17.5	7.5	0.909	0.912
456	38	286	5000	830	294	129	UDL-T	3	147	0.06	0.45	17.5	7.5	0.899	0.895
457	38	286	5000	830	294	107	UDL-T	3	147	0.06	0.38	17.5	7.5	0.892	0.891
458	38	286	5000	830	294	86	UDL-T	3	147	0.06	0.30	17.5	7.5	0.887	0.887
459	38	286	5000	830	294	64	UDL-T	3	147	0.06	0.23	17.5	7.5	0.883	0.883

Run No. (1)	Ply dimensions (mm)			Fastener			Load Type	Dimensionless Parameters						Present Study	Eq. (4.20)
				Stiffness (N/mm)	Pattern (mm)										
	b (2)	d (3)	L (4)	k (5)	S_p (6)	S_q (7)	Load Type (8)	n_p (9)	$\bar{k}$ (10)	$\frac{S_p}{L}$ (11)	$\frac{S_q}{d}$ (12)	$\frac{L}{d}$ (13)	$\frac{d}{b}$ (14)	C_L (15)	C_L (16)
460	38	286	5000	830	294	43	UDL-T	3	147	0.06	0.15	17.5	7.5	0.879	0.877
461	38	286	5000	830	80	98	UDL-T	3	147	0.02	0.34	17.5	7.5	0.869	0.869
462	38	286	5000	830	200	98	UDL-T	3	147	0.04	0.34	17.5	7.5	0.884	0.884
463	38	286	5000	830	334	98	UDL-T	3	147	0.07	0.34	17.5	7.5	0.892	0.891
464	38	286	5000	830	589	98	UDL-T	3	147	0.12	0.34	17.5	7.5	0.903	0.899
465	38	286	5000	830	844	98	UDL-T	3	147	0.17	0.34	17.5	7.5	0.904	0.903
466	38	286	5000	830	1098	98	UDL-T	3	147	0.22	0.34	17.5	7.5	0.905	0.906
467	38	286	5000	830	294	129	UDL-T	4	147	0.06	0.45	17.5	7.5	0.891	0.889
468	38	286	5000	830	294	107	UDL-T	4	147	0.06	0.38	17.5	7.5	0.884	0.885
469	38	286	5000	830	294	86	UDL-T	4	147	0.06	0.30	17.5	7.5	0.879	0.881
470	38	286	5000	830	294	64	UDL-T	4	147	0.06	0.23	17.5	7.5	0.875	0.877
471	38	286	5000	830	294	43	UDL-T	4	147	0.06	0.15	17.5	7.5	0.871	0.871
472	38	286	5000	830	80	98	UDL-T	4	147	0.02	0.34	17.5	7.5	0.863	0.863
473	38	286	5000	830	200	98	UDL-T	4	147	0.04	0.34	17.5	7.5	0.876	0.878
474	38	286	5000	830	334	98	UDL-T	4	147	0.07	0.34	17.5	7.5	0.884	0.886
475	38	286	5000	830	589	98	UDL-T	4	147	0.12	0.34	17.5	7.5	0.896	0.893
476	38	286	5000	830	844	98	UDL-T	4	147	0.17	0.34	17.5	7.5	0.899	0.897
477	38	286	5000	830	1098	98	UDL-T	4	147	0.22	0.34	17.5	7.5	0.900	0.900
478	38	286	5000	830	294	129	UDL-T	5	147	0.06	0.45	17.5	7.5	0.886	0.883
479	38	286	5000	830	294	107	UDL-T	5	147	0.06	0.38	17.5	7.5	0.878	0.880
480	38	286	5000	830	294	86	UDL-T	5	147	0.06	0.30	17.5	7.5	0.874	0.876
481	38	286	5000	830	294	64	UDL-T	5	147	0.06	0.23	17.5	7.5	0.870	0.871
482	38	286	5000	830	294	43	UDL-T	5	147	0.06	0.15	17.5	7.5	0.866	0.865
483	38	286	5000	830	80	98	UDL-T	5	147	0.02	0.34	17.5	7.5	0.860	0.857
484	38	286	5000	830	200	98	UDL-T	5	147	0.04	0.34	17.5	7.5	0.870	0.872
485	38	286	5000	830	334	98	UDL-T	5	147	0.07	0.34	17.5	7.5	0.878	0.880
486	38	286	5000	830	589	98	UDL-T	5	147	0.12	0.34	17.5	7.5	0.891	0.887
487	38	286	5000	830	844	98	UDL-T	5	147	0.17	0.34	17.5	7.5	0.894	0.891
488	38	286	5000	830	1098	98	UDL-T	5	147	0.22	0.34	17.5	7.5	0.896	0.894
489	65	500	5000	830	294	98	UDL-T	2	147	0.06	0.34	10.0	7.5	0.836	0.832
490	44	333	5000	830	294	98	UDL-T	2	147	0.06	0.34	15.0	7.5	0.875	0.874
491	38	294	5000	830	294	98	UDL-T	2	147	0.06	0.34	17.0	7.5	0.890	0.891
492	31	238	5000	830	294	98	UDL-T	2	147	0.06	0.34	21.0	7.5	0.922	0.925
493	43	286	5000	830	294	98	UDL-T	2	147	0.06	0.34	17.5	6.5	0.899	0.898
494	37	286	5000	830	294	98	UDL-T	2	147	0.06	0.34	17.5	7.5	0.896	0.895
495	33	286	5000	830	294	98	UDL-T	2	147	0.06	0.34	17.5	8.5	0.894	0.893
496	31	286	5000	830	294	98	UDL-T	2	147	0.06	0.34	17.5	9.0	0.893	0.891
497	65	500	5000	830	294	98	UDL-T	3	147	0.06	0.34	10.0	7.5	0.828	0.826
498	44	333	5000	830	294	98	UDL-T	3	147	0.06	0.34	15.0	7.5	0.868	0.868

Run No. (1)	Ply dimensions (mm)			Fastener			Load Type	Dimensionless Parameters						Present Study	Eq. (4.20)
				Stiffness (N/mm)	Pattern (mm)										
	b (2)	d (3)	L (4)	k (5)	S_p (6)	S_q (7)	Load Type (8)	n_p (9)	$\bar{k}$ (10)	$\frac{S_p}{L}$ (11)	$\frac{S_q}{d}$ (12)	$\frac{L}{d}$ (13)	$\frac{d}{b}$ (14)	C_L (15)	C_L (16)
499	38	294	5000	830	294	98	UDL-T	3	147	0.06	0.34	17.0	7.5	0.884	0.885
500	31	238	5000	830	294	98	UDL-T	3	147	0.06	0.34	21.0	7.5	0.916	0.919
501	43	286	5000	830	294	98	UDL-T	3	147	0.06	0.34	17.5	6.5	0.892	0.892
502	37	286	5000	830	294	98	UDL-T	3	147	0.06	0.34	17.5	7.5	0.890	0.890
503	33	286	5000	830	294	98	UDL-T	3	147	0.06	0.34	17.5	8.5	0.887	0.887
504	31	286	5000	830	294	98	UDL-T	3	147	0.06	0.34	17.5	9.0	0.886	0.885
505	65	500	5000	830	294	98	UDL-T	4	147	0.06	0.34	10.0	7.5	0.817	0.821
506	44	333	5000	830	294	98	UDL-T	4	147	0.06	0.34	15.0	7.5	0.858	0.863
507	38	294	5000	830	294	98	UDL-T	4	147	0.06	0.34	17.0	7.5	0.874	0.880
508	31	238	5000	830	294	98	UDL-T	4	147	0.06	0.34	21.0	7.5	0.906	0.913
509	43	286	5000	830	294	98	UDL-T	4	147	0.06	0.34	17.5	6.5	0.885	0.887
510	37	286	5000	830	294	98	UDL-T	4	147	0.06	0.34	17.5	7.5	0.882	0.884
511	33	286	5000	830	294	98	UDL-T	4	147	0.06	0.34	17.5	8.5	0.879	0.881
512	31	286	5000	830	294	98	UDL-T	4	147	0.06	0.34	17.5	9.0	0.878	0.880
513	66	500	5000	830	294	98	UDL-T	5	147	0.06	0.34	10.0	7.5	0.809	0.815
514	44	333	5000	830	294	98	UDL-T	5	147	0.06	0.34	15.0	7.5	0.851	0.857
515	38	294	5000	830	294	98	UDL-T	5	147	0.06	0.34	17.0	7.5	0.868	0.874
516	31	238	5000	830	294	98	UDL-T	5	147	0.06	0.34	21.0	7.5	0.901	0.907
517	43	286	5000	830	294	98	UDL-T	5	147	0.06	0.34	17.5	6.5	0.879	0.881
518	37	286	5000	830	294	98	UDL-T	5	147	0.06	0.34	17.5	7.5	0.876	0.878
519	33	286	5000	830	294	98	UDL-T	5	147	0.06	0.34	17.5	8.5	0.873	0.875
520	31	286	5000	830	294	98	UDL-T	5	147	0.06	0.34	17.5	9.0	0.872	0.874
521	36	238	5000	2027	80	129	UDL-T	3	360	0.016	0.45	21.0	6.5	0.906	0.901
522	36	238	5000	0	80	43	UDL-T	3	0	0.016	0.15	21.0	6.5	0.908	0.918
523	76	500	5000	2027	1098	43	UDL-T	3	360	0.220	0.15	10.0	6.5	0.783	0.798
524	76	500	5000	0	80	43	UDL-T	3	0	0.016	0.15	10.0	6.5	0.889	0.918
525	55	500	5000	2027	1098	43	UDL-T	3	360	0.220	0.15	10.0	9.0	0.796	0.788
526	55	500	5000	2027	1098	129	UDL-T	3	360	0.016	0.45	10.0	9.0	0.779	0.760
527	36	238	5000	2027	1098	43	UDL-T	3	360	0.22	0.15	21.0	6.5	0.891	0.929
528	38	286	5000	0	294	98	1-PL-T	2	0	0.06	0.34	17.5	7.5	0.891	0.891
529	38	286	5000	507	294	98	1-PL-T	2	90	0.06	0.34	17.5	7.5	0.879	0.873
530	38	286	5000	1013	294	98	1-PL-T	2	180	0.06	0.34	17.5	7.5	0.867	0.867
531	38	286	5000	1520	294	98	1-PL-T	2	270	0.06	0.34	17.5	7.5	0.859	0.862
532	38	286	5000	2027	294	98	1-PL-T	2	360	0.06	0.34	17.5	7.5	0.853	0.858
533	38	286	5000	0	294	98	1-PL-T	3	0	0.06	0.34	17.5	7.5	0.891	0.891
534	38	286	5000	507	294	98	1-PL-T	3	90	0.06	0.34	17.5	7.5	0.875	0.868
535	38	286	5000	1013	294	98	1-PL-T	3	180	0.06	0.34	17.5	7.5	0.862	0.861
536	38	286	5000	1520	294	98	1-PL-T	3	270	0.06	0.34	17.5	7.5	0.854	0.855
537	38	286	5000	2027	294	98	1-PL-T	3	360	0.06	0.34	17.5	7.5	0.849	0.850

Run No. (1)	Ply dimensions (mm)			Fastener			Load Type	Dimensionless Parameters						Present Study	Eq. (4.20)
				Stiffness (N/mm)	Pattern (mm)										
	b (2)	d (3)	L (4)	k (5)	S_p (6)	S_q (7)	Load Type (8)	n_p (9)	$\bar{k}$ (10)	$\frac{S_p}{L}$ (11)	$\frac{S_q}{d}$ (12)	$\frac{L}{d}$ (13)	$\frac{d}{b}$ (14)	C_L (15)	C_L (16)
538	38	286	5000	0	294	98	1-PL-T	4	0	0.06	0.34	17.5	7.5	0.891	0.891
539	38	286	5000	507	294	98	1-PL-T	4	90	0.06	0.34	17.5	7.5	0.870	0.864
540	38	286	5000	1013	294	98	1-PL-T	4	180	0.06	0.34	17.5	7.5	0.856	0.855
541	38	286	5000	1520	294	98	1-PL-T	4	270	0.06	0.34	17.5	7.5	0.850	0.848
542	38	286	5000	2027	294	98	1-PL-T	4	360	0.06	0.34	17.5	7.5	0.845	0.842
543	38	286	5000	0	294	98	1-PL-T	5	0	0.06	0.34	17.5	7.5	0.891	0.891
544	38	286	5000	507	294	98	1-PL-T	5	90	0.06	0.34	17.5	7.5	0.865	0.860
545	38	286	5000	1013	294	98	1-PL-T	5	180	0.06	0.34	17.5	7.5	0.851	0.849
546	38	286	5000	1520	294	98	1-PL-T	5	270	0.06	0.34	17.5	7.5	0.844	0.841
547	38	286	5000	2027	294	98	1-PL-T	5	360	0.06	0.34	17.5	7.5	0.840	0.834
548	38	286	5000	830	294	129	1-PL-T	2	147	0.06	0.45	17.5	7.5	0.883	0.884
549	38	286	5000	830	294	107	1-PL-T	2	147	0.06	0.38	17.5	7.5	0.873	0.872
550	38	286	5000	830	294	86	1-PL-T	2	147	0.06	0.30	17.5	7.5	0.867	0.865
551	38	286	5000	830	294	64	1-PL-T	2	147	0.06	0.23	17.5	7.5	0.863	0.860
552	38	286	5000	830	294	43	1-PL-T	2	147	0.06	0.15	17.5	7.5	0.859	0.858
553	38	286	5000	830	80	98	1-PL-T	2	147	0.02	0.34	17.5	7.5	0.843	0.843
554	38	286	5000	830	200	98	1-PL-T	2	147	0.04	0.34	17.5	7.5	0.862	0.863
555	38	286	5000	830	334	98	1-PL-T	2	147	0.07	0.34	17.5	7.5	0.870	0.870
556	38	286	5000	830	589	98	1-PL-T	2	147	0.12	0.34	17.5	7.5	0.873	0.875
557	38	286	5000	830	844	98	1-PL-T	2	147	0.17	0.34	17.5	7.5	0.875	0.878
558	38	286	5000	830	1098	98	1-PL-T	2	147	0.22	0.34	17.5	7.5	0.877	0.879
559	38	286	5000	830	294	129	1-PL-T	3	147	0.06	0.45	17.5	7.5	0.880	0.878
560	38	286	5000	830	294	107	1-PL-T	3	147	0.06	0.38	17.5	7.5	0.868	0.867
561	38	286	5000	830	294	86	1-PL-T	3	147	0.06	0.30	17.5	7.5	0.862	0.859
562	38	286	5000	830	294	64	1-PL-T	3	147	0.06	0.23	17.5	7.5	0.856	0.855
563	38	286	5000	830	294	43	1-PL-T	3	147	0.06	0.15	17.5	7.5	0.852	0.853
564	38	286	5000	830	80	98	1-PL-T	3	147	0.02	0.34	17.5	7.5	0.837	0.838
565	38	286	5000	830	200	98	1-PL-T	3	147	0.04	0.34	17.5	7.5	0.854	0.858
566	38	286	5000	830	334	98	1-PL-T	3	147	0.07	0.34	17.5	7.5	0.864	0.865
567	38	286	5000	830	589	98	1-PL-T	3	147	0.12	0.34	17.5	7.5	0.869	0.870
568	38	286	5000	830	844	98	1-PL-T	3	147	0.17	0.34	17.5	7.5	0.872	0.872
569	38	286	5000	830	1098	98	1-PL-T	3	147	0.22	0.34	17.5	7.5	0.873	0.874
570	38	286	5000	830	294	129	1-PL-T	4	147	0.06	0.45	17.5	7.5	0.874	0.873
571	38	286	5000	830	294	107	1-PL-T	4	147	0.06	0.38	17.5	7.5	0.861	0.862
572	38	286	5000	830	294	86	1-PL-T	4	147	0.06	0.30	17.5	7.5	0.855	0.854
573	38	286	5000	830	294	64	1-PL-T	4	147	0.06	0.23	17.5	7.5	0.849	0.849
574	38	286	5000	830	294	43	1-PL-T	4	147	0.06	0.15	17.5	7.5	0.845	0.848
575	38	286	5000	830	80	98	1-PL-T	4	147	0.02	0.34	17.5	7.5	0.835	0.832
576	38	286	5000	830	200	98	1-PL-T	4	147	0.04	0.34	17.5	7.5	0.849	0.852

Run No. (1)	Ply dimensions (mm)			Fastener			Load Type	Dimensionless Parameters						Present Study	Eq. (4.20)
				Stiffness (N/mm)	Pattern (mm)										
	b (2)	d (3)	L (4)	k (5)	S_p (6)	S_q (7)	Load Type (8)	n_p (9)	$\bar{k}$ (10)	$\frac{S_p}{L}$ (11)	$\frac{S_q}{d}$ (12)	$\frac{L}{d}$ (13)	$\frac{d}{b}$ (14)	C_L (15)	C_L (16)
577	38	286	5000	830	334	98	1-PL-T	4	147	0.07	0.34	17.5	7.5	0.859	0.859
578	38	286	5000	830	589	98	1-PL-T	4	147	0.12	0.34	17.5	7.5	0.865	0.864
579	38	286	5000	830	844	98	1-PL-T	4	147	0.17	0.34	17.5	7.5	0.868	0.867
580	38	286	5000	830	1098	98	1-PL-T	4	147	0.22	0.34	17.5	7.5	0.870	0.868
581	38	286	5000	830	294	129	1-PL-T	5	147	0.06	0.45	17.5	7.5	0.868	0.868
582	38	286	5000	830	294	107	1-PL-T	5	147	0.06	0.38	17.5	7.5	0.855	0.856
583	38	286	5000	830	294	86	1-PL-T	5	147	0.06	0.30	17.5	7.5	0.850	0.848
584	38	286	5000	830	294	64	1-PL-T	5	147	0.06	0.23	17.5	7.5	0.845	0.844
585	38	286	5000	830	294	43	1-PL-T	5	147	0.06	0.15	17.5	7.5	0.840	0.842
586	38	286	5000	830	80	98	1-PL-T	5	147	0.02	0.34	17.5	7.5	0.827	0.827
587	38	286	5000	830	200	98	1-PL-T	5	147	0.04	0.34	17.5	7.5	0.843	0.847
588	38	286	5000	830	334	98	1-PL-T	5	147	0.07	0.34	17.5	7.5	0.853	0.854
589	38	286	5000	830	589	98	1-PL-T	5	147	0.12	0.34	17.5	7.5	0.860	0.859
590	38	286	5000	830	844	98	1-PL-T	5	147	0.17	0.34	17.5	7.5	0.863	0.861
591	38	286	5000	830	1098	98	1-PL-T	5	147	0.22	0.34	17.5	7.5	0.864	0.863
592	65	500	5000	830	294	98	1-PL-T	2	147	0.06	0.34	10.0	7.5	0.820	0.819
593	44	333	5000	830	294	98	1-PL-T	2	147	0.06	0.34	15.0	7.5	0.852	0.852
594	38	294	5000	830	294	98	1-PL-T	2	147	0.06	0.34	17.0	7.5	0.865	0.865
595	31	238	5000	830	294	98	1-PL-T	2	147	0.06	0.34	21.0	7.5	0.890	0.892
596	43	286	5000	830	294	98	1-PL-T	2	147	0.06	0.34	17.5	6.5	0.873	0.871
597	37	286	5000	830	294	98	1-PL-T	2	147	0.06	0.34	17.5	7.5	0.870	0.869
598	33	286	5000	830	294	98	1-PL-T	2	147	0.06	0.34	17.5	8.5	0.869	0.867
599	31	286	5000	830	294	98	1-PL-T	2	147	0.06	0.34	17.5	9.0	0.868	0.865
600	65	500	5000	830	294	98	1-PL-T	3	147	0.06	0.34	10.0	7.5	0.813	0.813
601	44	333	5000	830	294	98	1-PL-T	3	147	0.06	0.34	15.0	7.5	0.846	0.846
602	38	294	5000	830	294	98	1-PL-T	3	147	0.06	0.34	17.0	7.5	0.859	0.860
603	31	238	5000	830	294	98	1-PL-T	3	147	0.06	0.34	21.0	7.5	0.886	0.886
604	43	286	5000	830	294	98	1-PL-T	3	147	0.06	0.34	17.5	6.5	0.866	0.865
605	37	286	5000	830	294	98	1-PL-T	3	147	0.06	0.34	17.5	7.5	0.864	0.863
606	33	286	5000	830	294	98	1-PL-T	3	147	0.06	0.34	17.5	8.5	0.862	0.861
607	31	286	5000	830	294	98	1-PL-T	3	147	0.06	0.34	17.5	9.0	0.861	0.860
608	65	500	5000	830	294	98	1-PL-T	4	147	0.06	0.34	10.0	7.5	0.807	0.808
609	44	333	5000	830	294	98	1-PL-T	4	147	0.06	0.34	15.0	7.5	0.840	0.841
610	38	294	5000	830	294	98	1-PL-T	4	147	0.06	0.34	17.0	7.5	0.853	0.854
611	31	238	5000	830	294	98	1-PL-T	4	147	0.06	0.34	21.0	7.5	0.880	0.881
612	43	286	5000	830	294	98	1-PL-T	4	147	0.06	0.34	17.5	6.5	0.860	0.860
613	37	286	5000	830	294	98	1-PL-T	4	147	0.06	0.34	17.5	7.5	0.857	0.858
614	33	286	5000	830	294	98	1-PL-T	4	147	0.06	0.34	17.5	8.5	0.855	0.856
615	31	286	5000	830	294	98	1-PL-T	4	147	0.06	0.34	17.5	9.0	0.854	0.855

Run No. (1)	Ply dimensions (mm)			Fastener			Load Type	Dimensionless Parameters						Present Study	Eq. (4.20)
				Stiffness (N/mm)	Pattern (mm)										
	b (2)	d (3)	L (4)	k (5)	S_p (6)	S_q (7)	Load Type (8)	n_p (9)	$\bar{k}$ (10)	$\frac{S_p}{L}$ (11)	$\frac{S_q}{d}$ (12)	$\frac{L}{d}$ (13)	$\frac{d}{b}$ (14)	C_L (15)	C_L (16)
616	66	500	5000	830	294	98	1-PL-T	5	147	0.06	0.34	10.0	7.5	0.800	0.802
617	44	333	5000	830	294	98	1-PL-T	5	147	0.06	0.34	15.0	7.5	0.832	0.836
618	38	294	5000	830	294	98	1-PL-T	5	147	0.06	0.34	17.0	7.5	0.845	0.849
619	31	238	5000	830	294	98	1-PL-T	5	147	0.06	0.34	21.0	7.5	0.870	0.876
620	43	286	5000	830	294	98	1-PL-T	5	147	0.06	0.34	17.5	6.5	0.853	0.854
621	37	286	5000	830	294	98	1-PL-T	5	147	0.06	0.34	17.5	7.5	0.850	0.852
622	33	286	5000	830	294	98	1-PL-T	5	147	0.06	0.34	17.5	8.5	0.848	0.850
623	31	286	5000	830	294	98	1-PL-T	5	147	0.06	0.34	17.5	9.0	0.847	0.849
624	36	238	5000	2027	80	129	1-PL-T	3	360	0.02	0.45	21.0	6.5	0.895	0.873
625	36	238	5000	0	80	43	1-PL-T	3	0	0.02	0.15	21.0	6.5	0.909	0.891
626	76	500	5000	2027	1098	43	1-PL-T	3	360	0.22	0.15	10.0	6.5	0.774	0.781
627	76	500	5000	0	80	43	1-PL-T	3	0	0.02	0.15	10.0	6.5	0.871	0.891
628	55	500	5000	2027	1098	43	1-PL-T	3	360	0.22	0.15	10.0	9.0	0.764	0.774
629	55	500	5000	2027	1098	129	1-PL-T	3	360	0.016	0.45	10.0	9.0	0.763	0.758
630	36	238	5000	2027	1098	43	1-PL-T	3	360	0.22	0.15	21.0	6.5	0.866	0.888
631	38	286	5000	0	294	98	2-PL-T	2	0	0.06	0.34	17.5	7.5	0.910	0.910
632	38	286	5000	507	294	98	2-PL-T	2	90	0.06	0.34	17.5	7.5	0.892	0.890
633	38	286	5000	1013	294	98	2-PL-T	2	180	0.06	0.34	17.5	7.5	0.880	0.882
634	38	286	5000	1520	294	98	2-PL-T	2	270	0.06	0.34	17.5	7.5	0.870	0.876
635	38	286	5000	2027	294	98	2-PL-T	2	360	0.06	0.34	17.5	7.5	0.863	0.871
636	38	286	5000	0	294	98	2-PL-T	3	0	0.06	0.34	17.5	7.5	0.910	0.910
637	38	286	5000	507	294	98	2-PL-T	3	90	0.06	0.34	17.5	7.5	0.886	0.885
638	38	286	5000	1013	294	98	2-PL-T	3	180	0.06	0.34	17.5	7.5	0.872	0.874
639	38	286	5000	1520	294	98	2-PL-T	3	270	0.06	0.34	17.5	7.5	0.863	0.866
640	38	286	5000	2027	294	98	2-PL-T	3	360	0.06	0.34	17.5	7.5	0.858	0.859
641	38	286	5000	0	294	98	2-PL-T	4	0	0.06	0.34	17.5	7.5	0.910	0.910
642	38	286	5000	507	294	98	2-PL-T	4	90	0.06	0.34	17.5	7.5	0.878	0.879
643	38	286	5000	1013	294	98	2-PL-T	4	180	0.06	0.34	17.5	7.5	0.863	0.866
644	38	286	5000	1520	294	98	2-PL-T	4	270	0.06	0.34	17.5	7.5	0.854	0.856
645	38	286	5000	2027	294	98	2-PL-T	4	360	0.06	0.34	17.5	7.5	0.849	0.848
646	38	286	5000	0	294	98	2-PL-T	5	0	0.06	0.34	17.5	7.5	0.910	0.910
647	38	286	5000	507	294	98	2-PL-T	5	90	0.06	0.34	17.5	7.5	0.873	0.873
648	38	286	5000	1013	294	98	2-PL-T	5	180	0.06	0.34	17.5	7.5	0.857	0.858
649	38	286	5000	1520	294	98	2-PL-T	5	270	0.06	0.34	17.5	7.5	0.849	0.846
650	38	286	5000	2027	294	98	2-PL-T	5	360	0.06	0.34	17.5	7.5	0.844	0.836
651	38	286	5000	830	294	129	2-PL-T	2	147	0.06	0.45	17.5	7.5	0.894	0.889
652	38	286	5000	830	294	107	2-PL-T	2	147	0.06	0.38	17.5	7.5	0.888	0.886
653	38	286	5000	830	294	86	2-PL-T	2	147	0.06	0.30	17.5	7.5	0.883	0.883
654	38	286	5000	830	294	64	2-PL-T	2	147	0.06	0.23	17.5	7.5	0.880	0.878

Run No. (1)	Ply dimensions (mm)			Fastener			Load Type	Dimensionless Parameters						Present Study	Eq. (4.20)
				Stiffness (N/mm)	Pattern (mm)										
	b (2)	d (3)	L (4)	k (5)	S_p (6)	S_q (7)	Load Type (8)	n_p (9)	$\bar{k}$ (10)	$\frac{S_p}{L}$ (11)	$\frac{S_q}{d}$ (12)	$\frac{L}{d}$ (13)	$\frac{d}{b}$ (14)	C_L (15)	C_L (16)
655	38	286	5000	830	294	43	2-PL-T	2	147	0.06	0.15	17.5	7.5	0.877	0.872
656	38	286	5000	830	80	98	2-PL-T	2	147	0.02	0.34	17.5	7.5	0.859	0.856
657	38	286	5000	830	200	98	2-PL-T	2	147	0.04	0.34	17.5	7.5	0.878	0.878
658	38	286	5000	830	334	98	2-PL-T	2	147	0.07	0.34	17.5	7.5	0.887	0.887
659	38	286	5000	830	589	98	2-PL-T	2	147	0.12	0.34	17.5	7.5	0.890	0.894
660	38	286	5000	830	844	98	2-PL-T	2	147	0.17	0.34	17.5	7.5	0.894	0.897
661	38	286	5000	830	1098	98	2-PL-T	2	147	0.22	0.34	17.5	7.5	0.898	0.899
662	38	286	5000	830	294	129	2-PL-T	3	147	0.06	0.45	17.5	7.5	0.879	0.882
663	38	286	5000	830	294	107	2-PL-T	3	147	0.06	0.38	17.5	7.5	0.880	0.879
664	38	286	5000	830	294	86	2-PL-T	3	147	0.06	0.30	17.5	7.5	0.875	0.876
665	38	286	5000	830	294	64	2-PL-T	3	147	0.06	0.23	17.5	7.5	0.870	0.871
666	38	286	5000	830	294	43	2-PL-T	3	147	0.06	0.15	17.5	7.5	0.866	0.865
667	38	286	5000	830	80	98	2-PL-T	3	147	0.02	0.34	17.5	7.5	0.848	0.848
668	38	286	5000	830	200	98	2-PL-T	3	147	0.04	0.34	17.5	7.5	0.869	0.871
669	38	286	5000	830	334	98	2-PL-T	3	147	0.07	0.34	17.5	7.5	0.879	0.879
670	38	286	5000	830	589	98	2-PL-T	3	147	0.12	0.34	17.5	7.5	0.884	0.886
671	38	286	5000	830	844	98	2-PL-T	3	147	0.17	0.34	17.5	7.5	0.888	0.890
672	38	286	5000	830	1098	98	2-PL-T	3	147	0.22	0.34	17.5	7.5	0.894	0.892
673	38	286	5000	830	294	129	2-PL-T	4	147	0.06	0.45	17.5	7.5	0.881	0.874
674	38	286	5000	830	294	107	2-PL-T	4	147	0.06	0.38	17.5	7.5	0.871	0.872
675	38	286	5000	830	294	86	2-PL-T	4	147	0.06	0.30	17.5	7.5	0.866	0.868
676	38	286	5000	830	294	64	2-PL-T	4	147	0.06	0.23	17.5	7.5	0.860	0.864
677	38	286	5000	830	294	43	2-PL-T	4	147	0.06	0.15	17.5	7.5	0.857	0.857
678	38	286	5000	830	80	98	2-PL-T	4	147	0.02	0.34	17.5	7.5	0.839	0.841
679	38	286	5000	830	200	98	2-PL-T	4	147	0.04	0.34	17.5	7.5	0.857	0.864
680	38	286	5000	830	334	98	2-PL-T	4	147	0.07	0.34	17.5	7.5	0.870	0.872
681	38	286	5000	830	589	98	2-PL-T	4	147	0.12	0.34	17.5	7.5	0.877	0.879
682	38	286	5000	830	844	98	2-PL-T	4	147	0.17	0.34	17.5	7.5	0.882	0.883
683	38	286	5000	830	1098	98	2-PL-T	4	147	0.22	0.34	17.5	7.5	0.888	0.885
684	38	286	5000	830	294	129	2-PL-T	5	147	0.06	0.45	17.5	7.5	0.875	0.867
685	38	286	5000	830	294	107	2-PL-T	5	147	0.06	0.38	17.5	7.5	0.864	0.864
686	38	286	5000	830	294	86	2-PL-T	5	147	0.06	0.30	17.5	7.5	0.859	0.861
687	38	286	5000	830	294	64	2-PL-T	5	147	0.06	0.23	17.5	7.5	0.855	0.856
688	38	286	5000	830	294	43	2-PL-T	5	147	0.06	0.15	17.5	7.5	0.852	0.850
689	38	286	5000	830	80	98	2-PL-T	5	147	0.02	0.34	17.5	7.5	0.834	0.834
690	38	286	5000	830	200	98	2-PL-T	5	147	0.04	0.34	17.5	7.5	0.850	0.856
691	38	286	5000	830	334	98	2-PL-T	5	147	0.07	0.34	17.5	7.5	0.863	0.865
692	38	286	5000	830	589	98	2-PL-T	5	147	0.12	0.34	17.5	7.5	0.870	0.872
693	38	286	5000	830	844	98	2-PL-T	5	147	0.17	0.34	17.5	7.5	0.875	0.875

Run No. (1)	Ply dimensions (mm)			Fastener			Load Type	Dimensionless Parameters						Present Study	Eq. (4.20)
				Stiffness (N/mm)	Pattern (mm)										
	b (2)	d (3)	L (4)	k (5)	S_p (6)	S_q (7)	Load Type (8)	n_p (9)	$\bar{k}$ (10)	$\frac{S_p}{L}$ (11)	$\frac{S_q}{d}$ (12)	$\frac{L}{d}$ (13)	$\frac{d}{b}$ (14)	C_L (15)	C_L (16)
694	38	286	5000	830	1098	98	2-PL-T	5	147	0.22	0.34	17.5	7.5	0.881	0.877
695	65	500	5000	830	294	98	2-PL-T	2	147	0.06	0.34	10.0	7.5	0.820	0.816
696	44	333	5000	830	294	98	2-PL-T	2	147	0.06	0.34	15.0	7.5	0.866	0.862
697	38	294	5000	830	294	98	2-PL-T	2	147	0.06	0.34	17.0	7.5	0.884	0.880
698	31	238	5000	830	294	98	2-PL-T	2	147	0.06	0.34	21.0	7.5	0.920	0.917
699	43	286	5000	830	294	98	2-PL-T	2	147	0.06	0.34	17.5	6.5	0.890	0.889
700	37	286	5000	830	294	98	2-PL-T	2	147	0.06	0.34	17.5	7.5	0.887	0.885
701	33	286	5000	830	294	98	2-PL-T	2	147	0.06	0.34	17.5	8.5	0.883	0.881
702	31	286	5000	830	294	98	2-PL-T	2	147	0.06	0.34	17.5	9.0	0.881	0.880
703	65	500	5000	830	294	98	2-PL-T	3	147	0.06	0.34	10.0	7.5	0.812	0.809
704	44	333	5000	830	294	98	2-PL-T	3	147	0.06	0.34	15.0	7.5	0.858	0.855
705	38	294	5000	830	294	98	2-PL-T	3	147	0.06	0.34	17.0	7.5	0.876	0.873
706	31	238	5000	830	294	98	2-PL-T	3	147	0.06	0.34	21.0	7.5	0.913	0.910
707	43	286	5000	830	294	98	2-PL-T	3	147	0.06	0.34	17.5	6.5	0.882	0.881
708	37	286	5000	830	294	98	2-PL-T	3	147	0.06	0.34	17.5	7.5	0.879	0.878
709	33	286	5000	830	294	98	2-PL-T	3	147	0.06	0.34	17.5	8.5	0.875	0.874
710	31	286	5000	830	294	98	2-PL-T	3	147	0.06	0.34	17.5	9.0	0.873	0.872
711	65	500	5000	830	294	98	2-PL-T	4	147	0.06	0.34	10.0	7.5	0.799	0.801
712	44	333	5000	830	294	98	2-PL-T	4	147	0.06	0.34	15.0	7.5	0.846	0.847
713	38	294	5000	830	294	98	2-PL-T	4	147	0.06	0.34	17.0	7.5	0.865	0.866
714	31	238	5000	830	294	98	2-PL-T	4	147	0.06	0.34	21.0	7.5	0.903	0.902
715	43	286	5000	830	294	98	2-PL-T	4	147	0.06	0.34	17.5	6.5	0.874	0.874
716	37	286	5000	830	294	98	2-PL-T	4	147	0.06	0.34	17.5	7.5	0.870	0.870
717	33	286	5000	830	294	98	2-PL-T	4	147	0.06	0.34	17.5	8.5	0.866	0.867
718	31	286	5000	830	294	98	2-PL-T	4	147	0.06	0.34	17.5	9.0	0.864	0.865
719	66	500	5000	830	294	98	2-PL-T	5	147	0.06	0.34	10.0	7.5	0.791	0.794
720	44	333	5000	830	294	98	2-PL-T	5	147	0.06	0.34	15.0	7.5	0.840	0.840
721	38	294	5000	830	294	98	2-PL-T	5	147	0.06	0.34	17.0	7.5	0.859	0.858
722	31	238	5000	830	294	98	2-PL-T	5	147	0.06	0.34	21.0	7.5	0.897	0.895
723	43	286	5000	830	294	98	2-PL-T	5	147	0.06	0.34	17.5	6.5	0.866	0.866
724	37	286	5000	830	294	98	2-PL-T	5	147	0.06	0.34	17.5	7.5	0.863	0.863
725	33	286	5000	830	294	98	2-PL-T	5	147	0.06	0.34	17.5	8.5	0.859	0.859
726	31	286	5000	830	294	98	2-PL-T	5	147	0.06	0.34	17.5	9.0	0.857	0.858
727	36	238	5000	2027	80	129	2-PL-T	3	360	0.02	0.45	21.0	6.5	0.881	0.876
728	36	238	5000	0	80	43	2-PL-T	3	0	0.02	0.15	21.0	6.5	0.921	0.910
729	76	500	5000	2027	1098	43	2-PL-T	3	360	0.22	0.15	10.0	6.5	0.800	0.760
730	76	500	5000	0	80	43	2-PL-T	3	0	0.02	0.15	10.0	6.5	0.912	0.910
731	55	500	5000	2027	1098	43	2-PL-T	3	360	0.22	0.15	10.0	9.0	0.757	0.746
732	55	500	5000	2027	1098	129	2-PL-T	3	360	0.016	0.45	10.0	9.0	0.749	0.704

Run No. (1)	Ply dimensions (mm)			Fastener			Load Type	Dimensionless Parameters						Present Study	Eq. (4.20)
				Stiffness (N/mm)	Pattern (mm)										
	b (2)	d (3)	L (4)	k (5)	S_p (6)	S_q (7)	Load Type (8)	n_p (9)	$\bar{k}$ (10)	$\frac{S_p}{L}$ (11)	$\frac{S_q}{d}$ (12)	$\frac{L}{d}$ (13)	$\frac{d}{b}$ (14)	C_L (15)	C_L (16)
733	36	238	5000	2027	1098	43	2-PL-T	3	360	0.22	0.15	21.0	6.5	0.895	0.918

Appendix C: Application of Research Findings to Design Provisions in CSA O86-24

This appendix aims to demonstrate the integration of the current study's findings into the existing design framework of CSA O86:24 for obtaining the elastic lateral torsional buckling (LTB) capacity of built-up beams.

C-1 Present CSA framework for elastic LTB capacity of built-up beams

The critical moment due to the LTB of beams can be obtained using

$$M_{cr} = \gamma C_r C_b C_l C_p \frac{\pi}{L_u} \sqrt{E_{05} I_y G_{05} J} K_{SE} K_T \tag{C.22}$$

where L_u is the unbraced segment length, E_{05} and G_{05} are the fifth-percentile modulus of elasticity and shear modulus, respectively, I_y is the moment of inertia about the weak axis, and J is the torsional constant of the cross-section. Coefficients K_{SE} and K_T are stiffness modifiers, while γ is a calibration factor that depends on the timber product type.

The coefficient C_b accounts for the influence of the bending moment distribution within the unbraced segment. This factor accounts for the increase in the elastic buckling resistance when the moment diagram is non-uniform. It can be evaluated according to clause 7.5.6.4.4 in the standard. The load height factor C_l captures the detrimental position of gravity loads when they are applied above the shear centre of the cross-section. Loads applied above the shear center tend to destabilize the member, while those applied below it have a stabilizing effect. The load height factor C_l can be obtained from Table 7.5 in CSA-O86:24. The partial torsional restraint coefficient C_r represents

the degree of partial torsional restraint provided at the ends of the unbraced segment. The coefficient C_p accounts for the pre-buckling deformation effect.

The lateral stability factor K_L due to the elastic LTB can be obtained using

$$K_L = \frac{M_{cr}}{F_b S K_x} \tag{C.23}$$

in which M_{cr} = critical moment for elastic lateral-torsional buckling that is calculated in Eq. (C.22), $S = \left(n_p b d^2\right)/6$ is the elastic section modulus, n_p is the number of plies, b is the ply width, and d is the ply depth, $F_b = f_b K_D K_H K_{Sb} K_T$, in which f_b is the specified bending strength, K_D is the load-duration factor, K_H is the system factor, K_{Sb} is the service-condition factor for bending, and K_T is the treatment factor and K_x is the curvature factor. Clause 6.5.3.2.4 of CAN/CSA-O86:24 suggests that the elastic LTB capacity is based on the sum of the elastic LTB capacities of the individual plies. Therefore, the critical moment mentioned in Eq. (C.22) is based on the cross-sectional properties I_y and J of a single ply multiplied by the number of plies.

C-2 Suggested changes to CSA O86:24

The current study proposes three changes to the existing framework of CSA O86:24 to estimate the elastic LTB capacity of built-up beams:

1- Multiply the critical moment predicted by Eq. (C.22) by the magnification factor defined in Eq. (4.18) to account for partial composite action between plies.

2- Compute the moment gradient factor C_b using Eq. (4.19).

3- Compute the load height factor C_l using Eq. (4.20).